Contents

1. Introduction

1. 1 Extracellular Matrix

The extracellular matrix (ECM) is the noncellular component present within all tissues and organs, and provides not only essential physical scaffolding for the cellular constituents but also triggers crucial biochemical and biomechanical cues that are required for tissue morphogenesis, differentiation and homeostasis.

Although, fundamentally, the ECM is composed of water, proteins and polysaccharides, each tissue has an ECM with a unique composition and topology that is generated during tissue development through a dynamic and reciprocal, biochemical and biophysical dialogue between the various cellular components (e.g. epithelial, fibroblast, adipocyte, endothelial elements) and the evolving cellular and protein microenvironment. Indeed, the physical, topological, and biochemical composition of the ECM is not only tissue-specific, but is also markedly heterogeneous. Cell adhesion to the ECM is mediated by ECM receptors, such as integrins, discoidin domain receptors and syndecans.

Moreover, the ECM is a highly dynamic structure that is constantly being remodeled, either enzymatically or non-enzymatically, and its molecular components are subjected to a myriad of post-translational modifications. Through these physical and biochemical characteristics the ECM generates the biochemical and mechanical properties of each organ, such as its tensile and compressive strength and elasticity, and also mediates protection by a buffering action that maintains extracellular homeostasis and water retention. In addition, the ECM directs essential morphological organization and physiological function by binding growth factors (GFs) and interacting with cell-surface receptors to elicit signal transduction and regulate gene transcription. The biochemical and biomechanical, protective and organizational properties of the ECM in a given tissue can vary tremendously from one tissue to another and even within one tissue, as well as from one physiological state to another. In fact, the ECM is involved in several physiologic processes of degradation and remodeling and moreover in regulating the behavior of the cells that contact it, influencing their development, function, shape, proliferation, and migration. This last

phenomenon holds a pivotal role during the development of inflammatory and pathologic status, such as in the atherosclerosis and formation of metastasis.

The ECM is composed of two main classes of polysaccharides: glycosaminoglycans (GAGs), which are usually found covalently linked to protein in the form of proteoglycans (PGs) and fibrous proteins (Schaefer and Schaefer, 2010). The main fibrous ECM proteins are collagens, elastins, fibronectins and laminins. PGs fill the majority of the extracellular interstitial space within the tissue in the form of a hydrated gel (Jarvelainen et al. 2009). PGs have a wide variety of functions that reflect their unique buffering, hydration, binding and force-resistance properties.

1. 2 Glycosaminoglycans and Proteoglycans

Proteoglycans (PGs) are biological molecules composed of a specific core protein substituted with covalently linked glycosaminoglycan (GAG) chains. Hyaluronan (HA) is an exception to this definition, as it lacks a protein core. GAGs are linear, sulfated, negatively charged polysaccharides, which can be divided into two classes, namely sulfated GAGs comprising chondroitin sulfate (CS), dermatan sulfate (DS), keratan sulfate (KS), heparin, and heparin sulfate (HS), and non-sulfated GAGs such as HA. GAG chains are made up of disaccharide repeating regions containing acetylated amino sugar moieties (N-acetylgalactosamine or N-acetyl-glucosamine) and mainly uronic acid (glucoronic acid or iduronic acid).

The biosynthesis of proteoglycans, in addition to the ordinary biosynthetic processes of O- and N-linked oligosaccharide components as in other glycoproteins, further requires biosynthesis of glycosaminoglycans in the Golgi apparatus, which can be considered to be a most complex biosynthetic process for complex carbohydrates. It requires a number of glycosyltransferases and sulfotransferases and involves multiple subregions of the Golgi apparatus, which poses a great challenge for researchers in elucidating the organization and regulatory mechanisms involved in proteoglycan biosynthesis.

PGs can be classified into three main groups according to their localization, extracellularly secreted, those associated with the cell surface and intracellular.

The wide molecular diversity of PGs derives from the multitude of possible combinations of protein cores, O-linked and N-linked oligosaccharides, and various types and numbers of GAG chains. The specific structural characteristics of GAG types provide some of the structural basis for the multitude of their biological functions. PGs exhibit numerous biological functions acting as structural components in tissue organization, and affect several cellular parameters, such as cell proliferation, adhesion, migration and differentiation. PGs interact with growth factors and cytokines, as well as with growth factor receptors, and are implicated in cell signaling.

1. 3 Hyaluronan

Hyaluronan is considered the simplest of the GAGs because it consists of a regular repeating sequence of non sulfated disaccharide units and because it's not bound to a core protein. It is an unusual polysaccharide that has a simple chemical structure but extraordinary properties. It is synthesized as a large, negatively charged, unbranched polymer that is composed of repeating disaccharides (from 2000 to 25000) of glucuronic acid and *N* acetylglucosamine linked with β-1,3 and β-1,4 glycosidic bonds respectively (Figure 1).

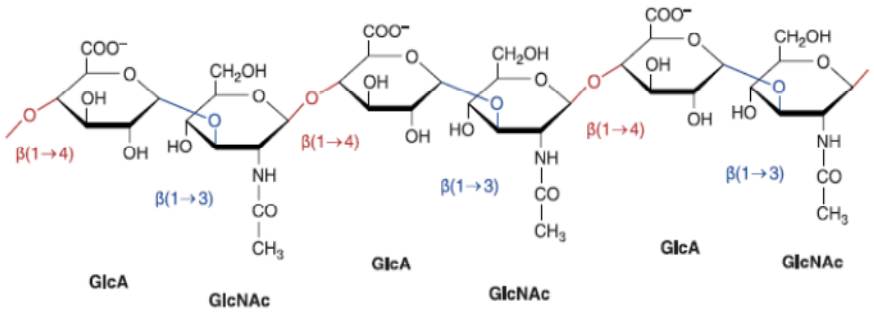

Figure 1- Repeated disaccharidic structure of hyaluronan

Although HA belongs to the family of glycosaminoglycans it differs from these in many ways. Other GAGs are made as PGs that are synthesized and assembled in the rough endoplasmic reticulum and Golgi apparatus, and are secreted in a similar way to other glycoproteins.
Moreover, whereas other GAGs are synthesized inside the cell and released by exocytosis, HA is spun out directly from the cell surface by an enzyme complex that is embedded in the plasma membrane.
Many of the functions of HA depend on specific hyaluronan-binding proteins and proteoglycans, some of which are constituents of the extracellular matrix, while others are integral components of the surface of cells.
HA has multiple functions, such as space filling, hydration, lubrication of joints, and provision of a matrix through which cells can migrate (Toole, 2004). HA is actively produced during tissue injury, tissue repair, and wound healing (Slevin et al. 2002). In addition to providing a framework for ingrowth of blood vessels and fibroblasts, HA also regulates many aspects of molecular mechanisms of tissue repair, such as activation of inflammatory cells to mount an immunological response and regulation of behavior of epithelial cells and fibroblasts. Elucidation of the role and mechanisms of HA is crucial in aiding the development of novel therapy for many diseases.

1. 4 Biosynthesis of Hyaluronan

HA is synthesized as an unmodified polysaccharide by three different, but related, hyaluronic acid synthases (HASs). These are multipass transmembrane enzymes, the active sites of which protrude from the inner face of the plasma membrane. HA is extruded through porelike structures onto the cell surface or into the ECM during its polymerization.
HA biosynthesis requires not only HASs participation but it needs also the synthesis of UDP-sugars throughout a complex pathway organized in several steps. The enzymes use UDP-β-*N*-acetyl-D-glucosamine and UDP-β-D-glucuronate as substrates. Two additional enzymes are necessary for the

glucuronic acid biosynthesis: the UDP-glucose pyrophosphorylase (UGPP) and the UDP-glucose dehydrogenase (UGDH). The first enzyme transfers glucose-1-phosphate to the UTP, producing UDP-glucose. This sugar is used as a substrate by the UGPP in an NAD^+-dependent, 2-fold oxidative reaction to generate UDP-glucuronic acid. The conversion of glucose to UDP-GlcNAc is mediated by the hexosamine biosynthetic pathway (HBP). This pathway merges from glycolysis using fructose-6-phosphate (Fruc-6-P) to form glucosamine-6-P (GlucN-6-P) and this main reaction is catalyzed by the rate-limiting enzyme glutamine:fructose-6-phosphate-amidotransferase (GFAT). GlucN-6-P is rapidly acetylated, isomerized to N-Acetylglucosamine-6-phosphate (GlucNAc-1-P) and activated to UDP-N-acetylglucosamine (UDP-GlucNAc) that serves as common precursor for all amino sugars used for the synthesis of glycoproteins, glycolipids, and PGs (Figure 2).

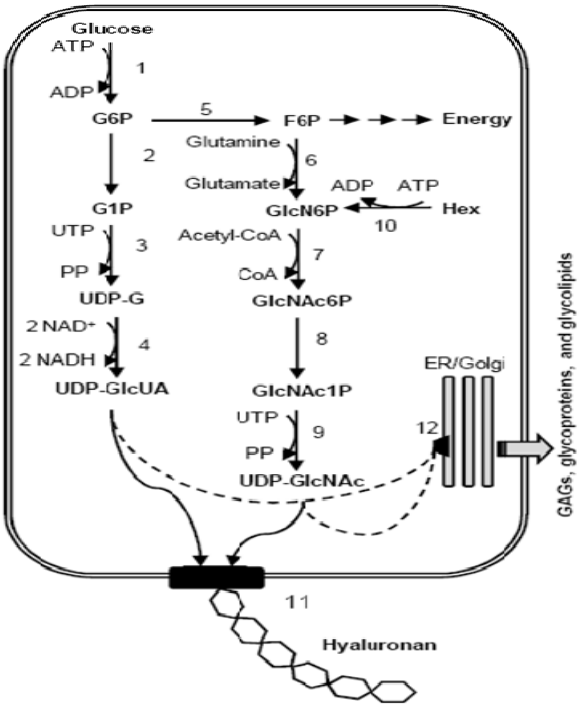

Figure 2- HA biosynthesis

In mammals the synthesis of HA is guaranted by three enzymes on the cell membrane (HAS1, 2 and 3); they differ in kinetic characteristics and product size. The existence of three different HAS isoforms with different characteristics implies that these enzymes have distinct biological and physiological roles. All the HAS isozymes are highly homologous in their amino acid sequences and have similar hydropathic features, suggesting that they are similarly organized within the membrane. (Itano et al. 1996). In human the genes encoding for the three HAS's are located on different autosome: HAS1 is located on Chr 19q13.4, HAS2 on Chr 8q24.12 and HAS3 on Chr 16q22.1. The expression profile of HAS genes during development are spatially and temporally regulated, suggesting that HA may play a different role during development in different tissues or cell types (Itano, 2008). Structurally, all HAS enzymes are integral membrane proteins composed of seven membrane-spanning regions with hydrophobic amino acid cluster and large cytoplasmatic loops (Figure 3). Unlike typical glycosiltransferases, this enzyme is localized in the plasma membrane.

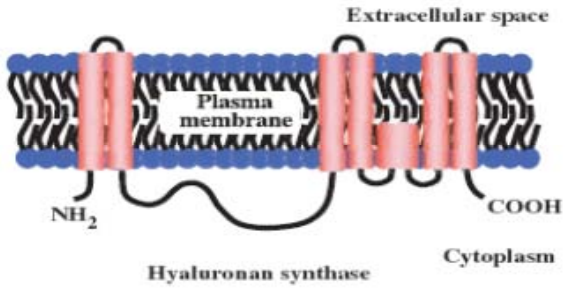

Figure 3- Structure of mammalian hyaluronan synthase

To complete the rapid HA-turn over in physiological conditions, this GAG is cleaved by enzymes known as hyaluronidases. In human there are six different genes encoding for hyaluronidases with different properties and cellular locations (Stern, 2004).

1. 5 The exosamine biosynthetic pathway

Uridine diphosphate-N-acetylglucosamine (UDP-GlcNAc) is synthesized from glucose as the final product of the hexosamine biosynthetic pathway (HBP) (Figure 4).

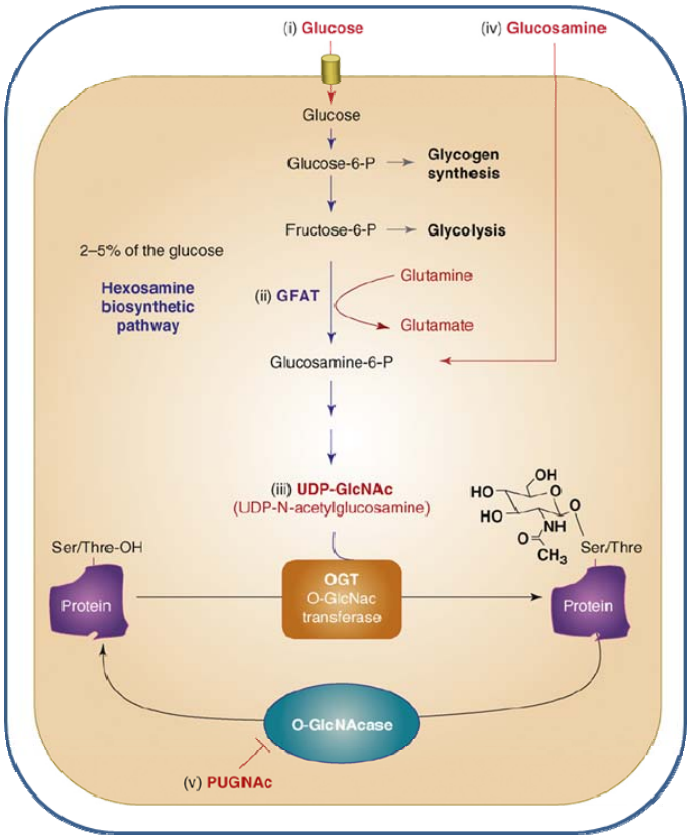

Figure 4- the exosamine pathway

Only a small percentage of the glucose entering in the cells, approximately 2–5% of intracellular glucose, depending on cell type, is routed to the HBP. Furthermore, flux through the pathway is thought to be regulated largely by the levels of glucose and the rate-limiting enzyme GFAT

(glutamine:fructose-6-phosphate amidotransferase). In fact, after entering the cells, glucose is rapidly phosphorylated and converted to fructose-6-phosphate (F-6-P), which is mainly metabolized through the glycolytic pathway. However, under chronic hyperglycemic conditions of a diabetic state, a greater part of F-6-P is diverted by the action of GFAT and converted into glucosamine-6-phosphate (GlcN-6-P). GlcN-6-P is then metabolized into various hexosamine products, including the main product UDP-GlcNAc. This elevated UDP-GlcNAc has three effects on the pathway. At first, UDP-GlcNAc feedback inhibits GFAT, thus blunting synthesis; also provide glycosidic precursors for the synthesis of glycoproteins, glycolipids and proteoglycans. Furthermore, it can be used to covalently modify proteins and affect their functions, through a single O-linked glycosylation, referred to O-GlcNAcylation. These O-GlcNAc modifications play critical roles in regulation of wide spectrum of cellular functions. Since its first discovery, it has been suggested that elevated *O*-GlcNAc contributes to many deleterious effects of hyperglycemia and glucotoxicity including insulin resistance, diabetic cardiovascular damage associated with oxidative stress and inflammation (Masson et al. 2006).

1. 6 O-GlcNac modification

The HBP connects a nutrient-sensing system to a signaling pathway by providing GlcN-6-P, the key precursor of UDP-GlcNAc, the substrate for O-GlcNAc modification. Indeed, O-GlcNAcylation results from the addition of a single UDP-GlcNAc on the hydroxyl groups of Ser and/or Thr residues of target proteins. O-GlcNAcylation is a unique type of glycosylation that it is not elongated to more complex glycan structures and is not restricted to the cell surface and/or luminal face of secreted proteins. This nucleocytoplasmic dynamic post-translational modification is rapidly responsive to hormones, nutrients, and cellular stress.

Enzymes that catalyze the addition and removal of O-GlcNAc have been cloned and characterized (Figure 5). Unlike protein phosphorylation, where ~650 genetically distinct enzymes regulate the addition and removal of

phosphate, just two catalytic polypeptides catalyze the turnover of O-GlcNAc; a uridine diphospho-N-acetylglucosamine: peptide β-N-acetylglucosaminyl transferase (OGT; EC 2.4.1) and a neutral β-N-acetylglucosaminidase (OGlcNAcase; EC 3.2.1.52).

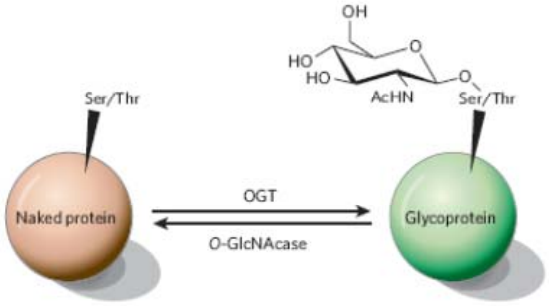

Figure 5- O-GlcNAcylation cycles

The sensitivity of O-GlcNAc levels to extracellular glucose concentrations supports a model in which O-GlcNAc plays a role as a nutritional sensor, regulating cell growth in response to the available nutrients by altering alters protein-protein interactions, intracellular localization, protein turnover and activity. Studies showing that altering UDP-GlcNAc levels, and increasing and decreasing levels of O-GlcNAc, disrupt cell cycle lend additional support to this model (Butkinaree et al. 2010).

Several studies have shown that such a crosstalk between GlcNAcylation and phosphorylation exists, as disturbing phosphorylation events affects GlcNAcylation levels and vice versa.

Site-mapping studies have shown that on some proteins *O*-GlcNAc and *O*-phosphate compete dynamically for the same serine or threonine hydroxyl moiety. This reciprocal occupancy seems to produce different activities or stability in the proteins (Figure 6).

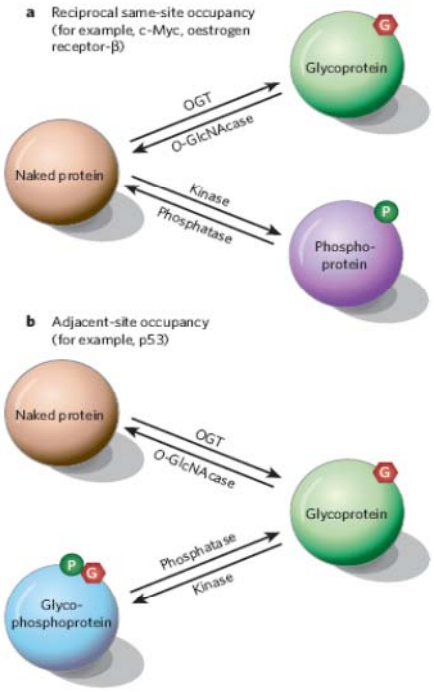

Figure 6- Dynamic interplay between O-GlcNAc and O-phosphate.

In certain proteins, *O*-GlcNAc and *O*-phosphate can also occur next to each other. Adjacent occupancy by each modification reciprocally influences the functions or turnover of proteins, as has recently been reported for the tumour suppressor p53 (Yang et al. 2006).

Our group demonstrated that HAS2 could be phosphorylated by AMPK in the intracytoplasmatic loop, which is important for HAS glycosyl transferase activity (Vigetti et al. 2011). Bioinformatic analysis have shown the presence of a putative AMPK phosphorylation consensus motif at treonine 110 (T110). Therefore, we mutated T110 to alanine (T110A) in order to prevent phosphorylation, and we found that the T110 residue can be target of AMPK and that the phosphorylation of HAS2 strongly reduces the HA synthetic activity. Because regulatory phosphorylation modulates the function of cellular proteins similar to that of O-GlcNAcylation, in the

present study we investigated whether HAS2 is subject to GlcNAc protein modification, and its consequence for the activity and the stability of HAS2.

1. 7 O-GlcNAc transferase (OGT)

OGT catalyses the addition of *O*-GlcNAc to protein. OGT was identified in and first purified from rat liver, and has since been cloned in rats, humans, *C. elegans* and other organisms. In mammals, OGT gene is highly conserved and is present as a single X linked gene localized near the centromere where recombination rates are low. This chromosomal region is linked to several neurological diseases, including Parkinson's disease (Nemeth et al. 1999). Although there is only one OGT gene present, mammalian has three different isoforms, all of which share an identical catalytic domain, but differ in the number of tetratricopeptide (TPR) repeat motifs found at the N-terminus. The longest form (116-kDa, ncOGT) is a nucleocytoplasmic isoform and the next longest isoform (103-kDa, mOGT) is mitochondrial. The shortest form of OGT (sOGT; 73-kDa) is also nuclear/cytoplasmic. In addition to the differential targeting of these isoforms, the level of expression varies depending on the target tissue. OGT is highly expressed in the pancreatic–β-cells and in the brain (Hanover et al. 1999). All OGT isoforms consist of two distinct domains: the N-terminal domain contains TPR motifs, which are common protein–protein interaction domains, while the C-terminal is the catalytic domain that is highly conserved. The main difference among OGT isoforms is the number of TPRs each isoform contains (Figure 7).

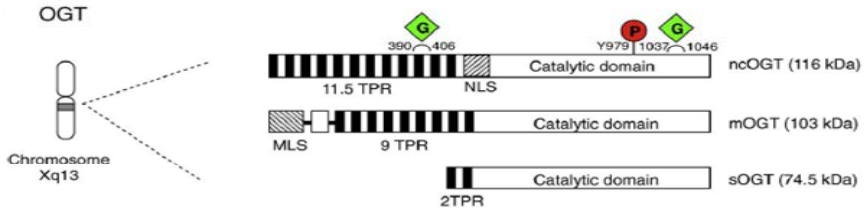

Figure 7- Structure of OGT isoforms

The mechanism by which OGT specifically modifies proteins are unclear, although it appears that UDP-GlcNAc concentration, protein–protein interactions, glycosylation, and phosphorylation may all play a role. The mRNA and protein expression levels of OGT are tissue-specific and are dependent upon specific cellular signaling, such as nutrient availability. Several proteins have been identified that interact with OGT (Yang et al, 2002), and while these interactions are not known to change the activity of OGT, they do act to anchor and/or target OGT to signaling and transcriptional complexes. These interactions may modulate the activity of OGT by affecting its localization, modulating the binding of substrate proteins, or targeting to complexes where it is specifically activated by signal transduction events. Notably, OGT is both O-GlcNAc modified and tyrosine phosphorylated (Lubas and Hanover, 2000). Finally, OGT activity is influenced by the levels of its donor substrate UDP-GlcNAc, suggesting that as levels of UDP-GlcNAc change within the cell, OGT will target a different population of substrates (Kreppel and Hart, 1999).
The coordinate regulation of substrate binding, substrate preference, association with target complexes, and post-translational modification may mediate OGT in such a way that it specifically modifies different proteins in response to diverse signals, appropriately regulating cellular function.

1. 8 O-GlcNAcase

O-GlcNAcase is a soluble, cytosolic β-N-acetylglucosaminidase expressed in all tissues examined and predominantly in brain (Wells et al. 2002). O-GlcNAcase is well conserved in mammals, with 97.8% identity between the human and mouse gene, and 29% identity (and 43% homology) between the human and C. elegans gene (Gao et al. 2001). O-GlcNAcase co-purifies with a complex of proteins suggesting that, like OGT, it is regulated by its interactions with other proteins (Gao et al. 2001). In addition, it has been shown that O-GlcNAcase is phosphorylated, suggesting an additional mechanism of regulation. O-GlcNAcase is efficiently inhibited by PUGNAC (O-(2-acetamido-2-deoxy-D-glucopyranosylidene)amino-N-

phenylcarbamate; Haltiwanger et al. 1998). The gene encodes two alternatively spliced isoforms of OGA, the longest form of OGA has two distinct domains, an O-GlcNAcase domain at the N-terminus that shows high homology with bacterial hyaluronidases and a putative acetyltransferase domain at the C-terminus (Schultz and Pils, 2002). The acetyltransferase domain may have histone acetyltransferase (HAT) activity (Toleman et al. 2004) but its sequence is dissimilar to other, canonical HAT domains (Figure 8). Interestingly, OGA contains a caspase-3 cleavage site between these domains (Wells et al. 2002). Two variants of O-GlcNAcase, in which amino acids 250–345 and 250–398 (exons 6 and 7) are deleted, have no activity suggesting that the O-GlcNAcase active site is within the N-terminal half of this protein.

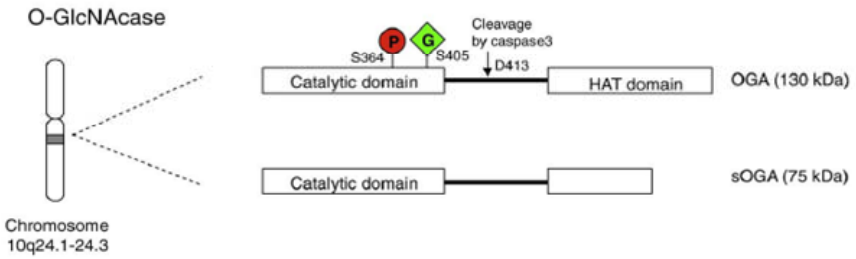

Figure 8- O-GlcNAcase structure

1. 9 O-GlcNAc and disease

The HBP connects a nutrient-sensing system to a signaling pathway by providing the substrate for O-GlcNAc modification of cytosolic and nuclear proteins in all cell types, including those involved in the cardiovascular system. This dynamic post-translational modification is rapidly responsive to hormones, nutrients, and cellular stress. It is reciprocal with phosphorylation on some proteins and is thought to play an analogous role to this modification in cellular regulation. O-GlcNAc modification alters protein-protein interactions, intracellular localization, protein turnover and activity (Zachara and Hart, 2002). The list of proteins targeted by O-

GlcNAcylation is ever growing and includes key intracellular proteins such as transcription factors, cytoskeletal proteins, tumor suppressor and oncogenes, nuclear and cytosolic proteins and enzymes. Accumulating data suggest that global O-GlcNAc protein modification is regulated in a cell-cycle dependent manner and that any disruption of this cycling results in major cell-cycle defects. In this connection, a recent study by Slawson et al. showed that excessive O-GlcNAc modification alters cell-cycle progression while intact O-GlcNAcylation is nevertheless necessary for proper cell cycle function. Several studies indicate that O-GlcNAc might induce nuclear localization of some transcription factors and may affect their DNA binding activities. For instance, transcriptional activation of Sp1, a ubiquitous transcription factor, has been reported several times to be induced (Goldberg et al. 2005), or inhibited (Yang et al. 2001) by O-GlcNAcylation. Other transcription factors have also been shown to be modified by O-GlcNAc including cAMP response element-binding protein (CREB) (Lamarre-Vincent and Hsieh-Wilson, 2003) and pancreatic duodenal homeobox (PDX-1) (Gao Y et al. 2003). More recent findings have strengthened that increased levels of O-GlcNAc have been implicated as a pathogenic contributor to glucose toxicity and insulin resistance, which are major hallmarks of type 2 diabetes and diabetes-related cardiovascular complications. Marshall and collegue demonstrated that flux through the HBP is responsible for the development of insulin resistance and remarked that the development of insulin resistance requires glucose, insulin, and glutamine. The role of glutamine in the development of insulin resistance has been found to occur via the regulation of GFAT, the rate limiting enzyme in the HBP. Inhibition of GFAT with either azaserine or DON abrogated the effects of hyperglycemia on the development of insulin resistance (Rajapakse et al. 2009). Studies have shown that an increase in cellular UDP-GlcNAc and O-GlcNAcylation levels on target proteins due to high glucose and glucosamine treatments leads to oxidative stress and endoplasmic reticulum stress, which have been shown to cause chronic inflammation and insulin resistance (Werstuck et al. 2006). Increasing the level of O-GlcNAc using either PUGNAC, a chemical inhibitor of OGA, or elevating O-GlcNAc levels with glucosamine induces insulin resistance in

3T3-L1 adipocytes (Vosseller et al. 2002). Insulin resistance and the corresponding decrease in glucose uptake are correlated with a defect in the translocation of the glucose transporter GLUT4 to the plasma membrane (Yang et al. 2008).

1. 10 O-GlcNAcylation on smooth muscle cell

Vascular smooth muscle cell dysfunction is a major risk factor of diabetic cardiovascular disease. AoSMCs are highly specialized cells whose principal functions are the contraction of blood vessels and the regulation of blood vessel tone-diameter, which regulate the blood pressure and the blood flow, respectively. Under diabetic conditions, an increased flux of glucose through the HBP has been proposed to cause vascular disease. It has been observed that prolonged exposure to high glucose leads to the increase of GFAT expression in VSMCs (Nerlich et al. 1998) indicating that GFAT is possibly involved in the development of the diabetic vascular complications. Inhibition of GFAT activity using DON decreases the hyperglycemia-induced tumor growth factor-alpha (TGF-α) expression in VSMCs, suggesting that the adverse effects of hyperglycemia in VSMCs are mediated by the HBP. Hall et al. (2001) demonstrated that expressions of GLUT1 and GLUT4 are increased in the neointima of the aorta after balloon injury. Increased proliferation and decreased apoptosis of AoSMCs provides a possible linkage with the increased risks of restenosis and atherosclerosis in patients with diabetes. Akimoto et al. (2001) found that the pattern of O-GlcNAc modification of proteins changed when rat aortic smooth muscle cells (RASMCs) were cultured in medium containing a high concentration of glucose. High glucose also elevates both the expression and activity of OGT. In addition, high glucose and glucosamine also induced an increase in the expression of growth factors in RASMCs. The effects of O-GlcNAc on cell growth and division may also contribute to the increase in VSMC proliferation seen in diabetes. Based on the above findings, it is clear that O-GlcNAcylation on specific vascular proteins has an important role in the regulation vascular reactivity, and further research is necessary to

determine the impact of O-GlcNAcylation on vascular reactivity. Thus, altering the O-GlcNAc levels in vascular tissues may represent a novel therapeutic approach for the treatment of diabetic cardiovascular disease.

1. Materials and Methods

2.1 Cell Culture and treatments

Human primary aortic smooth muscle cells (hAoSMC) were purchased from Lonza and grown in SmGm2 complete culture medium (Lonza) supplemented with 5% fetal bovine serum (FBS) (Lonza) and 1% glutamax (Lonza). 3x 10^5 cells were seeded in 35 mm dishes, and after 6 hours, SmGm2 medium was replaced with high glucose DMEM (Lonza) supplemented with 0,2% FBS. After 48 h to induce quiescence, the media was changed to low glucose (5 mM) DMEM-F12 (Euroclone) supplemented with 10% FBS. Cells were stimulated with 30 mM glucose, 2 mM glucosamine (GluN), 40 μM 6-diazo 5-oxonorleucine (DON), 5 mM alloxan, 100 μM *O*-(2-acetamido-2-deoxy-D-glucopyranosylidene) amino-*N*-phenylcarbamate (PUGNAc), 1mM benzyl-2-acetamido-2-deoxy-α-D-galactopyranoside (BG) for 24 h (all from Sigma) to modulate O-GlcNacylation.

NIH3T3 cells were grown to confluence in high glucose DMEM medium supplemented with 10% FBS and 1% glutamax. After preliminary experiments, a final concentration of 4 mM GluN, 150 μM PUGNAc, 2mM BG, 40 μM DON was used for 24 h treatments. Cultures were maintained in an atmosphere of humidified 95% air, 5% CO_2 at 37°C.

2.2 Transient and stable transfection

8x 10^5 hAoSMCs were cultured before nucleofection in SmGm2 complete culture medium until 70%-80% confluency. Cells were transiently transfected with 5 μg of plasmid DNA using *Human AoSMC Nucleofector Kit* (AMAXA) as described previously (Vigetti et al, 2006) to have high efficiency and low mortality.

1.5x 10^5 NIH3T3 cells were transiently transfected with 3 μg of total DNA using *ExGen 500 in Vitro Transfection Reagent* (Fermentas) following the manufacturer's protocol. Cells were incubated for 24-48 hours for the following analyses. For stable transfections, human HAS2 with N-terminal

c-myc tag in pcDNA3.1 was transfected in NIH3T3 using ExGen 500 and clones were selected in 400 μg/ml G-418 (Euroclone). Protein expression levels was assayed by immunoblot analysis with anti-C-Myc monoclonal antibody (Santa Cruz Biotecnology).

2.3 Gene expression determination by RT-PCR

RNAs extraction were performed using *TRI Reagent Solution* (Sigma) following the manufacturer's protocol. To remove DNA contamination, DNase treatment (Ambion) was done in all samples. 5 μg of extracted RNA were retrotranscribed using the *High Capacity cDNA synthesis kit* (Applied Biosystems). Quantitative RT-PCR was done on an *Abi Prism 7000 instrument* (Applied Biosystems) using *Taqman Universal PCR Master Mix* (Applied Biosystems) following the manufacturer's instructions. The following *TaqMan Gene Expression Assays* were used: HAS1 (Hs00155410), HAS2 (Hs00193435), HAS3 (Hs00193436), YY1 (Hs00231533), GAPDH (Hs99999905). Fluorescent signals generated during PCR amplifications were monitored and analyzed with *Abi Prism 7000 SDS Software* (Applied Biosystems). To check the SP1 abrogation we used a SYBR Green based quantitative RT-PCR (Applied Biosystem) using primers CTCCAGACCATTAACCTCAGTG and TGTATTCCATCACCACCAGC.
Comparison of the amount of each gene transcript among different samples was made using GAPDH as the reference and the $\Delta\Delta Ct$ method.

2.4 Human siRNA

Small interfering RNA (siRNA) was used to reduce the expression of human YY1 and SP1 in AoSMCs. SiRNA antisense sequence was the following: YY1 (IDs14958, 5'-UGAACUCUCAACAAAAGCUtt-3'), SP1 (ID13319, 5'-UGAGUUGUAAAGGUCUGCCct-3'), and negative control siRNA #1 kit (scramble, code 4611), a siRNA sequence not homologous to any known

gene, were purchased from Ambion. The transfections were done using the *Human AoSMC Nucleofector Kit* as previously described. After 24 h of incubation, cells were treated and the next day the silencing efficiency was quantified by quantitative RT-PCR measuring gene expression. The working concentration of siRNA in cell experiments was 50 nM.

2.5 Glycosaminoglycans determinations

GAGs released into the culture medium were purified by proteinase K (Finnzyme) digestion and ethanol precipitation. Δ-disaccharides obtained by the enzymatic digestions with hyaluronidase SD and chondroitinase ABC (Seikagaku Corporation) were fluorotagged with *2-aminoacridone* (AMAC, Molecular Probes). AMAC-tagged disaccharides were separated and quantified by PAGEFS and HPLC analyses as previously described (Karousou et al, 2004). Identification and quantification of sample bands in PAGEFS gel were done by comparing their migration and pixel density with standard Δ-disaccharides using *ImageJ software*. Separation and analysis of AMAC-derivatives of Δ-disaccharides were performed using an HPLC system coupled with a *Jasco-Borwin chromatograph system* with a fluorophore detector. Sample peaks were identified and quantified comparing the fluorescence spectra with standard Δ-disaccharides, using *Jasco-Borwin software.* Pericellular HA matrices were visualized by using a particle exclusion assay (Knudson W and Knudson CB, 1991). Representative cells were photographed at a magnification of ×40 and matrices and cellular areas were quantify using ImageJ software.

2.6 hAoSMCs mobility and adhesion assay

Confluent hAoSMc were scratched by pipette tip and then cultured in DMEM-F12 supplemented with 10% FBS in the presence of several

treatment. Migrated cells were quantified after 6 and 24 h as previously described (Vigetti et al, 2009). To test the adhesiveness of hAoSMCs in different condition, we performed the monocyte adhesion assay by using the monocyte U937 cell line (Vigetti et al, 2009). The quantification of adhered monocytes was done using an inverted microscope (Olympus) counting seven independent fields.

2.7 Western Blot Analysis

Wester blotting experiment were performed using the monoclonal antibody CTD110.6 (Sigma) in order to detected O-GlcNacylated proteins, polyclonal anti-GAPDH antibodies (Santa Cruz Biotechnology) or monoclonal anti-tubulin antibodies (Sigma). In some experiment monoclonal anti C-Myc antibodies (Santa Cruz Biotechnology) was also used to detected recombinant fused c-myc-HAS2 protein.

2.8 Immobilization of O-GlcNAc-modified Proteins with Wheat Germ Agglutinin

NIH 3T3 and hAoSMC cells are transfected with C-Myc-HAS2 or C-Myc-HAS2 and OGT coding plasmid or empty vector (pcDNA3.1). The next day, cells were treated to modulate protein O-GlcNAcylation and after 24 h growth medium was removed. Cells were scrapered in lysis buffer (10 mM Tris, 1.5 mM $MgCl_2$, 10 mM KCl in mQ water supplemented with proteases inhibitors (ROCHE)). The lysates were incubated on ice for 5 min, sonicated and the protein content was quantified using *Bradford Assay* (Sigma). 100 μg of total protein was incubated with 100 μl of (WGA)-conjugated agarose beads (Vector Laboratories). The preparation was rotated for 20 h at 4 °C and WGA-coniugated beads were collected by centrifugation; washed three times with lysis buffer and immobilized proteins were eluted by boiling in a waterbath for 5 min in lysis buffer with

1 M GluN. The eluited materials containing WGA-binding glycoproteins were assayed by western blot.

2.9 Microsome purification and HASs Activity Assay

Microsomes containing vesciculated fragments of the plasma membrane were obtained from control or transfected NIH3T3 cells as previously described (Vigetti et al, 2011). The quantification of HAS enzymatic activity was also carried out on proteins eluited from WGA-agarose beads. In some experiments, hexosaminidase digestions were conducted by treating cell lysates with *N*-acetylglucosaminidase from jack beans (Sigma). Lysates not digested with hexosaminidase were protected from deglycosylation by the addition of 50 μM PUGNAc in lysis buffer that inhibits endogenous *O*-GlcNAcase; as a control prior to determine HAS activity N-acetylglucosaminidase was boiled.

2.10 C-myc HAS2 stability

Stably transfected clones with high expression of c-myc-HAS2 were selected by growing NIH3T3 cells in the presence of 400 μg/mL of G418 (Euroclone) as described elsewhere (Badi et al. 2009). Cells were plated 24h prior to treatment with 150 μg/mL cycloheximide (CHX), GluN, PUGNAC and MG132 at 5 μM. At different time points, Western blotting analyses were carried out as described above to detect c-myc-HAS2 decay.

2.11 Luciferase gene reporter assay

hAOSMc were nucleofected with a -2118/+43 HAS2 promoter-luciferase reporter construction; a gift of Katri Makkonen. 24 h post-trasfection, cells

were treated to modulate protein O-GlcNAcylation. Cells extract were assayed using a *luciferase reporter gene assay kit (ROCHE)* at different time point as indicated. Protein concentration in cell lysates were analyzed using bratdford assay and the activity of luciferase was normalized to total protein concentration in lysates as previously described (Badi et al,2009).

2.12 Statistical Analyses

Unpaired Student's *t*-tests were done for statistical analyses. Probability values of $P<0.05$ were considered statistically significant (*). Experiments were repeated three times each time in duplicate, and data are expressed as mean ± standard error (SE).

3. Results

3. 1 O-GlcNAcylation induces HA secretion

It is generally known that an increase flux of glucose through the HBP is correlated with a global increase of the UDP-GlcNac level and subsequently can augment protein O-GlcNAcylation. This post translational modification could be a signal of nutrient abundance and modulates several cellular responses (Issad et al. 2008). Our hypothesis is to study whether O-GlcNacylation could regulate ECM polysaccharides synthesis. Since UDP-GlcNac, with UDP-GlcUA, is a precursor of HA, one of the main component of the ECM, we investigated the role of O-GlcNAcylation in the control of the cellular microenvironment with particular attention to HA synthesis.

To find out whether the HBP is required for GAG synthesis by O-GlcNAcylation, we treated cells with different compound that are able to interfere with protein glycosylation. Western blotting of hAoSMC and NIH3T3 cells lysates using a specific anti O-GlcNAc antibody, CTD110.6, revealed increase protein glycosylation as compared with control cells after glucosamine and PUGNAC treatments (Figure 9).

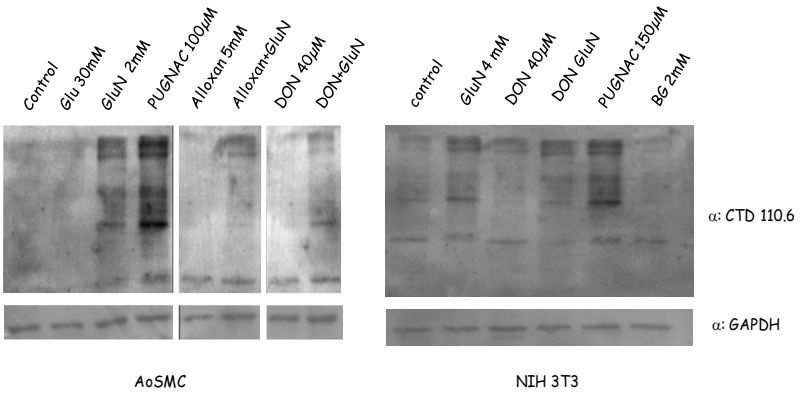

Figure 9- Representative immunoblot for O-linked glycoprotein

GluN, which bypasses the rate-limiting enzyme of the HBP, GFAT, is known to induce protein modification in the same cell lines (Raman et al, 2007); PUGNAC, a potent inhibitor of the enzyme O-GlcNAcase mimicking the enzyme-stabilized transition state, increases O-glycosylation of intracellular protein. To confirm that the HBP mediate protein glycosylation, we used specific inhibitors of GFAT and direct glycosylation inhibitors that interfered with the transfer of a sugar moiety to a protein. Preincubation of hAoSMCs with DON and alloxan, in order to inhibit the glucose flux through the HBP by inhibiting GFAT and OGT respectively, revealed a marked decrease in protein glycosylation as compared with cells not treated. The inhibitory effect of DON was reversed by GluN, confirming the specifity of DON effect; conversely, the simultaneous treatment with alloxan and GluN still inhibit O-GlcNAcylation as alloxan block OGT that acts downstream GluN entry point. Interestingly, in our condition, treatments with 30mM of glucose did not induce protein glycosylation suggesting that hAoSMCs used in the experiments were insulin-dependent for glucose uptake as previously described (Chisalita et al. 2009).

To verify whether the HBP and protein glycosylation could control GAG biosynthesis and secretion we performed an HPLC quantification of the unsaturated disaccharides (Δ) deriving from HA, chondroitin 4 sulfate (C4S) and chondroitin 6 sulfate (C6S) secreted into the hAoSMCs culture medium treated with the previous compound. As shown in figure 10, HPLC highlights that after GluN treatment, that induce UDP-GlcNAc level, both HA and chondroitins accumulate in the medium. DON and alloxan did not change GAG quantification, but the same treatments with GluN increased HA and chondroitins. On the contrary, modulation of protein O-GlcNAcylation with PUGNAC treatment, showed a specific HA augment without any effect on other GAG; while the simultaneous treatment with PUGNAC and GluN still increased both HA and chondroitins. These results suggested that an elevated UDP-GlcNac availability is critical for the biosynthesis of HA as well as that of other GAGs, while protein O-GlcNAcylation seems to be critical only for HA metabolism.

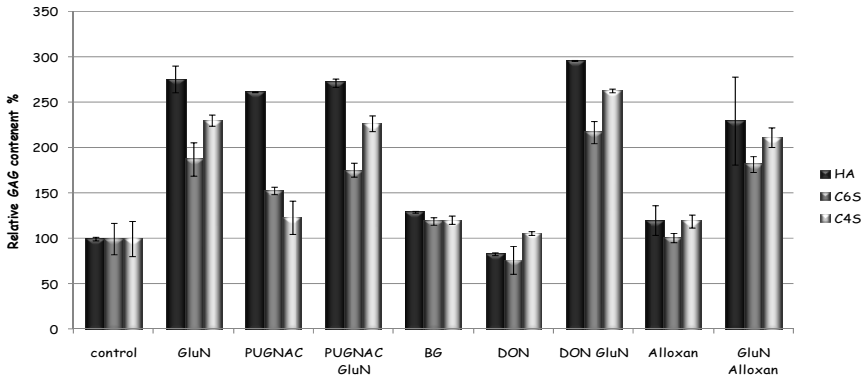

Figure 10- HPLC analyses on the hAoSMCs conditioned medium

We also investigated the correlation between protein O-GlcNAcylation and HA biosynthesis in NIH3T3 cells; the experiments confirmed the results obtained in SMCs. After treatments we used the culture media for PAGEFS and HPLC analyses, in order to quantify the amount of HA synthesized and secreted by the cells. In both PAGEFS and HPLC analyses, treatments that markedly induced UDP-GlcNac level also induce a significant increase of HA synthesis. Moreover, NIH3T3 cells treated with DON or alloxan showed a complete abolishment of this biosynthetic process, whereas the control cells cultured in medium enriched with DON+GluN or alloxan+GluN treatment were able to synthesize and secrete a large amount of HA, as shown in figure 11.

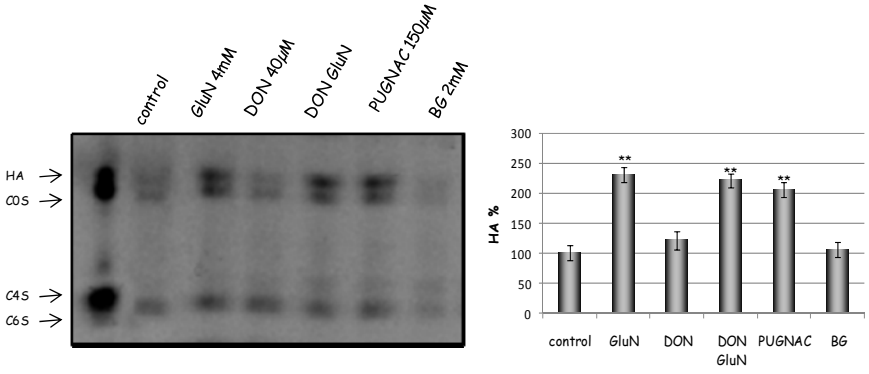

Figure 11- PAGEFS and HPLC analyses on the NIH3T3 conditioned cell medium

In addition, also in this cell line, is important to underline the specificity of this effect. In fact, PUGNAC treatments revealed the ability of this compounds to selectively regulate only HA synthesis by PAGEFS analysis: the amount of the other GAGs, as chondroitins, appears to be unchanged after treatments that modified O-GlcNAcylated protein level.

3. 2 O-GlcNAcylation regulates hAoSMCs cell behavior and microenvironment

As hAoSMCs are involved in vascular pathology through their proliferation, migration and immune cells recruitment, and HA has a pivotal role in these phenomena, we investigated the existence of correlation between HA biosynthesis due to protein O-GlcNAcylation analyzing its amount in pericellular coat by particle exclusion assay. Forty-eight hours after O-GlcNAc induction by GluN or PUGNAC treatments we observed an increment of pericellular space respect to the cells without any treatment (Figure 12). In contrast, treatments that reduce protein O-GlcNAcylation, as DON or BG, also reduce pericellular HA amount. This space between hAoSMCs and red blood cells is predominantly filled by HA, as demonstrated by digestion with hyaluronidase.

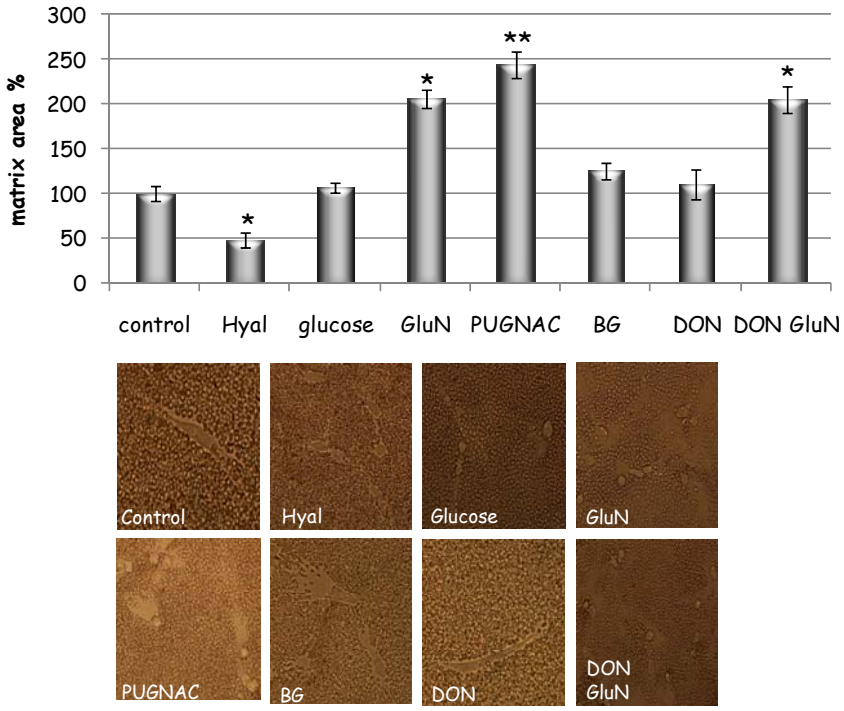

Figure 12- Particle exclusion assay quantification and microphotograph

One of the earlier events in vessel thickening is SMCs proliferation and migration from the tunica media to the intima, which determines neointima formation. SMC motility in vivo can depend on different factor, but it is well accepted that HA is a critical molecule favoring migration. Thus we evaluated if O-GlcNAcylation is able to regulate this process through the induction of HA-synthesis. As shown in figure 13, GluN or DON+GluN treatments, that increased O-GlcNAcylation, also induced hAoSMCs migration. To test the involvement of HA in migration, we adding in the medium 4-MU, a compound that decrease HA synthesis and secretion without any effect on chondroitins. We found that the addition of GluN to 4-MU treated cells is not able to restored the migration to levels similar to cells treated with GluN alone, indicating the specificity of HA in this phenomenon.

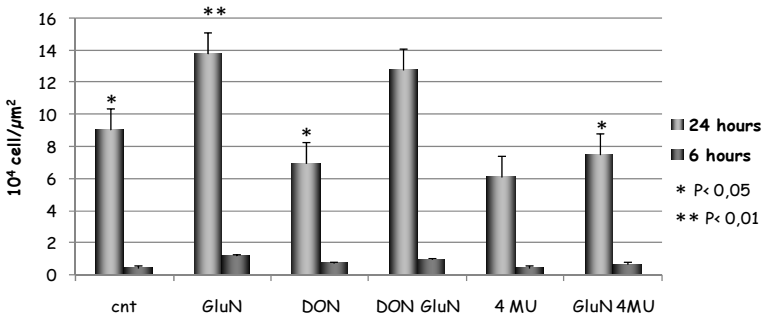

Figure 13- Cell migration using scratch wounding assay

At last, we verified the HA role in monocytes adhesion, process involved in inflammatory response. In addition to integrins and selectins, by means of CD44 circulating monocytes can adhere to HA. Therefore an accumulation of such GAG can be considered a proinflammatory signal. We quantified the number of adhesive U937 monocytes on hAoSMCs after treatments that induce or decrease O-GlcNAcylation and subsequently HA secretion. The induction of protein O-GlcNAcylation after PUGNAC or GluN treatments

showed a significant increase of U937 adhesion to hAoSMCs respect to the control cells (Figure 14).

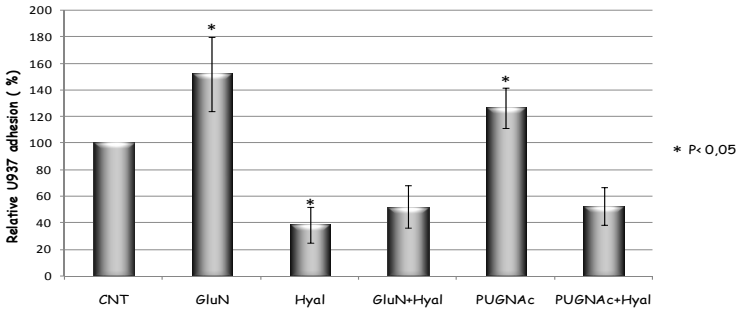

Figure 14- U937 monocytes adhesion on hAoSMCs

As a control, we treated hAoSMCs with hyaluronidase and interestingly, this pretreatment inhibited U937 binding, underlining that the interaction of monocytes with SMCs was due to HA and not to other GAGs.

3. 3 O-GlcNAcylation could regulate HAS 2 metabolism

O-GlcNAc modifications can occur either in the cytosplasm or in the nucleus and correspond to a dynamic process. This reversible O-GlcNAcylation is distinct from stable, complex glycosylations of membrane or secreted proteins, that take place in the lumen of the endoplasmic reticulum and in the Golgi apparatus. In contrast, O-GlcNAcylation/deglycosylation constitutes a dynamic regulatory mechanism that can modify the activity, the localization or the stability of cytosolic and nuclear proteins. Moreover, serine and threonine residues, that are targets for O-GlcNAc modifications, often correspond to residues that can also be phosphorylated, resulting in additional levels of protein regulation (Kuo et al. 2008). Our group recently demonstrated that HAS2 could be phosphorylated by AMPK at the Thr-110 and also the phosphorylation of this amino acid drastically reduces the HA synthetic activity (Vigetti et al. 2011). Infact this residue is localized in the intracytoplasmatic loop, which is important for HAS glycosyl transferase activity. As our preliminary experiments showed that treatments that increase protein O-GlcNAcylation or inhibit their deglycosylation could affect HA accumulation only, we hypothesized that the large cytoplasmic loops, critical for the enzymatic functions of HASes, could be accessible to nucleo-cytoplasmic OGT. In order to evaluate if the Thr-110 could be the target of OGT, we mutated this amino acid to alanine (T110A) in the C-Myc-HAS2 plasmid and transfected the mutant construct with or without OGT. After 48h, we quantified the HAS enzymatic activity in microsomes and we found a strong increase of HAS activity only after OGT cotransfection, whereas the functionality of c-myc HAS2+OGT was not affected by alloxan and GlcNAcase treatments. These results strongly suggest that Thr-110 could not be the target of OGT even if this enzyme drastically induce the HA synthetic activity (Figure 15).

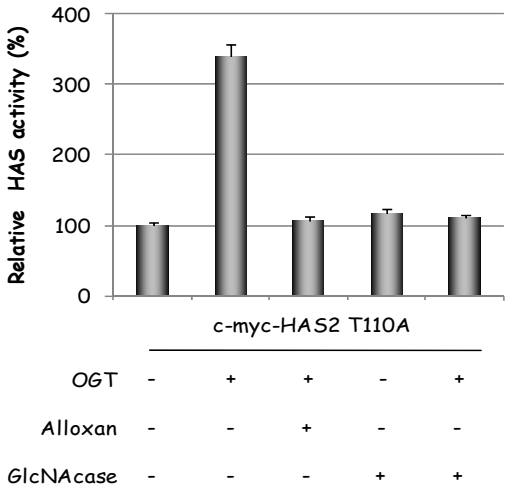

Figure 15- HAS2 activity in NIH3T3 cells transfected with c-Myc-HAS2 T110A

In order to evaluate if HAS2 is modified by O-GlcNAc we transiently transfected NIH3T3 cells with plasmids coding for c-myc-HAS2 or OGT or empty vector (pcDNA3.1). After treatments with GluN and PUGNAC, O-GlcNAcylated proteins are purified by agarose WGA beads bindings. Complexes was incubated and analyzed by western blotting using anti C-Myc antibody. The results show that HAS2 is recognized by WGA when is cotransfected with OGT or after glucosamine and PUGNAC treatments. Interestingly, after transfection with HAS2 C-Myc alone no O-GlcNAc modification is detectable (figure 16). As a control, we detected c-myc-HAS2 in all total protein extracts and in the wash fraction. These data suggested that HAS2 is O-Glycosylated after treatments that increase O-GlcNAcylation or impair deglycosylation.

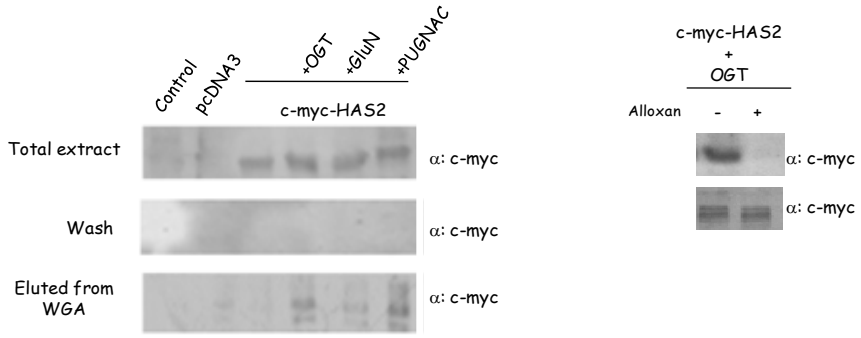

Figure 16- HAS2 is modified by O-GlcNAc in NIH3T3 cells

To confirm that HAS2 is O-GlcNacylated by cytoplasmatic OGT we transiently transfected NIH3T3 cells with plasmids coding for c-myc-HAS2 and OGT and treated them with alloxan. As shown in figure 15, HAS2 binding to WGA was markedly reduced after alloxan treatment. This experiment was performed also in hAoSMCs and confirmed the results obtained in NIH3T3 cells (data not shown). Together, these results indicate that HAS2 is subject to modification by O-GlcNAc. To identify putative O-GlcNAcylated residue, bioinformatic searches revealed the presence of a critical site in HAS2 protein at serine 221 (S221). Further, this residue is localized in the intracytoplasmatic loop that was previously shown to be important for HAS glycosyl transferase activity. For that reason, we mutated S221 to alanine (S221A) in the 6myc-HAS2 plasmid in order to prevent O-GlcNAylation and transfected the mutated construct in NIH3T3 cells with OGT. Since WGA binds O-GlcNAc residues, S221A mutants were used to determine whether HAS2 binding to WGA was mediated by O-GlcNAc. After 48h from transfections, microsomes were prepared by centrifugation, O-GlcNacylated proteins purified by binding with agarose WGA beads and HAS2 tested in the eluate by western blotting using anti C-Myc antibody. As shown in Figure 17, we found that the S221A mutation prevented HAS2 identification after WGA beads elution; this result strongly suggests that the S221 residue can be the target of OGT and that the mutation of this aminoacid drastically reduces HAS2 O-GlcNAcylation.

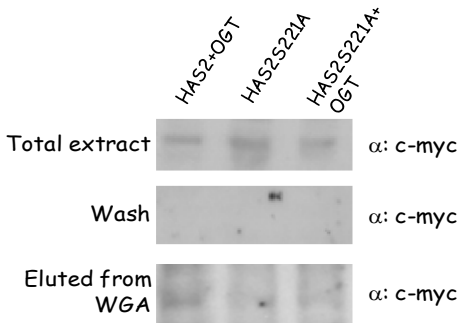

Figure 17- Identification of the critical residue involved in HAS2 O-GlcNAcylation

As the highly abundant and dynamic post-translational modification, *O*-GlcNAcylation, is implicated in several biological processes and in protein metabolism, we studied whether the HAS2 O-GlcNacylation could regulate its functionality. We quantified the HAS enzymatic activity in microsomes containing plasma membranes after NIH3T3 cells transfection and treatment as described above. As shown in Figure 18, the transfection of c-myc-HAS2 alone slightly increased HA synthetic activity, whereas the cotransfection with OGT, or the treatment with GluN or PUGNAC increased HAS2 activity. These results support the idea that HAS2 O-GlcNAcylation induces its HA synthetic capability. To confirm this point, two methods were used to determine whether HAS2 activity was mediated by O-GlcNAc. Firstly, we treated with alloxan cells cotransfected with c-myc-HAS2+OGT and we found a highly reduction of HAS activity. Secondly, *N*-acetylglucosaminidase (GlcNAcase) incubation, which removes O-GlcNAc, restored HAS activity to the control level. As a control we incubated an aliquots of sample with boiled *N*-acetylglucosaminidase; this enzyme inactivation did not affected HAS2 synthetic capability, which strongly suggests that one or more O-GlcNAcylation sites in the HAS2 enzyme can induce HAS2 activity.

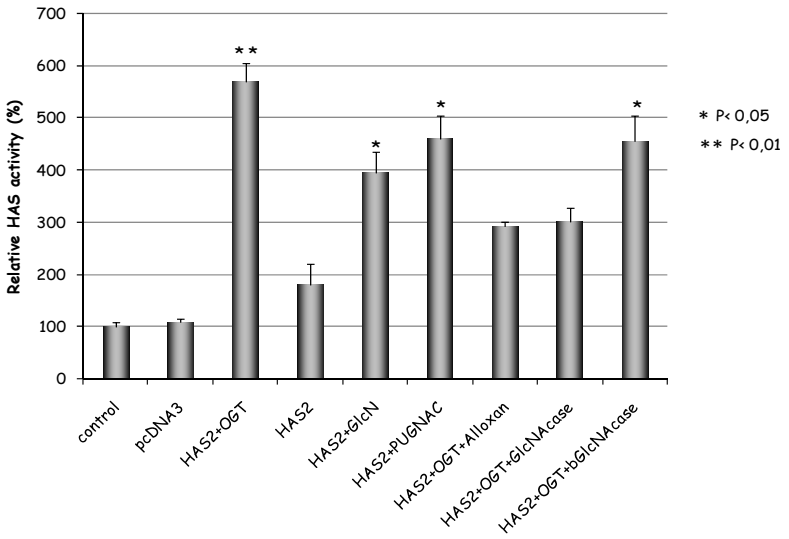

Figure 18- Relative quantification of HAS2 activity after O-GlcNAc modulation

To test the efficiency of N-acetylglucosaminidase used before, lysates were incubated with excess GlcNAcase or with boiled GlcNAcase, and then proteins were immunoblotted for CTD110.6. As shown in Figure 19A, N-acetylglucosaminidase had a high efficiency to hydrolize O-GlcNacylation. Interestingly, the activity of HAS3, the other HAS expressed in hAoSMCs, was not affected by O-GlcNacylation (Figure 19B).

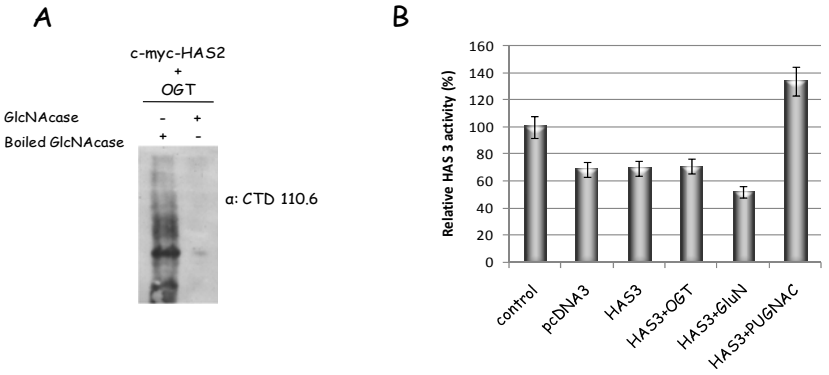

Figure 19- A:Jack bean N-acetylglucosaminidase efficiency. B: HAS3 activity assay

Our studies have shown that O-GlcNAc has a relationship with HA biosynthesis and has been implicated in modulating HAS2 synthetic activity. Since *O*-GlcNAcylation has been shown to regulate a great number of cellular functions we studied whether such HAS2 glycosylation could modify its stability. To investigate this issue, we generated a stable cell line overexpressing wild-type c-myc-HAS2 in order to eliminate the problem to have the same transfection efficiency of transient transfections. After the selection of a highly expressing clone (clone 8) by Western blotting (data not shown), we treated such clone with the protein synthesis inhibitor cycloheximide (CHX) and we visualized c-myc-HAS2 protein by Western blotting after different incubation time. In these experiments, the level of c-myc-HAS2 protein decreased rapidly and after 30 min completely disappeared (Figure 20A); showing that c-myc-HAS2 is a short-lived protein. We then turned out attention to the intracellular pathway responsible for the rapid HAS2 turnover. As recently HAS2 has been described to be an ubiquitinated protein (Karousou et al. 2010), we investigated whether 26S proteasome was involved in the degradation of c-myc-HAS2. We treated the clone 8 with CHX in the presence or absence of MG132, a specific 26S proteasome inhibitor. Cell extracts were then subjected to immunoblotting analysis using anti c-myc and tubulin antibodies to determine the presence of c-myc-HAS2. As shown in Figure 20B, a significant stabilization of the wild-type HAS2 protein was observed after 60 min of incubation with MG132 suggesting that this protein can be targeted to a 26S proteasome.

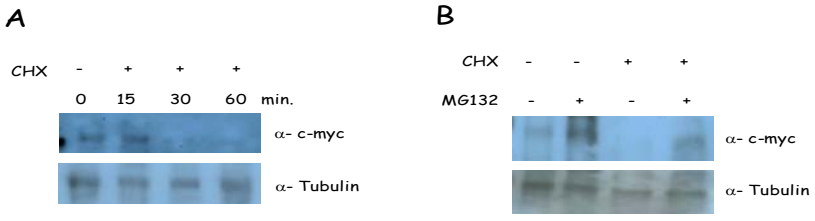

Figure 20- A: Determination of c-myc-HAS2 half-life. B: Proteasome system is involved in HAS2 degradation.

Since O-GlcNAc generally protects from protein degradation, we investigated O-GlcNAcylation ability to affect the intracellular stability of wild-type c-myc-HAS2. To study this issue, we treated stable NIH3T3 cell lines overexpressing wild-type c-myc-HAS2 with CHX+GluN, in order to induce O-GlcNAcylation, or CHX+GluN+Alloxan, to prevent O-GlcNAcylation. After different incubation times, cell extracts were immunoblotted to visualize c-myc-HAS2. As shown in Figure 21A, c-myc-HAS2 stability was greatly induced after GluN treatment allowing the detection of c-myc-HAS2 band until 3 hours after CHX addition. Such an effect was clearly dependent on the O-GlcNAcylation, since the OGT specific inhibitor, alloxan, caused HAS2 degradation (Figure 21B). This experiment provided a very strong support for a role of the O-GlcNAcylation in the control of HAS2 turnover.

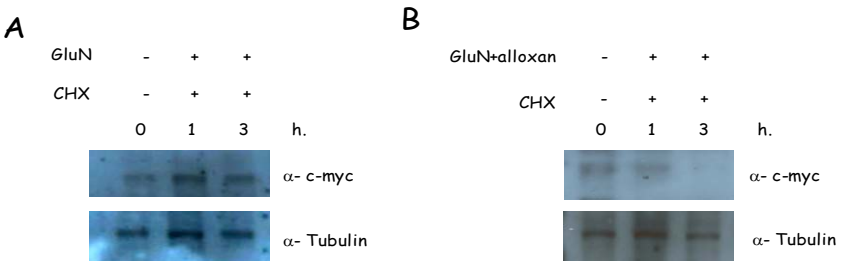

Figure 21- Determination of c-myc-HAS2 half-life after GluN (panel A) or GluN+alloxan treatments (panel B).

To further evaluate the role of protein stability on GAG metabolism, we treated hAoSMCs with CHX for 24 hours and analyzed GAG secreted into the conditioned cell medium using PAGEFS analysis. As shown in Figure 22A, HA was clearly the unique GAG susceptible to a very high turnover, since its production levels were significantly decrease by CHX treatments. This issue is confirmed by HPLC analyses that permitted us to quantify HA after CHX treatments, either in presence or absence of GluN or PUGNAC treatments (Figure 22B).

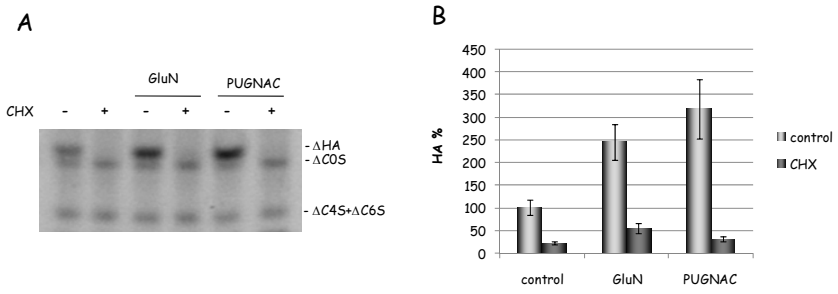

Figure 22- PAGEFS (panel A) and HPLC (panel B) analysis performed after GluN and PUGNAC treatments in hAoSMCs.

Our results showed that O-GlcNAcylation induction, which is implicated in HAS2 activation and stabilization, did not protect the HA degradation suggesting a complex mechanism of regulation that probably involved both 26S proteasome-mediate degradation and also hyaluronidases. We investigated the role of proteasomal degradation in HA biosynthesis by treatments of quiescent hAoSMCs with CHX and\or GluN for 24 hours, followed by incubation of the cells, at different times, in the presence or absence of MG132. Notably, a decrease of HA release into the culture medium was confirmed after CHX+GluN treatment (figure 23).

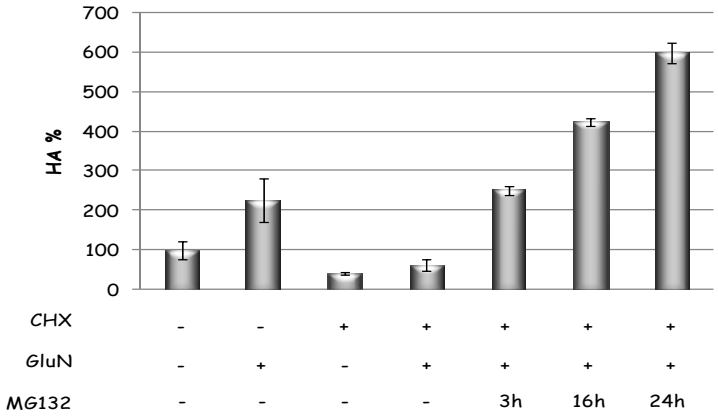

Figure 23- Determination of the role of proteasome mediate degradation in HA secretion by HPLC analysis.

Interestingly, a clear time-dependent increase of HA secretion was observed after blocking the proteasome-mediated degradation confirming that HA possessed a very rapid turnover that is completely rescue after 3 hours from the blocking of protein degradation.

3. 4 O-GlcNAc could regulate HAS 2 gene expression

O-GlcNAc modifications are tightly dependent on the concentration of UDP-GlcNAc produced by the HBP which itself depends on how much glucose enters the cell. Therefore, our results suggested that the extent of UDP-GlcNAc is essential for the synthesis of HA as well as that of other GAGs while O-GlcNAcylation seems to be critical only for HA synthesis. As the amount of protein O-GlcNAc modification is directly related to HA metabolism, we next studied the effect of this dynamic protein modification on the gene expression levels involved in HA biosynthesis. We treated quiescent hAoSMCs in order to modulate O-GlcNAcylation as previously described, and quantified the mRNA level using a quantitative RT-PCR. We studied the gene coding for the three HASs and also UGPP and UGDH, genes required for the reaction to generate UDP-glucuronic acid. Interestingly, treatments that induce O-GlcNAc or UDP-GlcNAc content did not change HAS3, UGDH and UGPP transcription level (Figure 24A and 24B); HAS1 mRNA expression was not detectable. On the contrary, as shown in Figure 24A, the HBP is a candidate for the up-regulation of HAS2 mRNA levels.

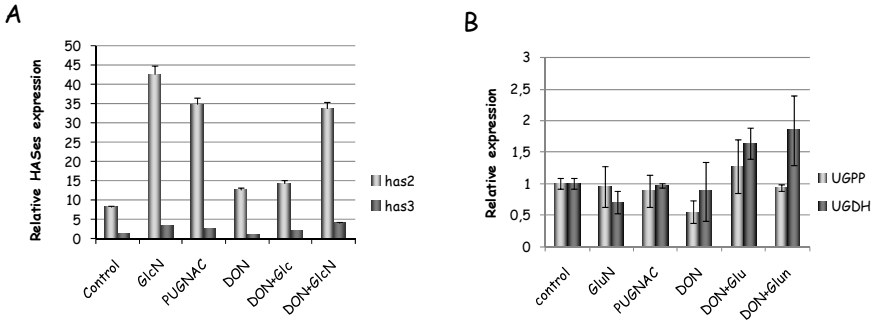

Figure 24- HASs (Panel A), UGDH and UGPP (Panel B) relative expression by quantitative RT-PCR analysis.

To confirm that the activation of the HBP results in increased expression of HAS2, we incubated hAoSMCs for 24 h with GluN and PUGNAc. As shown in Figure 25, HAS2 mRNA expression in response to GluN or PUGNAC was induced up by 5-fold and 3-fold, respectively, as compared with control cells. To confirm that the UDP-GlcNAc level and protein glycosylation mediate the up-regulation of HAS2, we used specific inhibitors of GFAT, the rate limiting enzyme of the hexosamine pathway, and direct glycosylation inhibitors that interfered with the transfer of a sugar moiety to a protein. Preincubation of hAoSMCs with DON inhibited the increase of HAS2 mRNA level. To show that the effect of GFAT inhibitors on HAS2 expression is the result of specific inhibition of the HBP and that the addition of downstream metabolites can overcome the effect of GFAT inhibitors, GluN was used to stimulate cells treated with DON. The inhibitory effect of DON on HAS2 mRNA expression was completely reversed when cells were treated with GluN. Similarly, when cells were preincubated with alloxan, that directly inhibit OGT, there was no increase in HAS2 mRNA expression. This inhibitor also down-regulated the level of HAS2 in the presence of GluN, suggesting that the O-GlcNAcylation is critical for the regulation of HAS2 transcription.

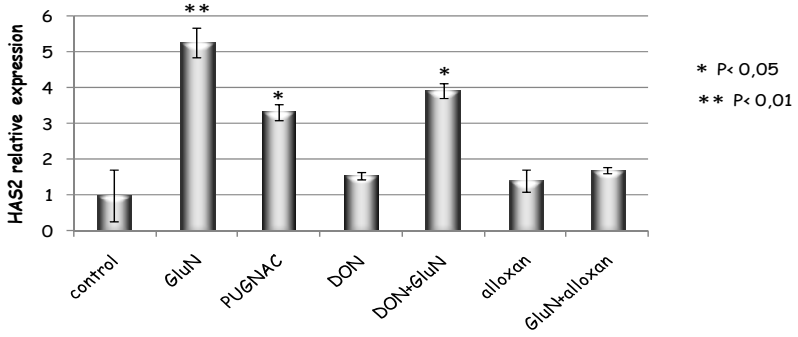

Figure 25- Effect of activation and inhibition of the HBP and protein O-GlcNAcylation on HAS2 mRNA expression in hAoSMCs.

We, therefore, proceeded with the aim to identify the molecular mechanism of up-regulation of HAS2 mRNA by GluN in hAoSMCs to confirm that the

hexosamine pathway affects this mechanism directly. Cells were incubated with or without GluN for 24h, then treated with actinomycin D (ActD) and lysed at 1h to 2h. Although HAS2 mRNA levels increased dramatically after stimulation with GluN (Figure 26), the inhibition of RNA synthesis with ActD maintained the relative amount of HAS mRNA unchanged after 1 or 2 h after the treatments. Therefore, the increment of HAS2 transcript seen after GluN addition can not be ascribed to a change in HAS2 transcript turnover rate (i.e., messenger stabilization). Our hypothesis is that HAS2 mRNA has a constant degradation rate and the increase of HAS2 transcript after GluN can be due to gene induction the involve RNA synthesis rather than messenger stabilization.

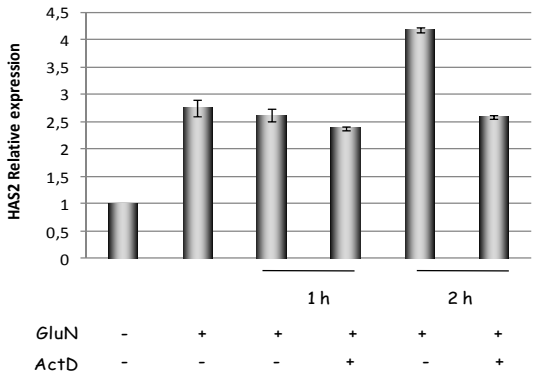

Figure 26- Effect of GluN treatment on HAS2 mRNA stability.

To determine whether the transcription of the endogenous HAS2 gene is increased in response to acute GluN stimulation we transiently transfected cultured hAoSMCs with a human HAS2 promoter-luciferase reporter gene construct and compared its activation in GluN-stimulated and control cells at different time set. We used a -2118/+43 HAS2 promoter-luciferase reporter construction and a control vector, CMV, that has high level of basal activity. After GluN stimulation, the activity of the HAS2 -2118/+43 luciferase reporter construct was not increased (Figure 27). Taken together, these results showed that GluN could not activates directly the HAS2 gene at the level of transcription.

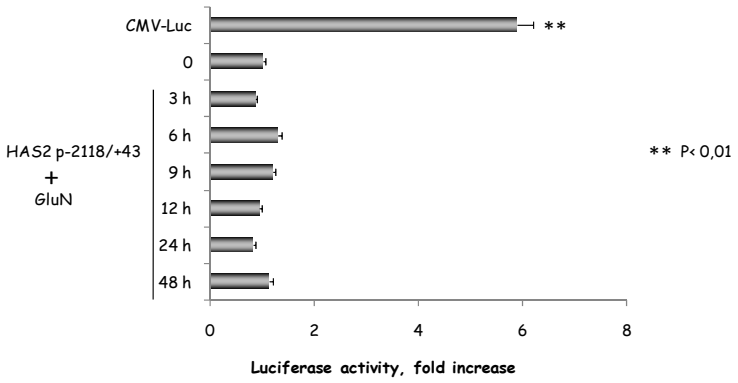

Figure 27- Effect of GluN treatment on HAS2 promoter activity.

Gene transcription in response to extracellular and intracellular stimuli depends both on the promoter structure and on the signal- and cell type–specific patterns of activation of transcriptional activators, coactivators, and suppressors. Many transcription factors are modified by O-GlcNAcylation in response to physiological stimuli, cell cycle stage, and developmental stage, and this modification can modulate their function in different ways. Since our results highlighted that HAS2 expression is induced by O-GlcNAc we wanted to investigate the role of Sp1 and YY1 in transcriptional regulation. In fact, it is known that a great number of transcription factors, such as YY1 and Sp1, which are regulated by O-GlcNAcylation, are involved in the regulation of HAS2 mRNA synthesis (Saavalainen K et al. 2007). YY1 was shown to act as a transcriptional activator or repressor depending on the context of its binding site within a particular promoter and on other cell type-specific factors. In order to investigate whether YY1 was involved in HAS2 transcription we silenced its expression using a siRNA approach. After 48 h from siRNA transfections, we assayed the gene silencing efficiency and HAS2 gene expression by quantitative RT-PCR. As shown in Figure 28B, we observed an about 80% reduction of YY1 transcripts; moreover, the YY1 expression rate was comparable in cells with or without GluN treatment. We found a non specific and not statistically significant reduction of HAS2 transcripts

respect to scrambled negative control siRNA (siSCR) after YY1 silencing, furthermore HAS2 gene expression did not subjected to siYY1 after GluN treatments suggesting that this transcription factor was not involved in HAS2 gene regulation in our cell system.

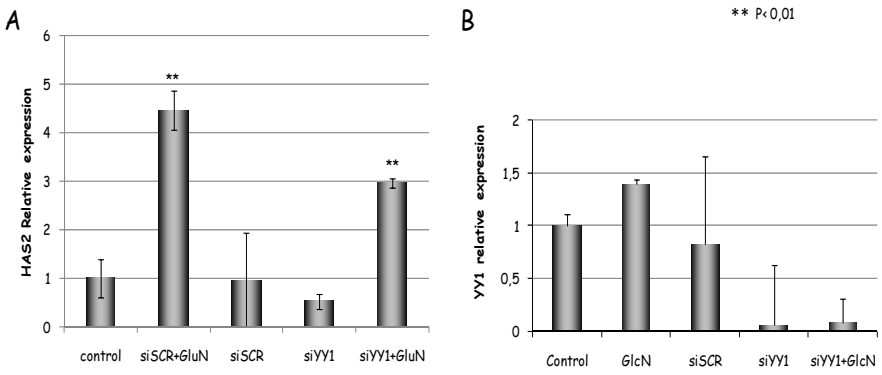

Figure 28- YY1 silencing effect on HAS2 (Panel A) and YY1 (Panel B) gene expression.

We then turned our attention to Sp1, a ubiquitously expressed zinc finger transcription factor. Beyond constitutive activation of housekeeping genes, hundreds of genes are regulated by this protein, and its activity is controlled by numerous post-translational modifications, including at least eight O-GlcNAc sites. Sp1 can be also phosphorylated and acetylated by several factors in response to different stimuli making it extensively involved in gene regulation. We thus decided to investigate its role in HAS2 trascription. Relative expression of HAS2 mRNA was evaluated by quantitative RT-PCR 48 h following siRNA transfection. Knockdown of Sp1 mRNA decreased HAS2 transcription by 80% indicating that such transcription factor is needed for the basal transcription of HAS2 gene as already reported (Monslow et al. 2006). Interestingly, reduction of HAS2 gene expression is also maintained after GluN treatment suggesting that Sp1 could induce HAS2 expression after O-GlcNAcylation (Figure 29A). The ability of siSp1 to knock down its respective mRNA was also confirmed and the result of this experiment is shown in Figure 29B.

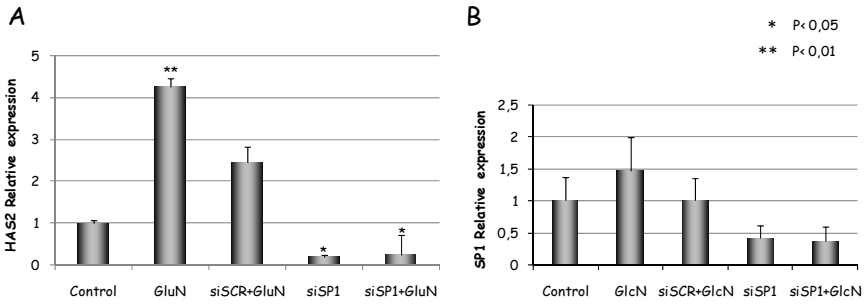

Figure 29- Sp1 silencing effect on HAS2 (Panel A) and Sp1 (Panel B) gene expression.

To support the idea that O-GlcNAcylation induces HAS2 expression via Sp1 we overexpressed this transcription factor in hAoSMC. Interestingly Sp1 overexpression did not induce HAS2 transcription in a significant fashion as GluN treatment. When Sp1 overexpression and GluN treatment were combined, the HAS2 mRNAs level increased to those observed in the control cells treated with GluN alone, even if without a statistically significant difference respect to samples without GluN (Figure 30). To confirm that protein glycosylation mediate the up-regulation of HAS2 via Sp1, we treated transfected hAoSMCs with GluN and alloxan, that block O-GlcNAcylation, and we found a highly reduction of HAS2 expression. These results could support the idea that HAS2 gene expression is regulated by Sp1 O-GlcNAcylation.

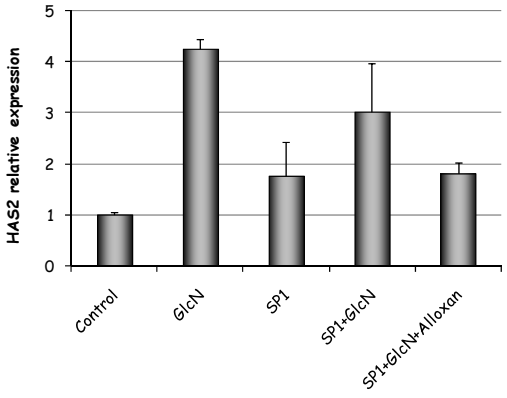

Figure 30- Sp1 overexpression effect in hAoSMCs.

O-GlcNAc modification of transcription factors is important in regulation of gene expression in various tissues. O-linked GlcNAc moieties on transcription factors may be recognized by various components of the transcriptional machinery, serve as a nuclear localization signal, antagonize the action of protein kinases by masking the potential serine and threonine sites for phosphorylation, modulate the DNA binding activity or the half-life, and increase the stability of transcription factors in the cell. To further confirm that Sp1 O-GlcNAcylation activate the transcription of HAS2 gene, we transfected hAoSMC with a -2118/+43 HAS2 promoter-luciferase reporter gene construct, that is known to contain several Sp1 binding sites, and compared its activation in GluN stimulated and control cells. After GluN stimulation, the activity of the HAS2 -2118/+43 luciferase reporter construct was not increased, confirming data obtained previously (see Figure 27). Interestingly, after cotrasfection of Sp1 with the reporter vector we observed an increase luciferase activity. Surprisingly, when we treated with GluN the cells cotransfected, as described above, we could not observed the transcriptional activation of the HAS2 promoter (Figure 31). This data demonstrated that Sp1 acts as an activator of the HAS2 gene as already reported (Monslow et al. 2006) but probably other unidentified transcription factors and coactivators form signal- and cell type–specific multiprotein complexes on the HAS2 promoter after O-GlcNAcylation.
Very recently, it has been reported that SP1 O-GlcNacylation inhibited HAS2 transcription (Jokela et al. 2011, paper in press).

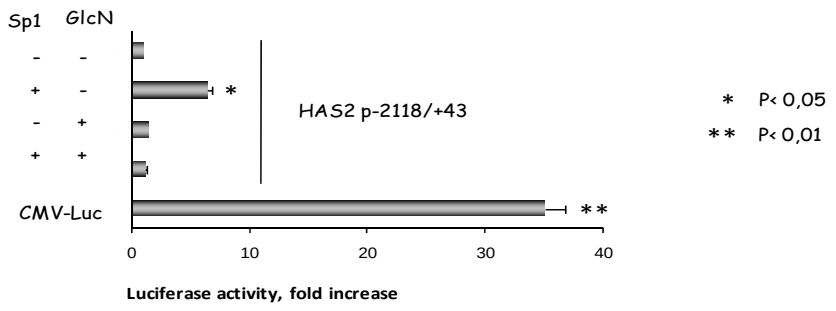

Figure 31- Effect of Sp1 expression and GluN treatment on HAS2 promoter activity.

4. Discussion

Hyperglycemia and insulin resistance are major causative factors for diabetes type 2 and its vascular complications, which are the first causes of death in the western countries. The development of vascular pathology is often coupled to dramatic alterations of the ECM, which provides critical support for vascular tissue as a scaffold for maintaining the organization of vascular cells into blood vessels, for blood vessel stabilization, morphogenesis, and for cell proliferation, migration, and survival (Davis et al. 2005). Thus, it is critical to understand how cells regulate ECM synthesis. In recent paper, it was demonstrated that HA accumulates in arteries in diabetic patient and in a porcine model for diabetes and this strongly influences atherosclerotic lesion formation (Heickendorff et al. 1994; Suzuki et al. 2001). Hyperglycemia can induce vascular complications via several different mechanisms, and one of the mechanisms is an increase of the HBP flux of glucose and O-GlcNAcylation of target protein (Karunakaran and Jeoung, 2010). Thus, the purpose of this study was to characterize, in a hAoSMCs model, how protein O-GlcNAcylation affect content of specific ECM components, in particular HA. Changes in HA production have mostly been associated with the regulation of HASs via different mechanism including the expression level of Has genes (Vigetti et al. 2009), UDP-sugar substrates availability and ubiquitination (Karousou et al. 2010). Our research and that of others have revealed the critical role of the UDP-sugar precursors in the regulation of HA synthesis. This synthesis requires ATP, UTP, and other critical metabolic molecules, including glucose, glutamine, glucosamine, and acetyl-CoA, which makes GAGs production an energy-consuming process. Our group recently demonstrated that the energy charge is critical for the regulation of HA metabolism, in fact at low ATP/AMP ratios, AMPK activity can block HA synthesis without altering the synthesis of other GAGs (Vigetti et al. 2011). Moreover, previous studies presented evidence that the cellular concentration of UDP-GlcUA and UDP-GlcNAc can become limiting in HA synthesis. Increasing the UDP-GlcUA level by overexpression of UGDH, HA production was enhanced (Vigetti et al. 2006); also HA synthesis was negatively influenced by mannose treatments through its ability to decrease the UDP-GlcNAc content (Jokela et al. 2008). HA synthesis

required UDP-GlcNAc, the end product of the HBP, which itself reflects the flux through this pathway and, therefore, could serve as a glucose sensor (Issad et al. 2008). The UDP-GlcNAc increment, induced by the nutrient availability, brings to protein O-GlcNAcylation which controls a plethora of cellular enzymes. This thesis is focused on the hypothesis that the rate of HA synthesis could be regulated by the level of HAS substrate concentration with particular attention to protein O-GlcNAcylation. Our results suggested that an elevated UDP-GlcNAc availability is critical for the biosynthesis of HA as well as that of other GAGs, while protein O-GlcNAcylation is critical only for HA metabolism. We found an augment of both HA and chondroitins by increasing the flux through the HBP with GluN treatments suggesting that the UDP-GlcNAc content may affect GAGs synthesis. This is probably due to the equilibrium between UDP-GlcNAc and UDP-N-acetylgalactosamine (UDP-GalNAc) mediated by UDP-galactose 4-epimerase resulting in UDP-GlcNAc/UDP-GalNAc ratio of 3:1 (Sweeney et al. 1993). Such results suggest that the UDP-GlcNAc induce all GAGs synthesis, in fact the nucleotide sugar transporter located on the Golgi membrane is necessary to furnish the substrates for the complex GAG synthesis systems (i.e., GAGosome). Moreover, PUGNAC treatments, that induce protein O-GlcNAcylation without any effect on UDP-GlcNAc content, seems to be critical only for HA biosynthesis without any change in the amount of the other GAGs. It is generally known that the nutrient availability induces an increment of UDP-GlcNAc concentration that brings to protein O-GlcNAcylation which controls a plethora of cellular enzymes. In fact, O-GlcNAc modifies various transcription factors and cellular proteins in a process dynamically reciprocal to phosphorylation of the same Ser and Thr residues or adjacent residues, and is important in regulating protein function (Love and Hanover, 2005; Hart et al. 2007). HASs are on plasma membrane and have large cytoplasmic loops which could be accessible to nucleo-cytoplasmic OGT. Bioinformatics searches revealed the presence of a putative O-GlcNAcylated residue in HAS2 protein at ser-221, which is localized in the intracytoplasmatic loop that was previously shown to be important for HAS glycosyl transferase activity (Weigel and DeAngelis, 2007). We were able to unequivocally detect O-GlcNAc on HAS2, which

could be significantly increased by co-expressed OGT, purifying O-GlcNAcylated proteins by agarose WGA beads bindings. Interestingly, mutation of ser-221 drastically reduces HAS2 O-GlcNAcylation. Interestingly, the Thr-110, that our group previously demonstrated to be phosphorylated by AMPK (Vigetti et al. 2010) could not be also glycosylated by O-GlcNAc. Furthermore, O-GlcNAcylation led to activation of the enzymatic activity of HAS2; although HASs share a high degree of amino acidic identity the O-GlcNAc effect seems to be specific only on HAS2. Such results suggest that HAS proteins, and HAS2 in particular, could have different regulatory mechanisms with several possibilities for post-translational modifications capable of modulating enzymatic activity. Since *O*-GlcNAcylation has been shown to regulate a great number of cellular functions including protein degradation (Zhang et al. 2003), we studied whether such HAS2 glycosylation could modify its stability. Our findings clearly indicate that c-myc-HAS2 has a very rapid turnover due to proteasomal activity and O-GlcNAcylation prevents its degradation as previously described for other proteins as SP1 (Zachara and Hart, 2004). Interestingly, at cellular level, the blocking of protein synthesis dramatically reduced only secreted HA maintaining unchanged the level of other GAGs indicating a complex mechanism of regulation that probably involved both 26S proteasome-mediate degradation as MG132 induced a rapid secretion of HA (Figure 32).

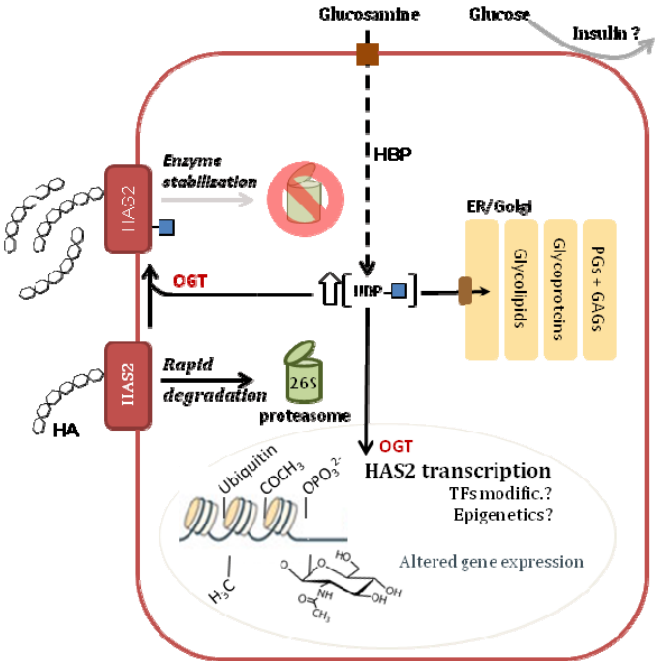

Figure 32- High UDP-GlcNAc mediate 26S proteasome degradation of HAS2.

We also confirmed the existence of correlation between HA biosynthesis due to protein O-GlcNAcylation analyzing its amount in pericellular coat. Interestingly, high glucose concentration did not affect O-GlcNAcylation level suggesting that hAoSMCs used in the experiments were insulin-dependent for glucose uptake as previously described (Chisalita et al. 2009). Actually, whether insulin, at physiological concentrations, has direct effects on SMCs remains controversial. Since the HA pericellular coat has been suggested to be involved as the cellular microenvironment in a variety of important biological and pathological events, its formation is probably strictly controlled (Toole, 2004). In fact, HA is increased in amount in atherosclerotic and restenotic lesions (Riessen et al. 1996) and has been implicated in tissue macrophage recruitment in other inflammatory diseases (De La Motte et al. 1999). Moreover, in the media and neointima, HA exert a proatherosclerotic effect (Vigetti et al. 2009); thus, HA could

mediate increased plaque inflammation. Consistent with this hypothesis, we found a crucial role of O-GlcNacylation favoring immune cells adhesion and SMC migration via HA. Therefore, hyaluronidase and 4-MU treatments of hAoSMCs after GluN treatment inhibited U937 binding and cells migration, respectively, underlining the crucial role of HA, and not to other GAGs, in SMCs behavior. From a functional point of view, it has been shown that GlcN ameliorates parameters of several diseases including adjuvant and rheumatoid arthritis and cardiac allograft survival. In cardiovascular system an increased of protein O-GlcNAcylation inhibits inflammatory and neointimal responses to acute endoluminal arterial injury suggesting a vasoprotective role of this post-translational modification in vivo (Xing et al. 2008). Our results seem to show a different role of O-GlcNacylation favoring immune cells adhesion and SMC migration and, therefore, highlighted simultaneous negative (i.e., increase insulin resistance, impair Ca2+ signaling, and increase angiotensin 2 synthesis) and positive (i.e., increase cardioprotection post trauma, and decrease ER and oxidative stresses) effects of O-GlcNacylation on cardiovascular system as already reported (Marsh et al. 2011; Laczy et al. 2009).

As the amount of protein O-GlcNAc modification is directly related to HA metabolism, we next studied the effect of this dynamic protein modification on the gene expression levels involved in HA biosynthesis. In fact, numerous transcription factors are O-GlcNAc modified, and the transcription of multiple genes is up- and downregulated when extracellular glucose/glucosamine concentrations are changed (Butkinaree et al. 2010). Quantitative RT-PCR study permitted to demonstrate that O-GlcNacylation and not a UDP-GlcNac increase up-regulated HAS2 mRNA levels. Moreover, these data demonstrated that the increased expression of HAS2 mRNA is not due to an increase in mRNA stability and suggested that RNA synthesis is involved in this mechanism of up-regulation. Interestingly, treatments that induce O-GlcNAcylation or UDP-GlcNAc content did not change the transcription level of HAS3, UGDH and UGPP, genes required for the reaction to generate UDP-glucuronic acid. Previous study, demonstrated that UDP-GlcUA content was able to regulate both HAS2 and HAS3 mRNA level (Vigetti et al. 2006), suggesting a different

mechanism that control HASs expression in response to the two substrates. On the other hand, GluN treatments could not modify the activation of the HAS2 promoter directly. It has been recently found that intracellular glucose metabolism, through UDP-GlcNAc content, inhibits HAS2 transcription through the transcription factors YY1 and Sp1 in keratinocytes (Tammi et al. 2011). The regulation of the HAS2 promoter by YY1 and Sp1 in hAoSMCs appears to be different; in fact, checking the GluN-induced changes in HAS2 expression we found a non specific and not statistically significant reduction of HAS2 transcript after YY1 silencing, suggesting that this transcription factor was not involved in HAS2 gene regulation. Surprisingly, it can be assumed that Sp1 contributes both to the basal mRNA expression of the HAS2 gene as well as to its super-induction after GluN treatment, although these data are not statistically significant; probably other unidentified transcription factors and coactivators form signal- and cell type–specific multiprotein complexes on the HAS2 promoter after O-GlcNAcylation. Recently it has been reported that histones can be O-GlcNacylated proteins, therefore the pathway that regulates HAS2 transcription could involve a more complex epigenetic mechanism (Slawson and Hart, 2011).

In conclusion, our results demonstrated that the availability of UDP-sugar substrates can modulate GAGs production and that protein O-GlcNAcylation influence only HA synthesis. We provided evidence that the HAS2 Ser-221 is O-GlcNacylated; this protein modification is correlated with HAS2 activity and stability. Moreover, we found that HAS2 has a very rapid turnover due to proteosomal activity and O-GlcNAcylation prevents its degradation. We also demonstrated that increasing UDP-GlcNAc in hAoSMC enhanced HAS2 gene expression; in this mechanism of up-regulation is not involved the mRNA stability. These results support the hypothesis that the synthesis of HA is tightly controlled both at substrate and gene expression levels.

5. Reference

Akimoto Y, Kreppel LK, Hirano H, Hart GW. (2001) Hyperglycemia and the O-GlcNAc transferase in rat aortic smooth muscle cells; elevated expression and altered patterns of O-GlcNAcylation. *Arch Biochem Biophys* 389: 166-75.

Badi I, Cinquetti R, Frascoli M, Parolini C, Chiesa G, Taramelli R, Acquati F. (2009) Intracellular ANKRD1 protein levels are regulated by 26S proteasome-mediate degradation. *FEBS Letters* 583, 2486-2492

Bouché C, Serdy S, Kanh CR, Goldfine AB. (2004) The cellular fate of glucose and its relevance in type 2 diabetes. *Endocr Review* 25, 807-830

Butkinaree C, Park K, Hart GW. (2010) O-linked β-N-acetylglucosamine (O-GlcNAc): Extensive crosstalk with phosphorylation to regulate signaling and transcription in response to nutrients and stress. *Biochim Biophys Acta* 1800(2): 96-106

Chisalita SI, Johansson GS, Liefvendahl E, Back K, Arnqvist HJ.. (2009) Human aortic smooth muscle cells are insulin resistant at the receptor level but sensitive to IGF1 and IGF2. *J Mol Endocrinol* 43: 231–239.

De La Motte CA, Hascall VC, Calabro A, Yen-Lieberman B, Strong SA (1999) Mononuclear leukocytes preferentially bind via CD44 to hyaluronan on human intestinal mucosal smooth muscle cells after virus infection or treatment with poly(I.C). *J Biol Chem* 274: 30747–30755

Davis GE, Senger DR. (2005) Endothelial extracellular matrix: biosynthesis, remodeling, and functions during vascular morphogenesis and neovessel stabilization. *Circ. Res.* 97:1093–1107.

Fulop N, Marchase RB, and Chatham JC. (2007) Role of protein O-linked N-acetyl-glucosamine in mediating cell function and survival in the cardiovascular system. *Cardiovasc Res* 73: 288-297.

Gao Y, Wells L, Comer FI, Parker GJ, Hart GW. (2001) Dynamic O-glycosylation of nuclear and cytosolic proteins: cloning and characterization of a neutral, cytosolic beta-N-acetylglucosaminidase from human brain. *J Biol Chem* 276: 9838–9845.

Gao Y, Miyazaki J, Hart GW. (2003) The transcription factor PDX-1 is post-translationally modified by O-linked N-acetylglucosamine and this modification is correlated with its DNA binding activity and insulin secretion in min6 beta-cells. Arch. Biochem. Biophys. 415: 155 – 163.

Goldberg HJ, Whiteside CI, Hart GW, Fantus IG. (2005) Posttranslational, reversible O-glycosylation is stimulated by high glucose and mediates plasminogen activator inhibitor-1 (PAI-1) gene expression and Sp1 transcriptional activity in glomerular mesangial cells. *Endocrinology* 147(1): 222 – 231.

Guinez C, Mir AM, Dehennaut V, Cacan R, Harduin-Lepers A, Michalski JC, Lefebvre T. (2008) Protein ubiquitination is modulated by O-GlcNAc glycosylation. *Faseb J* 22: 2901–2911.

Hall JL, Chatham JC, Eldar-Finkelman H, Gibbons GH. (2001) Upregulation of glucose metabolism during intimal lesion formation is coupled to the inhibition of vascular smooth muscle cell apoptosis: role of GSK3beta. *Diabetes* 50:1171-9.

Haltiwanger RS, Grove K, Philipsberg GA. (1998) Modulation of O-linked N-acetylglucosamine levels on nuclear and cytoplasmic proteins in vivo using the peptide O-GlcNAc-beta-N-acetylglucosaminidase inhibitor O- (2-acetamido-2-deoxy-D-

glucopyranosylidene)amino-Nphenylcarbamate. *J Biol Chem* 273: 3611–3617.

Han I, Kudlow JE. (1997) Reduced O glycosylation of Sp1 is associated with increased proteasome susceptibility, *Mol Cell Biol* 17: 2550–2558.

Hanover JA, Lai Z, Lee G, Lubas WA, Sato SM (1999) Elevated O-linked N-acetylglucosamine metabolism in pancreatic beta-cells. *Arch Biochem Biophys* 362:38-45

Hart GW, Housley MP, Slawson C (2007) Cycling of O-linked beta-N-acetylglucosamine on nucleocytoplasmic proteins. *Nature* 446:1017–1022

Heickendorff L, Ledet T, Rasmussen LM (1994) Glycosaminoglycans in the human aorta in diabetes mellitus: a study of tunica media from areas with and without atherosclerotic plaque. *Diabetologia* 37: 286–292.

Issad T, Kuo M (2008) O-GlcNAc modification of transcription factors, glucose sensing and glucotoxicity. *Cell* 19(10): 380-389.

Itano N and Kimata K (1996) Molecular cloning of Human hyaluronan synthase. *J Biol Chem* 271, 9875-9878

Itano N (2008) Simple primary structure, complex turnover regulation and multiple roles of hyaluronan. *J Biol Chem* 144, 131-137

Jarvelainen H, Sainio A, Koulu M, Wight TN, Penttinen R. (2009) Extracellular matrix molecules: potential targets in pharmacotherapy. *Pharmacol. Rev.* 61, 198-223.

Jokela TA, Jauhiainen M, Auriola S, Kauhanen M, Tiihonen R, Tammi MI, Tammi RH. (2008) Mannose inhibits hyaluronan synthesis by down regulation of the cellular pool of UDP-N-acetylhexosamines. *J Biol Chem* 283: 7666-7673.

Jokela TA, Makkonen KM, Oikari S, Kärnä R, Koli E, Hart GW, **Tammi RH, Carlberg C, Tammi MI.** (2011) Cellular content of UDP-N-acetylhexosamines controls hyaluronan synthase 2 expression and correlates with O-GlcNAc modification of transcription factors YY1 and SP1. *J Biol Chem* Paper in press

Karousou E, Militsopoulou M, Porta G, De Luca G, Hascall VC, Passi A. (2004) Polyacrylamide gel electrophoresis of fluorophore-labeled hyaluronan and chondroitin sulfate disaccharides: application to the analysis in cells and tissues. *Electrophoresis* 25:2919-2925.

Karousou E, Kamiryo M, Skandalis SS, Ruusala A, Asteriou T, Passi A, Yamashita H, Hellman U, Heldin C, Heldin P. (2010) The activity of Hyaluronan Synthase 2 Is regulated by dimerization and ubiquitination. *J Biol Chem* 285(31): 23647–23654

Karunakaran U, Jeoung NH. (2010) O-GlcNAc Modification: Friend or Foe in Diabetic Cardiovascular Disease. *Korean Diabetes J* 34: 211-219.

Knudson W, Knudson CB. (1991) Assembly of a chondrocyte-like pericellular matrix on non-chondrogenic cells. Role of the cell surface hyaluronan receptors in the assembly of a pericellular matrix. *J Cell Sci* 99(2):227–235.

Kreppel LK, Hart GW. (1999). Regulation of a cytosolic and nuclear O-GlcNAc transferase. Role of the tetratricopeptide repeats. *J Biol Chem* 274(45):32015-32022.

Kuo M, Zilberfarb V, Gangneux N, Christeff N, Issad T (2008). O-GlcNAc modification of FoxO1 increases its transcriptional activity: A role in the glucotoxicity phenomenon? *Biochimie* 90:679-685.

Laczy B, Hill BG, Wang K, Paterson AJ, White CR, Xing D, Chen YF, Darley-Usmar V, Oparil S, Chatham JC. (2009) Protein O-GlcNAcylation: a new signaling paradigm for the cardiovascular system. *Am J Physiol Heart Circ Physiol.* 296(1): 13-28

Lamarre-Vincent N and Hsieh-Wilson LC. (2003) Dynamic glycosylation of the transcription factor CREB: a potential role in gene regulation. *J Am Chem Soc* 125: 6612 – 6613.

Levesque H, Girard N, Maingonnat C, Delpech A, Chauzy C, Tayot J, Courtois H (1994) Localization and solubilization of hyaluronan and of the hyaluronan-binding protein hyaluronectin in human normal and arteriosclerotic arterial walls. *Atherosclerosis* 105:51–62

Love DC, Hanover JA (2005) The hexosamine signaling pathway: deciphering the 'O-GlcNAc code'. *Sci STKE* 2005:re13

Lubas WA, Hanover JA. (2000). Functional expression of O-linked GlcNAc transferase. Domain structure and substrate specificity. *J Biol Chem* 275: 10983-10988.

Macauley MS, Whitworth GE, Debowski AW, Chin D, Vocadlo DJ. (2005) OGlcNAcase uses substrate-assisted catalysis: kinetic analysis and development of highly selective mechanism-inspired inhibitors. *J Biol Chem* 280: 25313–25322.

Marsh SA, Dell'italia LJ, Chatham JC. (2011) Activation of the hexosamine biosynthesis pathway and protein *O*-GlcNAcylation

modulate hypertrophic and cell signaling pathways in cardiomyocytes from diabetic mice. *Amino Acids* 40 (3):819-828.

Marshall S, Bacote V, Traxinger RR. (1991) Discovery of a metabolic pathway mediating glucose-induced desensitization of the glucose transport system. Role of Hexosamine biosynthesis in the induction of insulin resistance. *J Biol Chem* 266:4706-12.

Masson E, Lagarde M, Wiernsperger N and El Bawab S. (2006) Hyperglycemia and Glucosamine-induced Mesangial Cell Cycle Arrest and Hypertrophy: Common or Independent Mechanisms? *Life* 58(7): 381-387

Monslow J, Williams JD, Fraser DJ, Michael DR, Foka P, Kift-Morgan AP, Luo DD, Fielding CA, Craig KJ, Topley N, Jones SA, Ramji DP, Bowen T. (2006) Sp1 and Sp3 Mediate Constitutive Transcription of the Human Hyaluronan Synthase 2 Gene. *J Biol Chem* 281(26): 18043–18050.

Nerlich AG, Sauer U, Kolm-Lilly V, Wagner E, Koch M, Schleicher ED. (1998) Expression of glutamine: fructose 6-phosphate amidotransferase in human tissues; evidence for high variability and distinct regulation in diabetes. *Diabetes* 47:170-8.

Nemeth AH, Nolte D, Dunne E, Niemann S, Kostrzewa M, Peters U, Fraser E, Bochukova E, Butler R, Brown J, Cox RD, Levy ER, Ropers HH, Monaco AP, Muller U. (1999) Refined linkage disequilibrium and physical mapping of the gene locus for X-linked dystonia-parkinsonism (DYT3). *Genomics* 60: 320-329.

Park SY, Ryu J, Lee W. (2005) O-GlcNAc modification on IRS-1 and Akt2 by PUGNAc inhibits their phosphorylation and induces insulin resistance in rat primary adipocytes. *Exp Mol Med* 37:220–229.

Rajapakse AG, Ming XF, Carvas JM, Yang Z. (2009) The hexosamine biosynthesis inhibitor azaserine prevents endothelial inflammation and dysfunction under hyperglycemic condition through antioxidant effects. *Am J Physiol Heart Circ Physiol* 296: H815-22.

Riessen R, Wight TN, Pastore C, Henley C, Isner JM (1996). Distribution of hyaluronan during extracellular matrix remodeling in human restenotic arteries and balloon-injured rat carotid arteries. *Circulation* 93: 1141–1147.

Saavalainen K, Tammi M, Bowen T, Schmitz ML, Carlberg C. (2007) Integration of the activation of the human Hyaluronan Synthase 2 gene promoter by common cofactors of the transcription factors retinoic acid receptor and nuclear factor KB. *J Biol Chem* 282(15):11530–11539.

Schaefer L and Schaefer RM. (2010) Proteoglycans: from structural compounds to signaling molecules. *Cell Tissue Res.* 339, 237-246.

Schalkwijk CG and Stehouwer CD. (2005) Vascular complications in diabetes mellitus: the role of endothelial dysfunction. *Clin Sci* 109:143-159.

Schultz J, Pils B. (2002) Prediction of structure and functional residues for O-GlcNAcase, a divergent homologue of acetyltransferases. *FEBS Lett* 529:179–82.

Shrikhande GV, Scali ST, da Silva CG, Damrauer SM, Csizmadia E, et al. (2010) O-Glycosylation Regulates Ubiquitination and

Degradation of the Anti-Inflammatory Protein A20 to Accelerate Atherosclerosis in Diabetic ApoE-Null Mice. *PLoS ONE* 5(12): e14240.

Slevin M, Kumar S, Gaffney J. (2002) Angiogenic oligosaccharides of hyaluronan induce multiple signaling pathways affecting vascular endothelial cell mitogenic and wound healing responses. *J Biol Chem* 277: 41046–41059.

Slawson C, Hart GW. (2011) O-GlcNAc signalling: implications for cancer cell biology. *Nat Rev Cancer* 11(9): 678-84.

Stern R. (2004) Hyaluronan catabolism: a new metabolic pathway. *European Journal of cell biology* 83:317-325.

Suzuki LA, Poot M, Gerrity RG, Bornfeldt KE (2001) Diabetes accelerates smooth muscle accumulation in lesions of atherosclerosis: lack of direct growth-promoting effects of high glucose levels. *Diabetes* 50: 851–860.

Sweeney C, Mackintosh D, Mason RM. (1993) UDP-sugar metabolism in Swarm rat chondrosarcoma chondrocytes. *Biochem. J.* 290, 563–570.

Tammi RH, Passi A, Rilla K, Karousou E, Vigetti D, Makkonen K, Tammi MI. (2011) Transcriptional and post-translational regulation of hyaluronan synthesis. *FEBS Journal* 278: 1419–1428

Toleman C, Paterson AJ, Whisenhunt TR, Kudlow JE. (2004) Characterization of the histone acetyltransferase (HAT) domain of a bifunctional protein with activable O-GlcNAcase and HAT activities. *J Biol Chem* 279:53665–73.

Toole BP. (2004) Hyaluronan: from extracellular glue to pericellular cue. *Nat Rev Cancer* 4: 528–539.

Yang WH, Kim JE, Nam HW, Ju JW, Kim HS, Kim YS, Cho JW. (2006) Modification of p53 with *O*-linked *N*-acetylglucosamine regulates p53 activity and stability. *Nature Cell Biol.* 8: 1074–1083.

Vigetti D, Clerici M, Deleonibus S, Karousou E, Viola M, Moretto P, Heldin P, Hascall VC, De Luca G, Passi A. (2011) Hyluronan synthesis is inhibited by adenosine monophosphate-activated protein kinase through the regulation of HAS2 activity in human aortic smooth muscle cells. *J Biol Chem* 286(10):7917-24.

Vigetti D, Ori M, Viola M, Genasetti A, Karousou E, Rizzi M, Pallotti F, Nardi I, Hascall VC, De Luca G, Passi A. (2006) Molecular cloning and characterization of UDP-glucose dehydrogenase from the amphibian xenopus laevis and its involvement in hyluronan synthesis. *J Biol Chem* 281(12):8254-63.

Vigetti D, Rizzi M, Viola M, Karousou E, Genasetti A, Clerici M, Bartolini B, Hascall VC, De Luca G, Passi A. (2009) The effects of 4-methylumbelliferone on hyaluronan synthesis, MMP2 activity, proliferation, and motility of human aortic smooth muscle cells. *Glycobiology* 537(19):537-546.

Vosseller K, Wells L, Lane MD, Hart GW. (2002) Elevated nucleocytoplasmic glycosylation by O-GlcNAc results in insulin resistance associated with defects in Akt activation in 3T3-L1 adipocytes. *PNAS USA* 99:5313–8.

Wang A, Hascall VC (2004) Hyaluronan structures synthesized by rat mesangial cells in response to hyperglycemia induce monocyte adhesion. *J Biol Chem* 279:10279–10285.

Weigel, PH, DeAngelis PL. (2007) *J. Biol.Chem.* 282, 36777–36781.

Wells L, Gao Y, Mahoney JA, Vosseller K, Chen C, Rosen A, Hart GW. (2002) Dynamic O-glycosylation of nuclear and cytosolic proteins— further characterization of the nucleocytoplasmic beta-N-acetylglucosaminidase. *J Biol Chem.* 277: 1755-1761.

Werstuck GH, Khan MI, Femia G, Kim AJ, Tedesco V, Trigatti B, Shi Y. (2006) Glucosamine-induced endoplasmic reticulum dysfunction is associated with accelerated atherosclerosis in a hyperglycemic mouse model. *Diabetes* 55:93-101.

Xing D, Feng W, Not LG, Miller AP, Zhang Y, Chen YF, Majid-Hassan E, Chatham JC, Oparil S. (2008) Increased protein O-GlcNAc modification inhibits inflammatory and neointimal responses to acute endoluminal arterial injury. Am J Physiol Heart Circ Physiol 295(1): 335-342.

Yang X, Zhang F, Kudlow JE. (2002) Recruitment of O-GlcNAc transferase to promoters by corepressor mSin3A: coupling protein O-GlcNAcylation to transcriptional repression. *Cell* 110: 69-80

Yang X, Su K, Roos MD, Chang Q, Paterson AJ, Kudlow JE. (2001) O-linkage of N-acetylglucosamine to Sp1 activation domain inhibits its transcriptional capability. *PNAS USA* 98:6611 – 6616.

Yang X, Ongusaha PP, Miles PD, Havstad JC, Zhang F, So WV. (2008) Phosphoinositide signalling links O-GlcNAc transferase to insulin resistance. *Nature* 451: 964–9.

Zachara NE, Hart GW. (2002) The emerging significance of O-GlcNAc in cellular regulation. *Chem Rev* 102: 431-438.

Zachara NE, Hart GW (2004) O-GlcNAc modification: a nutritional sensor that modulates proteasome function. *Trends Cell Biol* 14: 218–221.

Zhang F, Su K, Yang X, Bowe DB, Paterson AJ, Kudlow JE. (2003) O-GlcNAc Modification Is an Endogenous Inhibitor of the Proteasome. 115 (12): 715-725.

6. Acknowledgements

Acknowledgements

Few true words
To sincerely thank all the people
Who really helped me in these last years.

I wish to express my deep and sincere gratitude to ALL the lab member for their important support in these last months, which were so difficult for me. Your understanding, encouraging and personal guidance gave me the courage to face the complexities of life and complete successfully the best result of my life, Mattia!

Prof. De Luca,
Thank you to for giving me the possibility to came back to the "glycosaminoglycans world"

Prof. Passi,
My sincere thanks goes to you for recruiting me in your laboratory, for your encouragement, insightful comments and personal guidance during my PhD study.

Dondo,
I would like to express all my gratitude to you. Without you, this long work wouldn't have been possible! Your intuition of science is so impressive and discussing complicated question with you is always so easy and exciting. I'm really honored to work with you because you are not only my supervisor but above all my model for being a good researcher and in the same time a special person.

Paola,
Really thank you for being always present. Not only for lending me a hand in the lab but mainly for listening to me, for supporting me and for standing me…

I warmly thank Manuela, Jenny and all those who have helped me with my work. Thank you for your valuable advice and friendly help!

I owe my lovely thanks to my family and Paolo, for your love and for all the things that you always unconditionally do for me.

Sara

7. Publications

Supplemental Material can be found at:
http://www.jbc.org/content/suppl/2011/07/18/M111.268312.DC1.html

THE JOURNAL OF BIOLOGICAL CHEMISTRY VOL. 286, NO. 40, pp. 34487–34498, OCTOBER 7, 2011

Glycosaminoglycans and Glucose Prevent Apoptosis in 4-Methylumbelliferone-treated Human Aortic Smooth Muscle Cells*

Received for publication, June 6, 2011, and in revised form, July 5, 2011 Published, JBC Papers in Press, July 18, 2011, DOI 10.1074/jbc.M111.268312

Davide Vigetti[‡1], Manuela Rizzi[‡1], Paola Moretto[‡], Sara Deleonibus[‡], Jonathan M. Dreyfuss[§], Evgenia Karousou[‡], Manuela Viola[‡], Moira Clerici[‡], Vincent C. Hascall[¶], Marco F. Ramoni[§**], Giancarlo De Luca[‡], and Alberto Passi[‡2]

From the [‡]Dipartimento di Scienze Biomediche Sperimentali e Cliniche, Università degli Studi dell'Insubria, via J. H. Dunant 5, 21100 Varese, Italy, the [§]Harvard-Partners Center for Genetics and Genomics, Harvard Medical School, Boston, Massachusetts 02115, and the [¶]Biomedical Engineering ND20, The Cleveland Clinic, Cleveland, Ohio 44195

Smooth muscle cells (SMCs) have a pivotal role in cardiovascular diseases and are responsible for hyaluronan (HA) deposition in thickening vessel walls. HA regulates SMC proliferation, migration, and inflammation, which accelerates neointima formation. We used the HA synthesis inhibitor 4-methylumbelliferone (4-MU) to reduce HA production in human aortic SMCs and found a significant increase of apoptotic cells. Interestingly, the exogenous addition of HA together with 4-MU reduced apoptosis. A similar anti-apoptotic effect was observed also by adding other glycosaminoglycans and glucose to 4-MU-treated cells. Furthermore, the anti-apoptotic effect of HA was mediated by Toll-like receptor 4, CD44, and PI3K but not by ERK1/2.

Hyaluronan (HA)[3] is one of the most abundant glycosaminoglycans (GAGs) in extracellular matrices (ECMs) and is composed of linear, unsulfated repetitions of D-glucuronic acid and *N*-acetylglucosamine. In mammals, two specific HA synthases (HAS1 and -2) produce high molecular weight HA (HMW-HA), in the range of millions of Da, whereas the other isoenzyme (HAS3) synthesizes HA of lower molecular mass, in the range of several thousands of Da (1). The size of HA depends also on specific degrading enzymes (*i.e.* hyaluronidases) that can produce bioactive HA oligosaccharides. Therefore, *in vivo*, HA chains can greatly vary in lengths and can differently regulate cell behavior through interactions with several receptors, including CD44, RHAMM (receptor for HA-mediated motility), lymphatic vessel endothelial receptor 1 (Lyve-1), HA receptor for endocytosis (HARE), and Toll-like Receptor 4 (TLR4) (2).

In cardiovascular pathologies, HA accumulates during neointima formation and alters smooth muscle cell (SMC) behavior (3). In some pathological conditions, contractile SMCs dedifferentiate to form a synthetic phenotype characterized by a high production of ECM components, including HA and versican, by synthesis of ECM-modifying metalloproteinases (4) and by increased rates of proliferation and migration. Therefore, SMCs acquire the capability to invade the vascular tunica intima, thereby contributing to vessel wall thickening. HMW-HA is involved in the modulation of SMC migration and proliferation through interaction with CD44 (5–7), which can mediate a signaling cascade inside the cell that activates different pathways, including PI3K, AKT, and ERK1/2 (8).

We demonstrated previously that human aortic SMC (AoSMC) migration is strictly dependent on HA-CD44 signaling and recently reported that the HA synthesis inhibitor 4-methylumbelliferone (4-MU) reduced proatherosclerotic properties of AoSMCs by decreasing cell migration and proliferation and by inhibiting monocyte binding to the HA-rich ECM that contributes to inflammation (9, 10). Moreover, we found that the simultaneous addition of HMW-HA to 4-MU-treated AoSMCs restored cell proliferation to the levels of controls. Therefore, the aim of this study was to investigate at the molecular level the effects of HMW-HA after 4-MU treatment of AoSMCs and the pathways involved in its effect on the cells.

EXPERIMENTAL PROCEDURES

Cell Culture and Treatments—Human AoSMCs were purchased from Lonza and were grown for 2–6 passages in complete SmGm2 culture medium (Lonza) supplemented with 5% FBS. As we reported previously (9), a final concentration of 1 mM 4-MU (Sigma) in dimethyl sulfoxide (final concentration of 0.1%) inhibited HA synthesis −40% and reduced cell viability −25%. In some experiments, AoSMCs were grown in the presence of 25 μg/ml HMW-HA (~4 × 10[6] Da) (Healon, Abbott Medical Optics), 25 μg/ml chondroitin 4-sulfate (Seikagaku), 25 μg/ml chondroitin 6-sulfate (C6S, Seikagaku), 25 μg/ml der-

* This work was supported by the "Centro Grandi Attrezzature per la Ricerca Biomedica" Università degli Studi dell'Insubria and the PhD School in Biological and Medical Sciences Fellowships (to M. R., M. C., and S. D.). This work was also supported by grants from the University of Insubria (FAR) (to D. V., A. P., and G. D. L.), Centro Interuniversitario di Biotecnologie (to A. P.), Fondazione Comunitaria del Varesotto-ONLUS (to D. V.), and a young researcher award from Centro Insubre di Biotecnologie per la Salute Umana (to D. V.).

† This paper is dedicated to the memory of our wonderful friend Professor Marco Ramoni, who suddenly passed away on June 8, 2010.

[S] The on-line version of this article (available at http://www.jbc.org) contains supplemental Tables 1 and 2 and Figs. 1–5.

[1] Both authors contributed equally to this work.

[2] To whom correspondence should be addressed: Dipartimento di Scienze Biomediche Sperimentali e Cliniche, Università degli Studi dell'Insubria, via J. H. Dunant 5, 21100 Varese, Italy. Tel.: 39-0332-397142; Fax: 39-0332-397117; E-mail: alberto.passi@uninsubria.it.

[3] The abbreviations used are: HA, hyaluronan; GAG, glycosaminoglycan; HAS, HA synthase(s); HMW-HA, high molecular weight HA; AoSMC, aortic smooth muscle cell; 4-MU, 4-methylumbelliferone; ECM, extracellular matrix; C6S, chondroitin 6-sulfate; DS, dermatan sulfate; KS, keratan sulfate; TLR-4, Toll-like receptor 4; PAGE-FS, polyacrylamide gel electrophoresis of fluorophore-labeled saccharides.

matan sulfate (DS, Seikagaku), 25 μg/ml keratan sulfate (KS, Sigma), 25 mM (final concentration) glucose, 25 mM (final concentration) 2-deoxyglucose (2DG), 25 mM (final concentration) sorbitol, 10 μM U0126 (Sigma), 10 mM NH_4Cl (Sigma), 5 μM LY294002 (Sigma), 5 μg/ml anti-CD44 Hermes-1 monoclonal antibody (Developpment Studies Hybridoma Bank), 5 μg/ml anti-CD44 BRIC-235 monoclonal antibody (International Blood Group Reference Laboratory, Bristol, UK.), 5 μg/ml anti-tubulin monoclonal antibody (Sigma), 25 μg/ml purified, low endotoxin 34-mer HA oligosaccharide (6.8 kDa) (Glycoscience Laboratories) (11), 1 μg/ml anti-TLR4 monoclonal antibody (MTS510, Santa Cruz Biotechnology), or 15 ng/ml E5564 (eritoran, Eisai Inc.), a pharmacological inhibitor of TLR4 signaling (12). Such treatment concentrations were determined after preliminary dose-response experiments.

Microarray—Total RNA was extracted from three independent cultures of AoSMCs treated for 24 h with 1 mM 4-MU and from three independent untreated cell cultures using a commercial kit (Ambion). Bioanalyzer (Agilent) was used to quantify RNA, and only RNA samples with an RNA integrity number >7.5 were used. Two μg of total RNA were used to generate cDNA and digoxigenin-labeled cRNA. Ten μg of the cRNA were hybridized to a human genome survey microarray (Applied Biosystems, Foster City, CA). The signal was developed using a chemiluminescent detection kit (Applied Biosystems), and chips were scanned by using a 1700 chemiluminescent microarray analyzer (Applied Biosystems). The intensity distributions of the microarrays were highly similar, so normalization was not required. Probes whose FLAG value exceeded 5000 in more than four (of the six) arrays were filtered out. The data were assessed on the $\log_2$ scale, and differential expression analysis between the two groups was done using the *limma* package (13). Enrichment of KEGG pathways was computed by submitting the identified probes to DAVID (14) and using all human genes as background.

Quantitative RT-PCR—Quantitative RT-PCRs were done with an Abi Prism 7000 real-time instrument (Applied Biosystems) using the Taqman Universal PCR Master Mix and Human predeveloped TaqMan gene expression assays for p53, p21, CDK2, p16, CD44, and β-actin (Applied Biosystems). The relative quantification of gene expression levels was determined by comparing ΔC_T values as described previously (15–17).

DNA Content by Cytofluorimetry—AoSMCs were resuspended in PBS containing 1% IGEPAL for membrane permeabilization. Cell pellets obtained after centrifugation were resuspended in 1 ml of PBS with propidium iodide and RNase. The DNA contents of the cells were quantified by using a FACSCanto cytofluorimeter (Becton Dickinson).

HA Quantification—Polyacrylamide gel electrophoresis of fluorophore-labeled saccharides (PAGEFS) and HPLC were used to measure the amounts of unsaturated HA disaccharides in the conditioned cell culture media as described previously (18–20).

Cell Vitality and Motility Assays—Apoptotic cells were detected by using the Annexin-V-FITC kit (Roche Diagnostics), and necrotic cells were detected by staining with propidium iodide as described by the manufacturer. To quantify apoptosis and necrosis, green (apoptotic) and red (necrotic) cells were counted in 10 independent fields under a fluorescent microscope (Olympus). In experiments with chondroitin 4-sulfate, C6S, DS, KS, ammonium chloride, anti-CD44 antibody, anti-TLR4 antibody, and inhibitors, the numbers of viable cells were counted in a Burker's chamber by using trypan blue.

To measure cell motility, confluent AoSMCs were treated either with 1 mM 4-MU, or with 25 μg/ml HMW-HA, or 1 μg/ml of anti-TLR4 monoclonal antibody, or 15 ng/ml of E5564 and scratched by pipette tip. Migration was quantified after 24 h of incubation as described previously (9).

CD44 Silencing—siRNA was used to reduce expression of CD44 in AoSMCs. CD44 siRNA (s2681) and scramble negative control siRNA1 kit (code 4611) were both purchased from Ambion. The transfections were done using a Nucleofector apparatus (Amaxa) as described previously (4, 21). After 48 h of incubation, cells were treated with 4-MU, and HMW-HA and cell viability were measured.

Statistical Analyses—Statistical analysis of the data were done using analysis of variance, followed by post hoc tests (Bonferroni) using Origin software (version 7.5, OriginLab). Probability values of $p < 0.01$ or 0.05 were considered statistically significant. Experiments were repeated three times each time in duplicate, and data are expressed as means ± S.E.

RESULTS AND DISCUSSION

In vascular pathologies, vessel thickening is a very common problem and is determined by complex mechanisms that involve remodeling of the ECM. SMCs are primarily responsible for arterial wall ECM production, and when SMCs dedifferentiate to become atherosclerotic prone cells, they synthesize large amounts of specific ECM molecules, including HA (22). HA is known to accumulate in neointima and to induce SMC migration, which increases progression of lesions by the formation of a highly hydrated ECM that facilitates cell movements, and by triggering cell receptor signaling. Recently, we showed that the proatherosclerotic properties of AoSMCs are reduced by treating them with 4-MU, a well known HA synthesis inhibitor. At 1 mM 4-MU, we found a clear reduction of mRNA coding for HASes and decreased UDP-glucuronic acid levels, which decreased production of HA. Furthermore, cell migration and proliferation were also reduced (9). Interestingly, the addition of 25 μg/ml of exogenous HMW-HA to 4-MU-treated cells restored AoSMC proliferation and motility (9). The rescue of cell migration by HMW-HA was clearly mediated by CD44, whereas the rescue of cell proliferation was not investigated.

In this study, cellular pathways altered by 4-MU were investigated by whole genomic expression profiling by using a microarray approach to compare 10 μg of cRNA prepared from untreated and 4-MU-treated AoSMCs (at a concentration of 1 mM for 24 h). Bioinformatic analyses identified 107 probes (supplemental Table 1) with a false discovery rate <5%, and these yielded two enriched pathways the cell cycle pathway (p value <0.001) and the p53 signaling pathway (p value 0.012). The complete data set of the microarray experiment is reported in supplemental Table 2. As HA is known to regulate proliferation in a great number of cells (23), it was not surprising to find that inhibition of HA synthesis alters cell cycle genes. On the

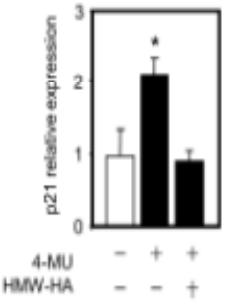

FIGURE 1. **Relative expression of p21 mRNA in untreated AoSMCs, after 24 h of treatment with 1 mM 4-MU alone, or with 1 mM 4-MU and 25 μg/ml of HMW-HA by quantitative RT-PCRs.** The lowest p21 expression in three different untreated samples was set at 1, and the S.E. is shown on each bar. *, $p < 0.01$ control versus treated samples. Relative expression is in arbitrary units.

other hand, the link between HA and p53 is not known, although recently, it was reported that reduction of an HA/versican ECM induced senescence and p53 accumulation in fibroblasts (24).

We showed previously that the addition of exogenous HMW-HA to 4-MU-treated AoSMCs rescued cell viability (9). Therefore, we measured the expression of several transcripts coding for cyclins, cyclin-dependent kinases, p53, BCL2, and several other proliferation-related genes in untreated AoSMCs and in AoSMCs treated for 24 h with 1 mM 4-MU and with 1 mM 4-MU + 25 μg/ml of HMW-HA by means of quantitative RT-PCR (results not shown). Interestingly, among the tested genes, only p21 mRNA responded to HMW-HA by returning to the level of untreated AoSMCs as shown in Fig. 1.

Because p21 is strictly related to cell cycle arrest, we measured the DNA content in AoSMCs after 4-MU or 4-MU + HMW-HA treatments by means of cytofluorimetric analyses (Fig. 2). Untreated cells were 50.9% in G_0, 21.5% in S, and 27.6% in G_2. After 4-MU treatment, the cells showed a clear G_1 arrest (84.1% in G_1, 10.8% in S, and 5.1% in G_2). Interestingly, in addition to the G_1 peak, another sharp peak appeared after 4-MU treatment, which is similar to the extra peak that has been associated with apoptosis in other cell types (25). Furthermore, in AoSMCs treated with 4-MU + HMW-HA, the extra peak disappeared, even though these cells continued to be blocked in G_1 (84.2% in G_1, 9.0% in S, and 6.9% in G_2). These results indicate that 4-MU inhibits cell growth through a G_1 block that is probably mediated through p21 or cyclin D1 as observed previously (7). Moreover, the cytofluorimetric analyses indicate the possibility that apoptosis could occur after 4-MU treatment, which can be prevented in the presence of HMW-HA. This would be consistent with the results of the microarray experiment that identified the p53 pathway and cell cycle as the most affected cellular functions, which fit well with cell growth arrest and apoptosis induction. Furthermore, p53 is known to induce apoptosis through mitochondrial outer membrane permeabilization and other mechanisms (26). Interestingly, during the preparation of this manuscript, Lokshwar and co-workers (27)

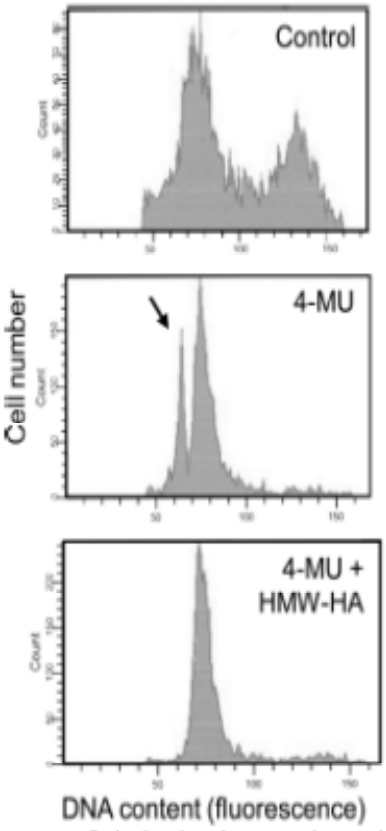

FIGURE 2. **Cytofluorimetric analyses of DNA content in untreated AoSMCs (control), after 24 h of treatment with 1 mM 4-MU, or after 24 h of treatment with 1 mM 4-MU and 25 μg/ml HMW-HA.** The *arrow* indicates the extra G_1 peak that has been associated with apoptosis. The peak is in 4-MU-treated samples but absent in 4-MU + HMW-HA treated cells.

published that 4-MU induced apoptosis in prostate tumor cells probably by activating the extrinsic pathway of apoptosis.

To confirm the induction of apoptosis in 4-MU-treated AoSMCs, we used a commercial kit to detect phosphatidylserine in the outer leaflet of the plasma membrane and found that the percentage of apoptotic cells increased ~8-fold in 4-MU-treated AoSMCs compared with untreated AoSMCs (Fig. 3A). Furthermore, the population of apoptotic cells in AoSMCs treated with 4-MU + HMW-HA was ~10% and not statistically different from untreated AoSMCs (Fig. 3A). There were no significant differences in the percentage of necrotic AoSMCs in the three treatments as measured by propidium iodine staining (data not shown). We also have measured viable cells after

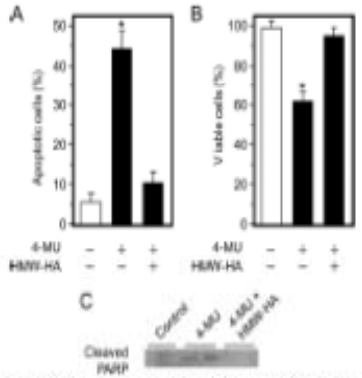

FIGURE 3. **Induction of apoptosis and reduction of cell viability after 4-MU treatment and anti-apoptotic effect of HMW-HA.** *A*, 5×10^5 AoSMCs were plated in the absence or in the presence of 1 mM 4-MU alone, or with 1 mM 4-MU + 25 μg/ml HMWHA for 24 h. Annexin V-FITC was used to mark apoptotic cells, and green fluorescent cells in 10 independent microscopic fields were counted. *, $p < 0.01$ control versus treated samples. *B*, AoSMCs were treated and incubated as in *A*, but stained with trypan blue. Viable cells were counted in 10 independent microscopic fields. *, $p < 0.01$ control versus treated samples. *C*, Western blots of 50 μg of protein extracted from untreated (control) or treated AoSMCs as described above using anti cleaved poly(ADP-ribose) polymerase (PARP) (active) antibody. In the figure, each band represents a different extract from a replicate culture.

4-MU treatment by means of trypan blue staining and found a reduction of ~40% of live cells, whereas in 4-MU + HMW-HA, vitality was similar to controls (Fig. 3*B*). Interestingly, the reduction of ~40% of viable cells after 4-MU treatment quantified by trypan blue correlates well with the ~40% increment of apoptotic cells determined with annexin-V kit (Fig. 3*A*), suggesting that trypan blue staining could be conveniently used to evaluate apoptosis in our conditions. To better demonstrate the effects of 4-MU and HMW-HA on cell viability, we treated AoSMCs with 0.5, 1, and 2 mM 4-MU and 25 μg/ml of HMW-HA finding a clear 4-MU dose-dependent reduction of cell proliferation (supplemental Fig. 1*A*). Similarly, apoptosis also had the same trend (supplemental Fig. 1*B*). The apoptotic process after 4-MU treatment was substantiated by showing that the cleaved poly(ADP-ribose) polymerase protein, a marker for apoptosis, was only present in AoSMCs treated with 4-MU (Fig. 3*C*, Western blot). The protective effect of HA against apoptosis has been reported for other cell types than vascular cells (28–32). However, it has been reported that HA-induced apoptosis in dendritic cells via inducible nitric-oxide synthase (33).

The transcripts for the antiapoptotic Bcl-2 protein and pro-apoptotic genes (Noxa, Puma, Bax, and Gadd45), which are known to be transcriptionally regulated by p53 (34–36), were measured by quantitative RT-PCR in the three AoSMC culture treatments. However, the expression analyses of these genes did not show any differences (results not shown), indicating that a different mechanism is involved for activation of apoptosis by 4-MU and rescue by HMW-HA.

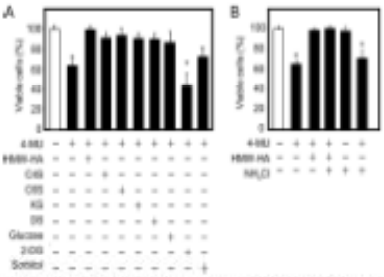

FIGURE 4. **Effects of exogenous lysosomal enzymes on inhibition of 4-MU-induced apoptosis.** *A*, 5×10^5 AoSMCs were plated for 24 h in the absence or in the presence of 1 mM 4-MU alone, with 1 mM 4-MU + 25 μg/ml HMW-HA, or with 1 mM 4-MU + 25 μg/ml of chondroitin 4-sulfate (C4S), 25 μg/ml of C6S, 25 μg/ml of KS, 25 μg/ml of DS, 25 mM (final concentration) of glucose, 25 mM of 2DG, or 25 mM sorbitol as osmotic control. Cells were stained with trypan blue, and viable ones were counted in 10 independent microscopic fields. *, $p < 0.01$ control versus treated samples. *B*, cells were plated as described above and treated with 1 mM 4-MU alone, with 1 mM 4-MU + 25 μg/ml HMW-HA, or with 1 mM 4-MU + 25 μg/ml HMW-HA + 10 mM NH_4Cl. After 24 h of incubation, the numbers of viable cells were quantified by using trypan blue staining. *, $p < 0.01$ control versus treated samples. Note that there was no statistically significant difference between cultures treated with 4-MU alone and 2DG.

Because 4-MU alters the cellular content of UDP glucuronic acid (9), we hypothesized that the inhibition of 4-MU-induced apoptosis by HA could be mediated by a metabolic effect. Although the inhibitory effect of 4-MU was specific for HA synthesis, we added other polysaccharides usually present in the ECM to 4-MU-treated AoSMCs to test for possible rescue from apoptosis: 25 μg/ml of each of the commercial GAGs (C4S, C6S, DS, KS). Moreover, to check the metabolic hypothesis in this process, we also used glucose and 2DG. We also treated AoSMCs with sorbitol as osmotic control, and it did not show any anti-apoptotic property. To check the purity of the GAG preparations, we verified absence of HA in sulfated GAG solutions by PAGEFS and HPLC (results not shown). As shown in Fig. 4*A*, among these compounds, only 2DG was not able to inhibit cell mortality induced by 4-MU supporting the metabolic hypothesis. In fact, 2DG is known to induce ATP depletion and energetic stresses in treated cells, which would be somewhat facilitative toward apoptosis. As far as glucose is concerned, we did not further investigate neither its anti-apoptotic mechanism nor whether it could trigger specific signals from HA receptors as CD44 or TLR4 (see below); in neurons and cancer cells, it was elegantly demonstrated that glucose can protect from apoptosis regulating glutathione and cytochrome *c* metabolism (37). The anti-apoptotic role of such GAGs after 4-MU treatment was also confirmed by detecting annexin V-FITC-positive cells (supplemental Fig. 2). Interestingly, among the GAGs, only KS does not contain glucuronic acid, suggesting that UDP-glucuronate is not critical in the anti-apoptotic effect, whereas it has a pivotal role to control HA synthesis (21).

However, GAGs would have to be degraded by the cells to furnish intermediate metabolites (i.e. UDP sugars or energy) through the action of several lysosomal glycosidases. To test

this possibility, we treated AoSMCs with NH_4Cl, a well known inhibitor of lysosomal enzymes. As shown in Fig. 4B, NH_4Cl alone did not decrease viability of the cells, and it did not alter the effect of HMW-HA to prevent the decrease in viability in the presence of 4-MU. Furthermore, NH_4Cl alone did not prevent the decrease of viability in the presence of 4-MU. To verify the effectiveness of ammonium chloride treatment, we measured an increment of ~50% in the content of HA after NH_4Cl treatment of AoSMCs by PAGEFS, demonstrating the inhibition of HA degrading enzymes (result not shown). Therefore, the blocking of lysosomal enzymes necessary to catabolize HA and the other polysaccharides is not involved in the anti-apoptotic effect of HMW-HA, suggesting that the metabolic hypothesis is not critical in this process.

Previous studies have demonstrated the central role of the HA receptor CD44 in regulating AoSMC behavior (5, 10) and have reported a link between p53 and CD44 (38). Moreover, another study with chondrocytes showed that the HA anti-apoptotic effect was due to CD44 (29). CD44 has several variants derived from alternative splicing events at the RNA maturation level. As CD44 interacts with many ECM components (i.e. collagen, fibronectin, laminin, HA, DS, and CS) (39, 40), such CD44 isoforms could be involved in receptor-ligand recognition, thereby explaining the evidence that other GAGs as CS and DS inhibited the 4-MU-induced apoptosis. To test this hypothesis, we inhibited the HA-CD44 interaction by using the CD44-blocking Hermes-1 or BRIC235 monoclonal antibodies and by attenuating HA-CD44 signaling with a 34-mer HA oligosaccharide as we previously showed in AoSMCs (10). As shown in Fig. 5A, neither Hermes-1 or BRIC235 nor the HA oligosaccharide were able to inhibit the rescuing effect of HMW-HA.

HA can be also recognized by other receptors (2), and among these, TLR4 could be a good candidate to mediate the rescuing process. TLRs mediate immune responses by sensing bacterial structures such as LPS, viral RNA, and endogenous molecules released by damaged host cells such as heat shock proteins (41). Notably, TLR4 has been described to interact with other polyanionic molecules, including heparan sulfate (42), and therefore could be involved also in the anti-apoptotic mechanism of the other GAGs. HA has been proposed to regulate TLR4, thereby modulating inflammation and apoptosis in mouse lung (2). To verify whether TLR4 was involved in the anti-apoptotic effect of HMW-HA, we treated AoSMCs with 4-MU, 4-MU+HMW-HA, 4-MU+HMW-HA+TLR4 blocking antibody, or with eritoran, a TLR4-directed endotoxin antagonist (12). Fig. 5B shows that both the blocking antibodies and eritoran prevented the rescuing effect of HMW-HA, thereby supporting the critical function of TLR4 in the anti-apoptotic effect mediated by HA in AoSMCs. Anti-TLR4 and eritoran alone (Fig. 5B) or in combination with 4-MU (data not shown) were not statistically significant from control cells. Interestingly, LPS, the main ligand of TLR4, at 1, 10, or 100 ng/ml was not able to reduce the mortality induced by 4-MU (supplemental Fig. 3), suggesting a specific response when HA reacts with TLR4. Although the direct binding of HA to TLR4 has never been demonstrated, it was shown that TLR4, CD44, and MD-2 form a complex that cooperates in HA recognition (43).

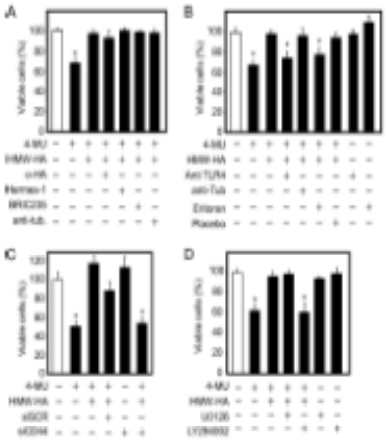

FIGURE 5. **Mechanism of anti-apoptotic effect of HMW-HA.** *A*, 5×10^5 AoSMCs were plated in the absence or in the presence of 1 mM 4-MU alone, with 1 mM 4-MU+25 μg/ml HMW-HA, with 1 mM 4-MU+25 μg/ml HMW-HA+25 μg/ml of the 34-mer HA oligosaccharide, with 5 μg/ml of two monoclonal antibody against CD44 (Hermes-1 and BRIC235), or with an irrelevant control antibody (anti-tubulin). *B*, cells were plated as described above and treated with 1 μg/ml of a monoclonal antibody against TLR4, with an irrelevant control antibody (anti-tubulin (anti-tub.)), with 15 ng/ml of eritoran, or with a placebo. *C*, 5×10^5 AoSMCs were nucleofected with siRNA against CD44 (siCD44), a scramble siRNA (siSCR), or subjected only to the electrical protocol and nucleofection reagent. After 24 h of incubation, cells were treated with 4-MU alone or 4-MU+HMW-HA as described above. *D*, cells were plated as described above and treated with 10 μM of U0126 or with 5 μM (final concentration) of LY294002. After 24 h of incubation, the numbers of viable cells were quantified by using trypan blue staining. *, $p < 0.01$ control versus treated samples.

Our data obtained with anti-CD44 antibodies and HA oligosaccharide prevented HA-CD44 interaction and signaling, but no information is available as to whether this treatment interferes with TLR4-CD44 complex formation, signaling, or stability. Therefore, we decided to abrogate CD44 expression by means of siRNA and verify whether or not the presence of CD44 protein was necessary for the HA anti-apoptotic effect. After the silencing, by quantitative RT-PCR, we measured the residual CD44 expression that ranged from 15 to 20% respect to control cells. As shown in Fig. 5C, the CD44 silencing alone did not influence cell viability, whereas the lack of CD44 inhibited the rescuing effect of HWM-HA after 4-MU treatment, indicating that CD44 is critical for HMW-HA the anti-apoptotic effect. The specificity of such data were confirmed by a scramble siRNA treatment that maintained the rescuing properties of HMW-HA as the untreated sample. The controversion between the anti-CD44 antibodies and CD44 silencing can be explained taking into consideration the fact that CD44 can form a complex with TLR4 (43, 44), and the beneficial effect of HMW-HA requires both of the receptors. We can speculate that HA could be recognized by TLR4, but, for the anti-apoptotic effect, the entire TLR4/CD44 complex is necessary for a survival signaling.

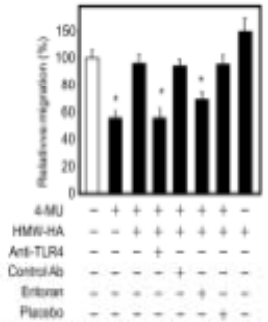

FIGURE 6. **TLR4 affects AoSMC motility.** Confluent AoSMCs were left untreated or treated with various combination of 1 mM 4-MU, 25 μg/ml HMW-HA, 1 μg/ml of anti-TLR4 monoclonal antibody, 1 μg/ml of unrelated antibody (anti-α-tubulin), 15 ng/ml of E5564, or placebo, scratched with a yellow tip, incubated for 24 h, and photographed under an inverted microscope. Images were analyzed by using NIH Image software, and the numbers of migrated cells into the scratched areas were counted. Relative data are expressed as mean ± S.E. in three different experiments. *, $p < 0.05$ versus untreated sample.

Although it is generally accepted that HA binds to TLR4 or TLR-4-MD-2 (myeloid differentiation factor 2) complex as the polyanionic nature as well as the disaccharide backbone with the β-glycosidic bond of known TLR4 agonist (LPS) and antagonist (eritoran) (44, 45), our results highlighted a central role of CD44 to regulate a specific TLR4 signaling triggered by HA (probably different form that evoked by LPS) as previously reported Taylor and collaborators (43).

We have also studied whether other GAGs as C6S and chondroitin 4-sulfate could abrogate 4-MU induced apoptosis through TLR4. As shown in supplemental Fig. 4, the blocking of the receptor with antibodies or the treatment with the antagonist did not prevent the rescuing indicating a different anti-apoptotic mechanism that could involve physical phenomena such as the "surface screening effect" theory (Gouy-Chapman-Stern theory) (46).

TLR4-mediated signaling leads to rapid activation of PI3K (47), one of a family of kinases involved in regulation of cell growth, apoptosis, and motility. As the PI3K-AKT signaling pathway is strictly related to cell survival, we evaluated whether this kinase was involved in the anti-apoptotic effect of HMW-HA. We used 5 μM LY294002 to inhibit PI3K and 10 μM of U0126 to block ERK1/2, which is also involved in apoptosis (48). Fig. 5*D* shows that the two inhibitors alone had little or no effect on AoSMC viability. However, the number of viable cells in 4-MU+HMW-HA treated AoSMCs decreased significantly only after LY294002 addition. This indicates that the PI3K pathway but not the ERK1/2 pathway is crucial for the rescuing effect mediated by HMW-HA.

Cell motility is crucial in atherogenesis. As HA interaction with TLR4 can regulate cell viability, we wondered whether this receptor is involved also in motility control. To address this issue, we repeated previously reported migration assays in which we demonstrated that HMW-HA enhanced AoSMC motility through CD44 (9). As shown in Fig. 6, after 24 h from the wound, the effect of HMW-HA to induce cell movement was abolished by treating AoSMCs with TLR4 blocking antibodies as well as by adding the TLR4 antagonist eritoran, whereas it was unaltered by unrelated antibodies or placebo. Additional control experiments with anti-TLR4 and eritoran alone (and in combination with 4-MU) without added HMW-HA did not show statistically significant differences from untreated cells (results not shown) clearly showing that TLR4 is able to participate to the modulation of AoSMC migration *in vitro*. As 4-MU reduced the number of vital cells by 40%, the delayed wound healing response may reflect the problem in proliferation rather than in migration. To exclude this issue, we repeated the experiments quantifying migration after 6 h from the wound finding comparable results (supplemental Fig. 5), suggesting a role of TLR4 in motility. Similar results were previously obtained in melanoma cells where the abrogation of TLR4 by short interference RNA inhibited the motility induced by short HA oligosaccharides (49). Another HA receptor (*i.e.* RHAMM) was shown to control SMC migration in response to HA (50). All these results highlight the importance of HA in the fine tuning of cell movement.

Overall, our results provide strong evidence that the apoptosis induced in AoSMCs in the presence of 4-MU can be blocked through the ability of HMW-HA and other GAGs to induce a PI3K anti-apoptotic signaling pathway through interaction with the TLR4-CD44 complex. Therefore, the role of CD44 in TLRs signaling is becoming critical in light of recent literature reporting the modulation of the NF-kB pathway throughout not only HA (16) but also other proinflammatory secreted molecules as tumor necrosis factor-inducible gene 6 (49).

Acknowledgments—We thank Adolfo Cangemi for cytofluorimetric analyses, Nicola Cirmi for microarray analyses, Akira Asari (Glycoscience Laboratories, Inc., Japan) for providing pure 34-mer HA oligosaccharide, the Eisai Research Institute for providing eritoran and placebo, the Developmental Studies Hybridoma Bank (maintained by The University of Iowa) for Hermes-1 antibody, and Maurizio Brivio for LPS. We gratefully acknowledge the "Centro Grandi Attrezzature per la Ricerca Biomedica" Università degli Studi dell'Insubria for use of its instruments facility.

REFERENCES

1. Tammi, R. H., Passi, A., Rilla, K., Karousou, E., Vigetti, D., Makkonen, K., and Tammi, M. I. (2011) *FEBS J.* **278**, 1419–1428
2. Jiang, D., Liang, J., and Noble, P. W. (2007) *Annu. Rev. Cell Dev. Biol.* **23**, 435–461
3. Vigetti, D., Viola, M., Karousou, E., Genasetti, A., Hascall, M., Clerici, M., Bartolini, B., Moretto, P., De Luca, G., and Passi, A. (2008) *Scientific World Journal* **8**, 1110–1118
4. Vigetti, D., Moretto, P., Viola, M., Genasetti, A., Hascall, M., Karousou, E., Pallotti, F., De Luca, G., and Passi, A. (2009) *FASEB J.* **23**, 1118–1130
5. Cuff, C. A., Kothapalli, D., Azonobi, I., Chun, S., Zhang, Y., Belkin, R., Yeh, C., Secreto, A., Assoian, R. K., Rader, D. J., and Puré, E. (2001) *J. Clin. Invest.* **108**, 1031–1040
6. Kothapalli, D., Flowers, J., Xu, T., Puré, E., and Assoian, R. K. (2008) *J. Biol. Chem.* **283**, 31823–31829
7. Kothapalli, D., Zhao, L., Hawthorne, E. A., Cheng, Y., Lee, E., Puré, E., and Assoian, R. K. (2007) *J. Cell Biol.* **176**, 535–544
8. Turley, E. P. (2004) *Nat. Rev. Cancer* **4**, 528–539

9. Vigetti, D., Rizzi, M., Viola, M., Karousou, E., Genasetti, A., Clerici, M., Bartolini, B., Hascall, V. C., De Luca, G., and Passi, A. (2009) *Glycobiology* **19**, 537–546
10. Vigetti, D., Viola, M., Karousou, E., Rizzi, M., Moretto, P., Genasetti, A., Clerici, M., Hascall, V. C., De Luca, G., and Passi, A. (2008) *J. Biol. Chem.* **283**, 4445–4458
11. Tawada, A., Mura, T., Oomiki, Y., Watanabe, A., Matsuzaki, Y., and Asari, A. (2002) *Glycobiology* **12**, 431–436
12. Mullarkey, M., Rose, J. R., Bristol, J., Kawata, T., Kimura, A., Kobayashi, S., Przetak, M., Chow, J., Gusovsky, F., Christ, W. J., and Rossignol, D. P. (2003) *J. Pharmacol. Exp. Ther.* **304**, 1093–1102
13. Smyth, G. K. (2005) in *Bioinformatics and Computational Biology Solutions Using R and Bioconductor* (Gentleman, R., Carey, V., Dudoit, S., Irizarry, R., and Huber, W., eds.), pp. 397–420, Springer, New York
14. Dennis, G., Jr., Sherman, B. T., Hosack, D. A., Yang, J., Gao, W., Lane, H. C., and Lempicki, R. A. (2003) *Genome Biol.* **4**, P3
15. Vigetti, D., Genasetti, A., Karousou, E., Viola, M., Clerici, M., Bartolini, B., Moretto, P., De Luca, G., Hascall, V. C., and Passi, A. (2009) *J. Biol. Chem.* **284**, 35584–35594
16. Vigetti, D., Genasetti, A., Karousou, E., Viola, M., Moretto, P., Clerici, M., Deleonibus, S., De Luca, G., Hascall, V. C., and Passi, A. (2010) *J. Biol. Chem.* **285**, 24039–24048
17. Vigetti, D., Clerici, M., Deleonibus, S., Karousou, E., Viola, M., Moretto, P., Heldin, P., Hascall, V. C., De Luca, G., and Passi, A. (2011) *J. Biol. Chem.* **286**, 7917–7924
18. Karousou, E. G., Viola, M., Genasetti, A., Vigetti, D., Luca, G. D., Karamanos, N. K., and Passi, A. (2008) *Biomed. Chromatogr.* **19**, 701–705
19. Viola, M., Karousou, E. G., Vigetti, D., Genasetti, A., Pallotti, F., Gozzini, G. F., Tira, E., De Luca, G., and Passi, A. (2006) *J. Pharm. Biomed. Anal.* **41**, 36–42
20. Vigetti, D., Viola, M., Gornati, R., Oir, M., Nardi, I., Passi, A., De Luca, G., and Bernardini, G. (2005) *Matrix Biol.* **23**, 511–517
21. Vigetti, D., Oir, M., Viola, M., Genasetti, A., Karousou, E., Rizzi, M., Deleonibus, F., Nardi, I., Hascall, V. C., De Luca, G., and Passi, A. (2006) *J. Biol. Chem.* **281**, 8254–8263
22. Bassuk, R., Wight, T. N., Pastores, C., Hanley, C., and Israel, J. M. (1996) *Circulation* **93**, 1141–1147
23. Sheehan, K. M., DeLoia, L. B., Wen, R. A., Bonnema, J. D., and DeNoyer, D. H. (2004) *Life Sci.* **75**, 3087–3102
24. Sawai, K., Chanchaey, K., Hatano, S., Kongtawelert, P., Kimata, K., and Watanabe, H. (2009) *J. Biol. Chem.* **284**, 8591–8604
25. Gorman, A. M., Samali, A., McGowan, A. J., and Cotter, T. G. (1997) *Cytometry* **29**, 97–105
26. Fetterman, J. L., Kraemer, R. T., and Kraemer, G. (2004) *Nat. Cell Biol.* **6**, 266–268
27. Lokeshwar, V. B., Lopez, L. E., Munoz, D., Chi, A., Shirodkar, S. P., Lokeshwar, S. D., Escudero, D. O., Dhir, N., and Altman, N. (2010) *Cancer Res.* **70**, 2613–2623
28. Kaneko, T., Saito, H., Toya, M., Sato, T., Nakahara, K., and Hirai, M. (2010) *J. Androl. Reprod. Genet.* **17**, 161–167
29. Lingrell, G., Grani, T., Zini, N., Tomagnini, S., Fiacrini, A., Guidolin, D., Berlanga, C., and Facchini, A. (2011) *Arthritis Rheum.* **63**, 1800–1807
30. Onoda, M., Nakanishi, C., Yokota, A., and Sato, Y. (2009) *Neurology* **14**, 213–219
31. Paulsen, T., Dutot, M., Joly, F., Warnet, J. M., and Rat, P. (2009) *Mol. Vis.* **15**, 577–585
32. Xu, H., Ito, T., Tawada, A., Maeda, H., Yamamichi, H., Inaba, K., Yoshida, K., Uchiyama, Y., and Asari, A. (2002) *J. Biol. Chem.* **277**, 17308–17314
33. Yang, T., Wilson, T. P., Villa, L., Erlé, M., Arnason, J., Watkins, S. Kondziolka, D., Okada, H., Pollack, I. F., and Chambers, W. H. (2002) *Cancer Res.* **62**, 2580–2591
34. Wei, M. C., Zong, W. X., Cheng, E. H., Lindsten, T., Panoutsakopoulou, V., Ross, A. J., Roth, K. A., MacGregor, G. R., Thompson, C. B., and Korsmeyer, S. J. (2001) *Science* **292**, 727–730
35. Oda, E., Ohki, R., Murasawa, H., Nemoto, J., Shibue, T., Yamashita, T., Tokino, T., Taniguchi, T., and Tanaka, N. (2000) *Science* **288**, 1053–1058
36. Yu, J., Wang, Z., Kinzler, K. W., Vogelstein, B., and Zhang, L. (2003) *Proc. Natl. Acad. Sci. U.S.A.* **100**, 1931–1936
37. Vaughn, A. E., and Deshmukh, M. (2008) *Nat. Cell Biol.* **10**, 1477–1483
38. Godar, S., Ince, T. A., Bell, G. W., Feldser, D., Donaher, J. L., Bergh, J., Liu, A., Miu, K., Watnick, R. S., Reinhardt, F., McAllister, S. S., Jacks, T., and Weinberg, R. A. (2008) *Cell* **134**, 62–73
39. Naor, D., Sionov, R. V., and Ish-Shalom, D. (1997) *Adv. Cancer Res.* **71**, 241–319
40. Chin, B. K., Carpenito, C., Dougherty, S. T., Hayes, G. M., and Dougherty, G. J. (1999) *Neoplasia* **1**, 445–452
41. Trant, M. F., and Gay, B. (2006) *J. Leukoc. Biol.* **79**, 514–519
42. Johnson, G. B., Brunn, G. J., Kodaira, Y., and Platt, J. L. (2002) *J. Immunol.* **168**, 5233–5239
43. Taylor, K. R., Yamasaki, K., Radek, K. A., Di Nardo, A., Goodarzi, H., Golenbock, D., Beutler, B., and Gallo, R. L. (2007) *J. Biol. Chem.* **282**, 18265–18275
44. Jiang, D., Liang, J., and Noble, P. W. (2011) *Physiol. Rev.* **91**, 221–264
45. Kim, H. M., Park, B. S., Kim, J. I., Kim, S. E., Lee, J., Oh, S. C., Enkhbayar, P., Matsushima, N., Lee, H., Yoo, O. J., and Lee, J. O. (2007) *Cell* **130**, 906–917
46. Vigetti, D., Andrini, O., Clerici, M., Negrini, D., Passi, A., and Moriondo, A. (2008) *Cell Physiol. Biochem.* **22**, 137–146
47. Laird, M. H., Rhee, S. H., Perkins, D. J., Medvedev, A. E., Piao, W., Fenton, M. J., and Vogel, S. N. (2009) *J. Leukoc. Biol.* **85**, 966–977
48. Jo, S. K., Cho, W. Y., Sung, S. A., Kim, H. K., and Won, N. H. (2005) *Kidney Int.* **67**, 458–466
49. Voelcker, V., Gebhardt, C., Averbeck, M., Saalbach, A., Wolf, V., Weih, F., Sleeman, J., Anderegg, U., and Simon, J. (2008) *Exp. Dermatol.* **17**, 100–107
50. Sewani, R. C., Wang, C., Yang, B., Zhang, S., Kinsella, M. G., Wight, T. N., Stern, R., Nance, D. M., and Turley, E. A. (1996) *J. Clin. Invest.* **98**, 1159–1168

THE JOURNAL OF BIOLOGICAL CHEMISTRY VOL. 286, NO. 10, pp. 7917–7924, March 11, 2011

Hyaluronan Synthesis Is Inhibited by Adenosine Monophosphate-activated Protein Kinase through the Regulation of HAS2 Activity in Human Aortic Smooth Muscle Cells*

Received for publication, October 12, 2010, and in revised form, December 3, 2010 Published, JBC Papers in Press, January 12, 2011, DOI 10.1074/jbc.M110.193656

Davide Vigetti[*1], Moira Clerici[*1], Sara Deleonibus[*], Evgenia Karousou[*], Manuela Viola[*], Paola Moretto[*], Paraskevi Heldin[§], Vincent C. Hascall[¶], Giancarlo De Luca[*], and Alberto Passi[*2]

From the [*]Dipartimento di Scienze Biomediche Sperimentali e Cliniche, Università degli Studi dell'Insubria, Via J. H. Dunant 5, 21100 Varese, Italy, the [§]Ludwig Institute for Cancer Research, Uppsala University Biomedical Center, SE-75124 Uppsala, Sweden, and the [¶]Department of Biomedical Engineering, The Cleveland Clinic, Cleveland, Ohio 44195

Hyaluronan (HA) is an extracellular matrix glycosaminoglycan (GAG) involved in cell motility, proliferation, tissue remodeling, development, differentiation, inflammation, tumor progression, and invasion and controls vessel thickening in cardiovascular diseases. Therefore, the control of HA synthesis could permit the fine-tuning of cell behavior, but the mechanisms that regulate HA synthesis are largely unknown. Recent studies suggest that the availability of the nucleotide-sugar precursors has a critical role. Because the formation of UDP-sugars is a highly energetically demanding process, we have analyzed whether the energy status of the cell could control GAG production. AMP-activated protein kinase (AMPK) is the main ATP/AMP sensor of mammalian cells, and we mimicked an energy stress by treating human aortic smooth muscle cells (AoSMCs) with the AMPK activators 5-aminoimidazole-4-carboxamide-1-β-D-ribofuranoside and metformin. Under these conditions, HA synthesis, but not that of the other GAGs, was greatly reduced. We confirmed the inhibitory effect of AMPK using a specific inhibitor and knock-out cell lines. We found that AMPK phosphorylated Thr-110 of human HAS2, which inhibits its enzymatic activity. In contrast, the other two HAS isoenzymes (HAS1 and HAS3) were not modified by the kinase. The reduction of HA decreased the ability of AoSMCs to proliferate, migrate, and recruit immune cells, thereby reducing the pro-atherosclerotic AoSMC phenotype. Interestingly, such effects were not recovered by treatment with exogenous HA, suggesting that AMPK can block the pro-atherosclerotic signals driven by HA by interaction with its receptors.

Hyaluronan (HA)[3] is a ubiquitous and atypical glycosaminoglycan (GAG) that is neither sulfated nor linked to any core protein. It is composed of GlcUA and *N*-acetyl-D-glucosamine GlcNAc and is synthesized by three plasma membrane HA synthases (HAS1, HAS2, and HAS3) that generate linear polymers with molecular masses ranging from thousands to several millions of daltons (1). Many cellular effects of HA depend on its viscoelastic properties, molecular mass, and membrane receptors, including CD44, RHAMM (receptor for HA-mediated motility), Lyve-1 (lymphatic vessel endothelial receptor 1), HARE (HA receptor for endocytosis), and TLR4 (Toll-like receptor 4), which trigger several signaling events (1). During development, HA has a role in many critical events, including cell migration and differentiation, through spatiotemporal regulation of HAS expression in amphibians as well as in mammals (2–5).

In cardiovascular pathologies, HA has critical pro-atherosclerotic properties (6). In normal arteries, HA is typically located in the tunica adventitia, but following injuries, HA can be found in the media and neointima (7), where it can modulate the behavior of smooth muscle cells (SMCs) and contribute to inflammatory responses, including recruitment of immune cells (8, 9). SMCs have a critical role in vessel wall thickening due to their proliferation, migration, and secretion of extracellular matrix (ECM)-modifying enzymes (10). Moreover, SMCs are responsible for HA matrix deposition after vessel injury, and HA itself can modulate SMC motility (11) and dedifferentiation (12). Several experiments confirmed the critical pro-atherosclerotic role of HA using CD44 knock-out animals (12) or HAS2 transgenic mice (13), by blocking HA/CD44 interaction (14), or by inhibiting HA synthesis (15).

Therefore, regulation of HA synthesis could provide new methods to treat vascular pathologies. Growth factors, cytokines, prostaglandins, PKA, and PKC are known to modulate HA synthesis through HAS activity and HAS gene expression, although their physiological roles are not completely understood (1). Our research and that of others have revealed the critical role of the UDP-sugar precursors (UDP-GlcUA and UDP-GlcNAc) in the regulation of HA synthesis (16, 17). The ratio of NAD^+ to NADH, which is influenced mainly by oxygen

* This work was supported by the Fondazione Comunitaria del Varesotto-ONLUS, PRIN 2007 (to G. D. L.), Fondo di Ateneo per la Ricerca, and a Centro Insubre di Biotecnologie per la Salute Umana young researcher award (to D. V.).

The on-line version of this article (available at http://www.jbc.org) contains supplemental Figs. S1–S6.

[1] Both authors contributed equally to this work.

[2] To whom correspondence should be addressed. Tel.: 39-332-397-142; Fax: 39-332-397-119; E-mail: alberto.passi@uninsubria.it.

[3] The abbreviations used are: HA, hyaluronan; GAG, glycosaminoglycan; HAS, HA synthase; SMC, smooth muscle cell; ECM, extracellular matrix; AMPK, AMP-activated protein kinase; AoSMC, aortic SMC; AICAR, 5-aminoimidazole-4-carboxamide-1-β-D-ribofuranoside; 2-DG, 2-deoxyglucose; CS, chondroitin sulfate; HS, heparan sulfate; MEF, mouse embryonic fibroblast; CA-AMPK, constitutively active AMPK; DN-AMPK, dominant-negative AMPK.

availability, is known to control UDP-GlcUA content through the activity of UDP-glucose dehydrogenase in cartilage and cornea, which can lead to keratan sulfate synthesis (18).

The synthesis of HA precursors requires ATP, UTP, and other critical metabolic molecules, including glucose, glutamine, glucosamine, and acetyl-CoA (supplemental Fig. S1), which makes GAG production an energy-consuming process. As energy charge is critical for the regulation of all cellular metabolism, we tested whether the ATP/AMP ratio could control the synthesis of HA and other GAGs. We focused our attention on AMP-activated protein kinase (AMPK), which is the main energy sensor of the eukaryotic cell (19). AMPK is a heterotrimeric protein with a catalytic α subunit and two regulatory subunits (β and γ) that, when the ATP/AMP ratio decreases, inhibit anabolic processes and induce catabolic pathways to restore ATP levels (20). The mechanism for activating AMPK is complex and involves phosphorylation of the critical Thr-172 on the catalytic α subunit. By altering gene expression or by directly phosphorylating several pivotal enzymes, AMPK regulates cellular metabolic processes, including glycolysis, gluconeogenesis, lipid metabolism, and protein synthesis. However, the consequences for the metabolism of ECM components are not yet known. Therefore, the aim of this study was to determine how modulation of AMPK affects the metabolism of HA and other GAGs in primary human aortic SMCs (AoSMCs).

EXPERIMENTAL PROCEDURES

Cell Cultures and Treatments—Primary human AoSMCs were purchased from Lonza and were grown for four to five passages in complete SmGm2 culture medium (Lonza) supplemented with 5% FBS as described previously (15). 2.5×10^5 cells were seeded in 35-mm dishes, and after 6 h, SmGm2 medium was replaced with high glucose DMEM supplemented with 0.2% FBS to induce quiescence. After 48 h, DMEM was maintained in the positive control (quiescent cells), whereas it was replaced with SmGm2 medium supplemented with 15% FBS in the negative control (growth cells). In the treated cells, DMEM was substituted with SmGm2 medium enriched with 15% FBS and supplemented with increasing concentrations of 5-aminoimidazole-4-carboxamide-1-β-D-ribofuranoside (AICAR), metformin, or 2-deoxyglucose (2-DG) (all from Sigma).

Western Blotting—Western blot experiments were performed as reported previously (14) using antibodies against AMPKα, phospho-AMPKα (Thr-172), or phospho-acetyl-CoA carboxylase (Ser-79) (all from Cell Signaling). To investigate the phosphorylation of HAS2 at the putative AMPK target residue Thr-110, we used a affinity-purified phospho-specific polyclonal antibody prepared in rabbit against the synthetic peptide RKCLQSVKRLpTYPGIKV, which resembles residues 100–116 of the human HAS2 sequence (Davids Biotechnologie, Regensburg, Germany). As a control, we also used a polyclonal antibody against the same peptide without threonine phosphorylation (generated by the same company).

GAG Determinations—HA, chondroitin sulfate (CS), and heparan sulfate (HS) released into the culture medium were purified by proteinase K (Finnzymes) and ethanol precipitation. *Streptomyces dysgalactiae* hyaluronidase, chondroitinase ABC, and heparinases I–III (all from Seikagaku) were used to obtain the unsaturated (Δ) disaccharides, which were quantified by HPLC analyses (21, 22). Pericellular HA matrices were visualized using a particle exclusion assay (15).

Gene Expression Determinations by Quantitative RT-PCR—Total RNAs were extracted from AoSMCs with TRIzol (Invitrogen), retrotranscribed using the High Capacity cDNA synthesis kit (Applied Biosystems), and amplified on an ABI Prism 7000 instrument (Applied Biosystems). The following human TaqMan gene expression assays were used: HAS1 (Hs00155410_m1), HAS2 (Hs00193435_m1), HAS3 (Hs00193436_m1), UDP-glucose dehydrogenase (Hs00163365_m1), UDP-glucose pyrophosphorylase (Hs00198879_m1), and β-actin (Hs99999903_m1). The relative gene expression was determined by comparing ΔC_t (14).

Cell Mobility and Adhesion Assays—Confluent AoSMCs were growth-arrested by culture in DMEM with 0.2% FBS for 2 days. The cells were scratched by blue tip and then cultured under different conditions for 24 h. Migrated cells were quantified as described previously (15). To assess the adhesiveness of AoSMCs under different conditions, we performed monocyte adhesion assays using the U937 monocyte cell line as reported previously (15).

Cell Transfections—Primary AoSMCs were nucleofected with 5 μg of plasmid DNA using a Nucleofector apparatus (Amaxa) and the human AoSMC Nucleofector kit as described previously (17) to have high efficiency and low mortality. Wild-type and knock-out mouse embryonic fibroblasts (MEF) and COS-1 and COS-7 cells were efficiently transfected using ExGen 500 (Fermentas) following the manufacturer's protocol.

Microsome Purification and HAS Activity Assay—Control or transfected COS-7 cells were lysed in 10 mM KCl, 1.5 mM $MgCl_2$, and 10 mM Tris-HCl (pH 7.4) supplemented with protease and phosphatase inhibitors (Roche Applied Science) by scraping and sonication. The lysate was centrifuged at $5000 \times g$ for 5 min at 4 °C, and the supernatant was centrifuged at $100,000 \times g$ for 40 min at 4 °C to obtain microsomes containing vesiculated fragments of the plasma membrane (23). The pellet was resuspended in the lysis buffer, and protein content was determined by Bradford assay. Twenty μg of proteins were used to determine HAS activity as described previously (8).

Statistical Analyses—Statistical analyses of the data were performed by analysis of variance, followed by Bonferroni post hoc tests using Origin 7.5 software (OriginLab). Probability values of $p < 0.01$ or 0.05 were considered statistically significant. Experiments were repeated three times, each time in duplicate, and data are expressed as means ± S.E.

RESULTS AND DISCUSSION

Effects of AMPK Activation on GAG Synthesis—To induce AMPK activation, AoSMCs were incubated for 2 days with 0.2% FBS to induce quiescence (positive control) and then treated for 48 h with 15% FBS (negative control) or with 15% FBS plus AICAR, a pharmacological activator of AMPK that mimics AMP, as previously reported in AoSMCs (24). By Western blotting, we demonstrated that AICAR induced phosphorylation of Thr-172 on the AMPK α subunit and that AICAR induced AMPK activation by detecting phospho-acetyl-CoA carboxyl-

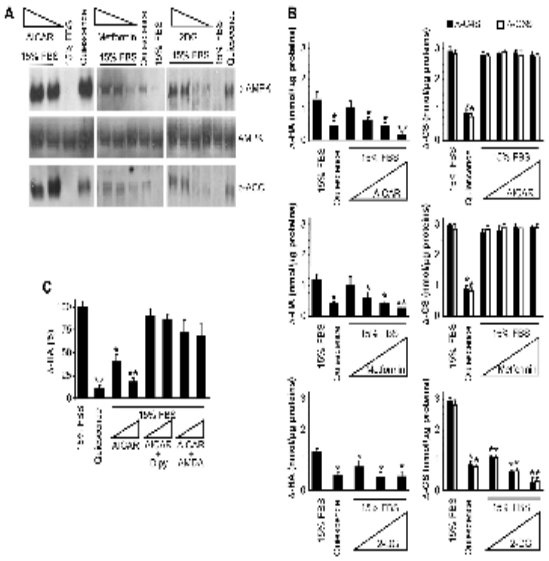

FIGURE 1. AICAR, metformin, and 2-DG inhibit HA synthesis but not CS synthesis in AoSMCs. *A*, Western blot analysis of 30 μg of protein extracts prepared from quiescent AoSMCs (0.2% FBS, 48 h) or quiescent cells treated with 15% FBS or 15% FBS plus AICAR (1 and 2 mM; 48 h), with 15% FBS plus metformin (2, 3, and 4 mM; 48 h), or with 15% FBS plus 2-DG (15, 25, 50, and 75 mM; 48 h; the high 2-DG concentrations were needed to compete with the 25 mM glucose contained in the AoSMCs growth medium) using specific anti-phospho-AMPKα (*p-AMPK*), anti-total AMPKα (*AMPK*), or anti-phospho-acetyl-CoA carboxylase (*p-ACC*) antibodies. In the 2-DG experiment, the 15% FBS sample also contained 50 mM sorbitol as an osmotic control. The images are representative of three independent experiments. *B*, quantification of Δ-HA, Δ-C4S, and Δ-C6S prepared from GAGs released into the culture medium of quiescent AoSMCs treated for 48 h with 15% FBS, with 15% FBS plus AICAR (0.5, 1, 2, and 4 mM), with metformin (0.5, 1, 2, and 4 mM), or with 2-DG (12, 25, and 50 mM) as described for *A*. *C*, relative quantification of Δ-HA prepared from GAGs released into the culture medium of quiescent AoSMCs treated with 15% FBS, with AICAR (1 and 2 mM), with AICAR plus 10 μM dipyridamole (*Dipy*), or with AICAR plus 10 μM 5′-amino-5′-deoxyadenosine (*AMDA*). Results are expressed as means ± S.E. in three different determinations. *, $p < 0.5$; **, $p < 0.01$, 15% FBS *versus* treatments, respectively.

ase, an AMPK target (Fig. 1*A*). In other experiments, quiescent AoSMCs were treated for 48 h with metformin and 2-DG (Fig. 1*A*), which induce AMPK phosphorylation and activation driven by different mechanisms from AICAR, *i.e.* through the upstream kinase complex LKB1-STRAD-MO25 (25) and by ATP depletion, respectively. These results showed that AICAR, metformin, and 2-DG sustained phospho-AMPK and phospho-acetyl-CoA carboxylase activities in 15% FBS in dose-dependent responses.

At this time point, we collected aliquots of cell medium and purified the secreted GAGs. Unsaturated (Δ) disaccharides from HA, CS, and HS were obtained by digestion with specific enzyme eliminases. The resulting Δ-disaccharides were then derivatized with 2-aminoacridone and quantified by HPLC (21, 22). The treatment of quiescent AoSMCs with 15% FBS induced an ~2.5-fold increase in HA, whereas the addition of 15% FBS plus AICAR or metformin caused a dose-dependent and statistically significant inhibition of HA synthesis (Fig. 1*B*). In contrast, the synthesis of CS (both 6- and 4-sulfated isomers) (Fig. 1*B*) as well as HS (supplemental Fig. S1) did not change after the treatments, and only minor and not statistically significant modification of sulfation patterns were observed. These results clearly demonstrate that HA synthesis, but not CS or HS synthesis, is inhibited by both AICAR and metformin. Previous studies showed that metformin does not decrease sulfate incorporation into GAGs (26). However, because HA is not sulfated, our results are novel and particularly interesting because of the critical functions of HA in the vasculature. The "conventional" GAG synthesis inhibitor 2-DG (27) was used as a control and indeed reduced synthesis of both HA and CS (Fig. 1*B*). Moreover, HA, which remains associated with cell membranes to form pericellular coats, also decreased after the treatments as evaluated by particle exclusion assays (supplemental Fig. S2). To confirm the results obtained with AICAR, AoSMCs were also treated with dipyridamole, which inhibits AICAR transport into cells by blocking an adenosine transporter, and with 5′-amino-5′-deoxyadenosine, which inhibits the cytosolic phosphorylation of AICAR by blocking the adenosine kinase (24). Both these treatments avoided the HA reduction induced by AICAR (Fig. 1*C*).

To confirm the involvement of AMPK in HA synthesis inhibition, we used Compound C, a specific AMPK inhibitor (25). As shown in Fig. 2*A*, Compound C in the presence of AICAR increased the HA level to near control levels. Therefore, these data substantiate the critical involvement of AMPK in regulating HA synthesis. Furthermore, AoSMCs were nucleofected

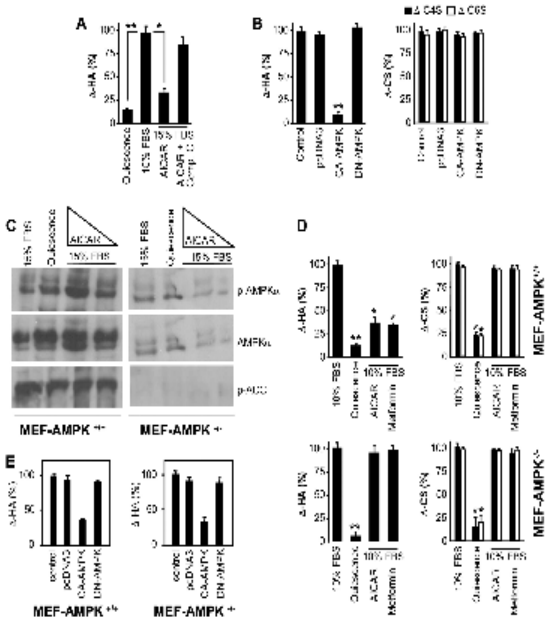

FIGURE 2. **AMPK is involved in AICAR- and metformin-dependent HA synthesis inhibition.** *A*, relative HPLC quantification of Δ-HA prepared from GAGs released into the culture medium of quiescent AoSMCs treated with 15% FBS (set as 100%), with 15% FBS plus 1 mM AICAR, or with 15% FBS plus 1 mM AICAR plus 100 μM Compound C (*Comp. C*). *B*, relative HPLC quantification of Δ-HA and Δ-CS prepared from GAGs released into the culture medium of AoSMCs nucleofected with an expression vector coding for CA-AMPK or DN-AMPK or with an empty vector (pcDNA3). The analyses were performed 48 h after the nucleofections. The content of Δ-HA, Δ-C4S, or Δ-C6S in control cells (*i.e.* subjected to the electrical protocol without DNA) was set to 100%. *C*, Western blot analysis of 30 μg of protein extracts prepared from quiescent (0.2% FBS, 48 h) wild-type ($AMPK^{+/+}$) MEFs, from $AMPK^{-/-}$ MEFs, or from quiescent cells treated with 15% FBS or with 15% FBS plus AICAR (1 and 2 mM, 48 h) using specific anti-phospho-AMPKα (*p-AMPK*), anti-total AMPKα, or anti-phospho-acetyl-CoA carboxylase (*p-ACC*) antibodies. The absence of phospho-acetyl-CoA carboxylase bands in $AMPK^{-/-}$ MEFs indicates the absence of AMPK activity. *D*, relative HPLC quantification of Δ-HA and Δ-CS prepared from GAGs released into the culture medium of $AMPK^{+/+}$ MEFs or $AMPK^{-/-}$ MEFs incubated for 48 h with 0.2% FBS (quiescent), with 10% FBS (set as 100%), with 10% FBS plus 2 mM AICAR, or with 10% FBS plus 4 mM metformin. *, $p < 0.5$; **, $p < 0.01$, 15% FBS (or control in *B* or 10% FBS in *C*) *versus* treatments, respectively. *E*, relative HPLC quantification of Δ-HA and Δ-CS prepared from GAGs released into the culture medium of $AMPK^{+/+}$ MEFs, untransfected $AMPK^{-/-}$ MEFs (control), or cells transfected with plasmid coding for CA-AMPK or DN-AMPK or with an empty vector (pcDNA3).

with a recombinant pcDNA3 plasmid coding for constitutively active AMPK (CA-AMPK) or for dominant-negative AMPK (DN-AMPK). The amount of HA secreted was dramatically decreased after CA-AMPK nucleofection but did not change after DN-AMPK nucleofection (Fig. 2*B*). Similarly, HA pericellular coats were abolished by CA-AMPK but not DN-AMPK treatment (supplemental Fig. S2). Interestingly, CS synthesis was not altered by either of the treatments (Fig. 2*B*), indicating a specific role of AMPK in HA synthesis.

To definitely demonstrate AMPK effects on HA synthesis, we used MEFs from animals null in the α1 and α2 subunits of AMPK ($AMPK^{-/-}$) or from wild-type ($AMPK^{+/+}$) mice, both kindly provided by Benoit Viollet (28). In preliminary control experiments, we verified the lack of AMPK activity in $AMPK^{-/-}$ MEFs by demonstrating the absence of the phospho-acetyl-CoA carboxylase band in Western blotting as well as the lack of cell cycle inhibition after AICAR addition (Fig. 2*C* and supplemental Fig. S3). $AMPK^{+/+}$ and $AMPK^{-/-}$ MEF cultures were treated with 15% FBS or with 15% FBS plus AICAR or metformin. After 48 h, AICAR and metformin reduced HA released into the medium by ~60% in $AMPK^{+/+}$ MEF cultures (Fig. 2*D*) and caused a near absence of cell-associated HA (supplemental Fig. S4). As expected, CS was not affected by the treatments (Fig. 2*D*). In contrast, HA in $AMPK^{-/-}$ MEF cultures was not changed by these treatments (Fig. 2*D*). These results demonstrate that cells without AMPK activity are not able to reduce HA synthesis in response to AICAR or metformin. The transfection of the CA-AMPK-coding plasmid into $AMPK^{-/-}$ MEFs restored their ability to inhibit HA synthesis (Fig. 2*E*). This clearly shows that the energy charge, through AMPK activity, regulates HA synthesis and therefore affects ECM composition.

HA Does Not Influence AMPK-mediated Reduction of Cell Proliferation, Migration, and Adhesiveness—SMCs are involved in vascular diseases through their proliferation, intima invasion, and recruitment of immune cells, and HA has a central role to control SMC behavior. Therefore, we investigated whether AICAR and metformin are able to modulate AoSMC cell cycle responses. Using cytofluorometric analyses, we confirmed the previously published data (24) indicating that AICAR and metformin, through AMPK, can block the cell cycle in G_0/G_1 phase without inducing cell death or apoptosis (data not shown). Furthermore, the exogenous addition of high molecular mass HA (average of $\sim 4 \times 10^6$ Da; Healon) and the exogenous addition of low molecular weight HA (prepared by digesting Healon with testicular hyaluronidase for 90 min, which generates oligosaccharides <500 kDa) to AICAR- or metformin-treated cells maintained AoSMCs arrested in G_0/G_1 (supplemental Fig. S5), suggesting that the HA-activated signaling by specific cell-surface receptors cannot bypass the block of the cell cycle induced by AMPK. These data confirm the finding that high molecular mass HA antagonizes mitogen-induced S phase entry in vascular SMCs by modulating cyclin D_1 and $p27^{kip1}$ (12, 29). On the other hand, by means of scratch tests, we found that AMPK activity reduced cell migration by ~70%, whereas AMPK inhibition by Compound C maintained cell motility (Fig. 3*A*). The exogenous addition of high molecular mass HA was not able to bypass the blocking effect of AMPK on cell migration (supplemental Fig. S5). This issue is interesting, as high molecular mass HA is generally known to greatly induce cell mobility, and by decreasing HA synthesis, AICAR or metformin could be useful to limit HA-dependent cell invasion that is critical in several pathologies, such as cancer metastasis or neointima formation. Interestingly, low molecular mass HA, which is known to strongly induce cell motility, was able to partially overcome the effects AICAR and metformin (supplemental Fig. S5). As *in vivo* HA can be fragmented during neointima formation due to an inflammatory response (30), the migration inhibitory effect of AMPK could be maintained also in the presence of HA oligosaccharides that physiologically are a strong activator of cell proliferation or motility.

AICAR and metformin treatments also strongly reduced adhesion of fluorescent U937 monocytes on AoSMCs, whereas AMPK inhibition with Compound C maintained the number of adherent monocytes comparable with the control (Fig. 3, *B* and *C*). Interestingly, the monocyte binding in the Compound C-treated samples confirmed the role of HA in cell adhesion because enzymatic removal of HA and the exogenous high molecular mass HA added to treated cells reduced monocyte adhesion to near control levels. It is known that HA can modulate inflammation triggering TLR4 signaling (1) or can mediate immune cell adhesion on the endothelium or SMCs via CD44 (9, 31, 32). The results of these experiments demonstrate that activation of AMPK *in vitro* inhibits proliferation, migration, and monocyte adhesion, thereby reducing AoSMC pro-atherosclerotic behaviors.

Vessel thickening involves a plethora of causes partially still unknown, but ECM remodeling is one of the main events affecting vascular cells (33). Previous studies have shown that administration of AICAR *in vivo* suppressed neointima forma-

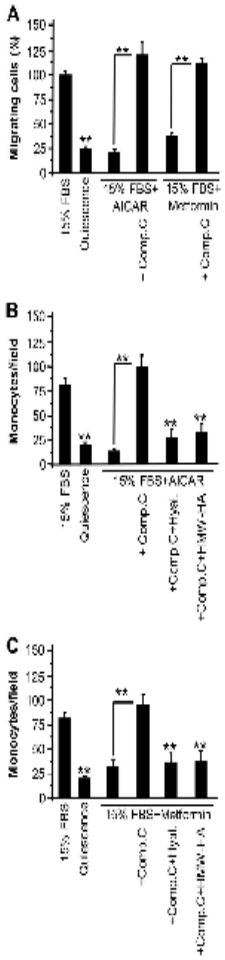

FIGURE 3. AICAR and metformin modulate AoSMC motility and adhesive properties through AMPK. *A*, relative quantification of AoSMC mobility. Quiescent confluent AoSMCs were treated with 15% FBS, with 15% FBS plus AICAR (1 mM), or with 15% FBS plus metformin (2 mM) with or without 100 μM Compound C (*Comp.C*). After 24 h, cells were scratched using a pipette tip, and after 24 h, migrated cells were counted. *B* and *C*, U937 monocyte adhesion assays performed on AoSMCs treated with AICAR (*B*) or metformin (*C*). Seventy percent quiescent confluent cells were treated with 15% FBS, with 15% FBS plus AICAR (1 mM), or with 15% FBS plus metformin (2 mM) with or without 100 μM Compound C. After 48 h, fluorescent U937 cells were added for 20 min at 37 °C, washed, and counted under a fluorescence microscope. Control experiments were done by treating AoSMCs with hyaluronidase (*Hyal*) or by competing for cell-associated HA adding high molecular weight HA (*HMW-HA*). Results are expressed as the number of adherent U937 cells per field and are represented as means ± S.E. **, $p < 0.01$, untreated *versus* treated samples.

tion after mechanical injury in the rat femoral artery, although no information was provided on ECM composition (34). Furthermore, it has been known for decades that metformin can inhibit vascular complications of type 2 diabetes patients (35), and AMPK has also been indicated as a therapeutic target for atherosclerosis and cancer (36). Therefore, in addition to its multiple effects on cell cycle progression and on protein, fatty acid, and cholesterol synthesis (36), our results indicate that AMPK can modulate ECM composition by inhibiting HA synthesis, suggesting its pivotal role in all the processes that contribute to matrix remodeling.

Molecular Mechanism of AMPK-mediated Inhibition of HA Synthesis—To elucidate the critical effect of AMPK activation only on HA synthesis, we determined whether AMPK can modulate the expression of genes involved in HA metabolism. In fact, it is known that AMPK controls the expression of several genes, including the critical glucose metabolism transcription factor FOXO (37). Therefore, by means of quantitative RT-PCR, we quantified the relative content of mRNAs coding for HA-metabolizing enzymes, including UDP-glucose pyrophosphorylase, UDP-glucose dehydrogenase, HASs, and hyaluronidases after AoSMCs treatments with AICAR and metformin, and we did not find any significant gene expression differences (supplemental Fig. S6). The finding that UDP-glucose pyrophosphorylase and UDP-glucose dehydrogenase genes are not modulated by AMPK could be reasonable considering that UDP-glucose and UDP-GlcUA are critical not only for HA synthesis but also for all other sulfated GAGs, glycogen, and other glycoconjugates that are necessary for cell survival. However, a proteomic study revealed that UDP-glucose pyrophosphorylase can be a target of AMPK in pigs, enhancing the complexity of this issue (38).

Although HASs are known to be regulated at the transcriptional level by several growth factors and cytokines (1), this seems not to be the case for AMPK. As HASs are transmembrane proteins, their activity can be phospholipid-dependent (39). Interestingly, AMPK can regulate mitochondrial cardiolipin content (40), and this lipid is known to regulate bacterial HAS (39). As cardiolipin is typically in the mitochondria, this issue could be not critical for eukaryotic HASs, although very recently, it was reported that the AMPK γ1 subunit can control erythrocyte membrane elasticity (41). Therefore, AMPK could modify membrane lipid composition indirectly by modulating HAS activity or stability.

On the other hand, AMPK could act on HASs at a post-translational level (*i.e.* phosphorylation), which would assure a rapid response. Interestingly, the AMPK β1 subunit has a myristoylation signal that localizes the AMPK complex in the plasma membrane (42), where AMPK could interact with HASs. Bioinformatic analyses have shown that HASs conserve several AMPK consensus sequences in the intracytoplasmic loop, which makes such enzymes hypothetical AMPK targets. To study this issue, we transiently transfected COS-7 cells, which are known to synthesize a limited amount of HA, with plasmid coding for FLAG-tagged human HAS1 (FLAG-HAS1), HAS2 (FLAG-HAS2), or HAS3 (FLAG-HAS3) and measured the HA released into the culture medium (Fig. 4*A*). Each construct increased HA synthesis significantly. However, only the

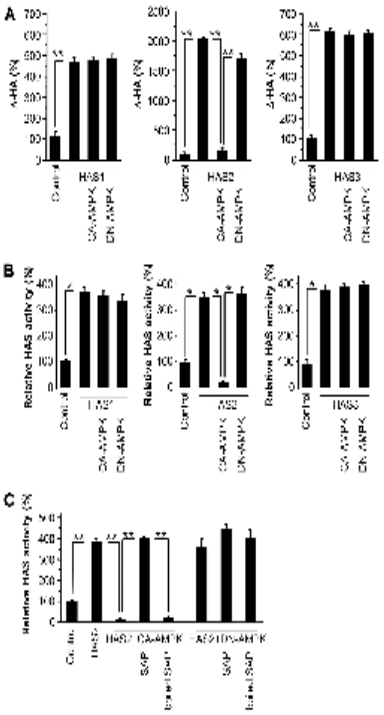

FIGURE 4. **AMPK inhibits HAS2 activity.** *A*, relative HPLC quantification of Δ-HA prepared from GAGs released into the culture medium 48 h after transfection of COS-7 cells with the FLAG-HAS1-, FLAG-HAS2-, or FLAG-HAS3-expressing vector alone, cotransfection with the CA-AMPK- or DN-AMPK-expressing vector, or transfection with the empty pcDNA3 vector alone (control). *B*, relative quantification of HAS enzymatic activity in microsomes prepared from COS-7 cells transfected as described for *A*. *C*, relative quantification of HAS activity in microsome proteins extracted from COS-7 cells transfected with FLAG-HAS2 or cotransfected with the FLAG-HAS2+CA-AMPK- or FLAG-HAS2+DN-AMPK-expressing plasmid. In some experiments, membrane fraction proteins were preincubated with shrimp alkaline phosphatase (*SAP*) to hydrolyze phosphate groups. Control experiments were done by preincubating the samples with heat-inactivated SAP (*boiled SAP*). Results are represented as means ± S.E. *, $p < 0.05$; **, $p < 0.01$, untreated *versus* treated samples.

FLAG-HAS2-transfected cells decreased HA synthesis to near control levels when cotransfected with CA-AMPK but not with DN-AMPK (Fig. 4*A*). This strongly suggests that only HAS2 can be targeted by AMPK. To evaluate whether AMPK can modulate HAS functionality, we quantified the HAS enzymatic activity in microsomes because HAS enzymes are transmembrane proteins, and their activity can be recovered only in crude cell membranes. We found a strong reduction of HAS activity only when FLAG-HAS2 was cotransfected with CA-AMPK, whereas the functionality of other HAS enzymes (*i.e.* HAS1 and HAS3) was not affected by CA-AMPK (Fig. 4*B*). Although HASs share a high degree of amino acidic identity, the inhibi-

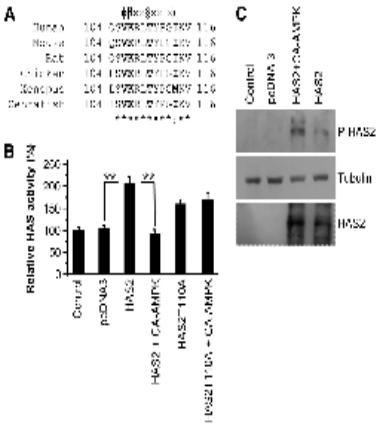

FIGURE 5. **Identification of the critical residue involved in AMPK-dependent HAS2 inhibition.** *A*, alignment of HAS2 sequences around Thr-110 from different organisms showing the conservation of the AMPK consensus site (with critical residues shown in *boldface*). ϕ, hydrophobic residue; β, basic residue; *x*, any residue; *S*, serine or threonine. *B*, relative quantification of HAS activity in microsome fractions prepared from COS-7 cells transfected with the wild-type 6-Myc-HAS2 (*HAS2*)- or 6-Myc-HAS2 T110A (*HAS2T100A*)-expressing plasmid or with the empty pcDNA3 vector alone (control) or cotransfected with the CA-AMPK-expressing vector. Results are expressed as means ± S.E. **, $p < 0.01$, pcDNA3 or HAS2+CA-AMPK *versus* HAS2 samples. *C*, Western blot analysis of 30 μg of protein extracts prepared from untransfected COS-7 cells (control) or from COS-7 cells transfected with plasmid coding for 6-Myc-HAS2 or an empty vector (pcDNA3) or cotransfected with plasmid coding for 6-Myc-HAS2 and CA-AMPK (HAS2+CA-AMPK) using the polyclonal antibody that recognizes phospho-Thr-110 (*P-HAS2*), tubulin (as a loading control), or HAS2 (as a transfection efficiency control).

tory effect only on HAS2 activity seems to be very specific. From a pathophysiological point of view, HAS2 transgenic mice exacerbate neointima formation after pro-atherosclerotic stimuli (13); therefore, the specific inhibitory effect of AMPK on the main HAS responsible of vessel thickening could be of crucial pharmacological importance. Interestingly, the enzymatic hydrolysis of protein phosphate groups in FLAG-HAS2+CA-AMPK microsomes, by treatment with shrimp alkaline phosphatase, restored HAS activity to the control level (Fig. 4C), which strongly suggests that one or more phosphorylation sites in the HAS2 enzyme or in an accessory protein present in the membrane can reduce HAS2 activity.

To identify critical phosphorylation residue(s), we searched the Human Protein Reference Database, which revealed the presence of a putative AMPK phosphorylation consensus motif in HAS2 protein at Thr-110. The sequence around this amino acid is very well conserved in HAS2 proteins from zebrafish to mouse (Fig. 5*A*), suggesting its importance. Moreover, this site is not shared with HAS1 or HAS3, which would explain why HAS1 and HAS3 are not regulated by AMPK. Furthermore, this residue is on a cytoplasmic loop of HAS2 that was previously shown to be important for glycosyltransferase activity (39). Therefore, we mutated Thr-110 to alanine (T110A) in the 6-Myc-HAS2 plasmid to prevent phosphorylation and transfected the mutant construct into COS-7 cells with or without CA-AMPK. After 48 h, we measured the HAS-specific activity in microsomes and found that the HA synthetic activity of the T110A-transfected COS-7 cells was comparable with wild-type HAS2 and that CA-AMPK was not able to inhibit HA synthesis (Fig. 5*B*). To determine whether Thr-110 could be phosphorylated, we used two polyclonal antibodies prepared against two peptides that represent the HAS2 sequence from amino acids 100 to 116 in which Thr-110 was phosphorylated or not. As shown in Fig. 5*C*, in Western blot experiments, the antibody generated against the phosphopeptide (*P-HAS2 panel*) was able to detect a band corresponding to HAS2 in protein extracts prepared in COS-7 cells cotransfected with plasmids coding for 6-Myc-HAS2 and CA-AMPK. A faint band was also visible in extracts prepared from transfection with only 6-Myc-HAS2, where a small amount of HAS2 phosphorylation could be due to endogenous COS-7 AMPK activity. The antibody generated against the unphosphorylated peptide (*HAS2 panel*) was able to detect HAS2 protein in both treatments, revealing similar transfection efficiency. These results strongly suggest that Thr-110 can be the target of AMPK and that the phosphorylation of this amino acid drastically reduces the HA synthetic activity. A previous study reported the phosphorylation of HAS3 without describing the effect on enzyme functionality (43), whereas another work clearly showed that ERK-mediated serine phosphorylation of all three HASs increased their specific activity (44). This finding suggests that HAS proteins could have different regulatory mechanisms in which the same post-translational modification (*i.e.* phosphorylation) in different sites could increase or decrease the enzymatic activity. Moreover, a recent work demonstrated that HAS2 and HAS3 can make homo- and heterodimers and that HAS2 activity can be modulated by ubiquitination at Lys-190 (45). Such results suggest that HASs (and HAS2 in particular) can be complex proteins with several possibilities for post-translational modifications capable of modulating enzymatic activity.

Our findings demonstrate that at low ATP/AMP ratios, AMPK activity can block HA synthesis without altering the synthesis of other GAGs. The mechanism of such regulation does not involve a change in gene expression but involves the phosphorylation of HAS2, which decreases its HA synthetic activity. When AMPK is active, cells are already known to be growth-arrested, and for this reason, AMPK was indicated as a therapeutic marker for cancer and vascular pathologies (36). Our results highlight this point, demonstrating that AMPK can deeply modify the ECM environment, thereby preventing cell mobility and reducing pro-inflammatory cell recruitment, which, *in vivo*, could be associated with reduced disease development or progression. The ATP/AMP ratio depends on nutrient availability, and glucose has a pivotal role in physiology. In hypoglycemic conditions, cells have a low energy charge, and by switching off non-vital anabolic processes (*i.e.* HA synthesis) and concomitantly switching on lipid catabolism, AMPK can thereby increase the ATP/AMP ratio and overcome stress periods. On the other hand, in hyperglycemic conditions, cells have a high energy charge and inactive AMPK but can initiate several intracellular stress responses that can lead to autophagy (46). In this condition, HA synthesis is known to be dramatically elevated, and HA cable-like structures can be produced extracel-

lularly that are strongly adhesive for inflammatory cells (47). In this context, a deeper knowledge of the mechanisms that control cell microenvironment metabolism (*i.e.* synthesis, degradation, and modifications) could identify critical factors involved in pathologies, such as the role of AMPK in cardiovascular diseases.

Acknowledgments—We are grateful to Benoît Viollet (Institut Cochin, University Paris 5, Paris, France) for knock-out and wild-type MEFs, Dave Carling (Medical Research Council Clinical Sciences Centre, Imperial College, London, UK) for the CA-AMPK vector, Morris J. Birnbaum (Howard Hughes Medical Institute, Philadelphia, PA) for the DN-AMPK vector, Paul H. Weigel (University of Oklahoma) for the HAS1 and HAS3 vectors, and Federica Cossu and Martino Bolognesi (University of Milan, Milan, Italy) for bioinformatic studies on HAS2. We acknowledge the Centro Grandi Attrezzature per la Ricerca Biomedica at the Università degli Studi dell'Insubria for instrument availability.

REFERENCES

1. Jiang, D., Liang, J., and Noble, P. W. (2007) *Annu. Rev. Cell Dev. Biol.* 23, 435–461
2. Camenisch, T. D., Spicer, A. P., Brehm-Gibson, T., Biesterfeldt, J., Augustine, M. L., Calabro, A., Jr., Kubalak, S., Klewer, S. E., and McDonald, J. A. (2000) *J. Clin. Invest.* 106, 349–360
3. Nardini, M., Ori, M., Vigetti, D., Gornati, R., Nardi, I., and Perris, R. (2004) *Gene Expr. Patterns* 4, 303–308
4. Ori, M., Nardini, M., Casini, P., Perris, R., and Nardi, I. (2006) *Development* 133, 631–640
5. Vigetti, D., Viola, M., Gornati, R., Ori, M., Nardi, I., Passi, A., De Luca, G., and Bernardini, G. (2003) *Matrix Biol.* 22, 511–517
6. Vigetti, D., Viola, M., Karousou, E., Genasetti, A., Rizzi, M., Clerici, M., Bartolini, B., Moretto, P., De Luca, G., and Passi, A. (2008) *TheScientificWorldJOURNAL* 8, 1116–1118
7. Riessen, R., Wight, T. N., Pastore, C., Henley, C., and Isner, J. M. (1996) *Circulation* 93, 1141–1147
8. Vigetti, D., Genasetti, A., Karousou, E., Viola, M., Clerici, M., Bartolini, B., Moretto, P., De Luca, G., Hascall, V. C., and Passi, A. (2009) *J. Biol. Chem.* 284, 30684–30694
9. Vigetti, D., Genasetti, A., Karousou, E., Viola, M., Moretto, P., Clerici, M., Deleonibus, S., De Luca, G., Hascall, V. C., and Passi, A. (2010) *J. Biol. Chem.* 285, 24639–24645
10. Vigetti, D., Moretto, P., Viola, M., Genasetti, A., Rizzi, M., Karousou, E., Pallotti, F., De Luca, G., and Passi, A. (2006) *FASEB J.* 20, 1118–1130
11. Savani, R. C., and Turley, E. A. (1995) *Int. J. Tissue React.* 17, 141–151
12. Cuff, C. A., Kothapalli, D., Azonobi, I., Chun, S., Zhang, Y., Belkin, R., Yeh, C., Secreto, A., Assoian, R. K., Rader, D. J., and Puré, E. (2001) *J. Clin. Invest.* 108, 1031–1040
13. Chai, S., Chai, Q., Danielsen, C. C., Hjorth, P., Nyengaard, J. R., Ledet, T., Yamaguchi, Y., Rasmussen, L. M., and Wogensen, L. (2005) *Circ. Res.* 96, 583–591
14. Vigetti, D., Viola, M., Karousou, E., Rizzi, M., Moretto, P., Genasetti, A., Clerici, M., Hascall, V. C., De Luca, G., and Passi, A. (2008) *J. Biol. Chem.* 283, 4448–4458
15. Vigetti, D., Rizzi, M., Viola, M., Karousou, E., Genasetti, A., Clerici, M., Bartolini, B., Hascall, V. C., De Luca, G., and Passi, A. (2009) *Glycobiology* 19, 537–546
16. Jokela, T. A., Jauhiainen, M., Auriola, S., Kauhanen, M., Tiihonen, R., Tammi, M. I., and Tammi, R. H. (2008) *J. Biol. Chem.* 283, 7666–7673
17. Vigetti, D., Ori, M., Viola, M., Genasetti, A., Karousou, E., Rizzi, M., Pallotti, F., Nardi, I., Hascall, V. C., De Luca, G., and Passi, A. (2006) *J. Biol. Chem.* 281, 8254–8263
18. Balduini, C., Brovelli, A., De Luca, G., Galligani, L., and Castellani, A. A. (1973) *Biochem. J.* 133, 243–249
19. Hardie, D. G. (2004) *J. Cell Sci.* 117, 5479–5487
20. Towler, M. C., and Hardie, D. G. (2007) *Circ. Res.* 100, 328–341
21. Karousou, E. G., Viola, M., Genasetti, A., Vigetti, D., Luca, G. D., Karamanos, N. K., and Passi, A. (2005) *Biomed. Chromatogr.* 19, 761–765
22. Viola, M., Vigetti, D., Karousou, E., Bartolini, B., Genasetti, A., Rizzi, M., Clerici, M., Pallotti, F., De Luca, G., and Passi, A. (2008) *Electrophoresis* 29, 3168–3174
23. Caride, A. J., Filoteo, A. G., Enyedi, A., Verma, A. K., and Penniston, J. T. (1996) *Biochem. J.* 316, 353–359
24. Igata, M., Motoshima, H., Tsuruzoe, K., Kojima, K., Matsumura, T., Kondo, T., Taguchi, T., Nakamaru, K., Yano, M., Kukidome, D., Matsumoto, K., Toyonaga, T., Asano, T., Nishikawa, T., and Araki, E. (2005) *Circ. Res.* 97, 837–844
25. Zhou, G., Myers, R., Li, Y., Chen, Y., Shen, X., Fenyk-Melody, J., Wu, M., Ventre, J., Doebber, T., Fujii, N., Musi, N., Hirshman, M. F., Goodyear, L. J., and Moller, D. E. (2001) *J. Clin. Invest.* 108, 1167–1174
26. de Dios, S. T., Frontanilla, K. V., Nigro, J., Ballinger, M. L., Ivey, M. E., Cawson, E. A., and Little, P. J. (2007) *J. Diabetes Complicat.* 21, 108–117
27. Tímár, J., Diczházi, C., Bartha, I., Pogány, G., Paku, S., Rásó, E., Tóvári, J., Ladányi, A., Lapis, K., and Kopper, L. (1995) *Int. J. Cancer* 62, 755–761
28. Laderoute, K. R., Amin, K., Calaoagan, J. M., Knapp, M., Le, T., Orduna, J., Foretz, M., and Viollet, B. (2006) *Mol. Cell. Biol.* 26, 5336–5347
29. Kothapalli, D., Zhao, L., Hawthorne, E. A., Cheng, Y., Lee, E., Puré, E., and Assoian, R. K. (2007) *J. Cell Biol.* 176, 535–544
30. de la Motte, C., Nigro, J., Vasanji, A., Rho, H., Kessler, S., Bandyopadhyay, S., Danese, S., Fiocchi, C., and Stern, R. (2009) *Am. J. Pathol.* 174, 2254–2264
31. DeGrendele, H. C., Estess, P., and Siegelman, M. H. (1997) *Science* 278, 672–675
32. Hascall, V. C., Majors, A. K., De La Motte, C. A., Evanko, S. P., Wang, A., Drazba, J. A., Strong, S. A., and Wight, T. N. (2004) *Biochim. Biophys. Acta* 1673, 3–12
33. Ross, R. (1999) *N. Engl. J. Med.* 340, 115–126
34. Nagata, D., Takeda, R., Sata, M., Satonaka, H., Suzuki, E., Nagano, T., and Hirata, Y. (2004) *Circulation* 110, 444–451
35. Kirpichnikov, D., McFarlane, S. I., and Sowers, J. R. (2002) *Ann. Intern. Med.* 137, 25–33
36. Motoshima, H., Goldstein, B. J., Igata, M., and Araki, E. (2006) *J. Physiol.* 574, 63–71
37. Greer, E. L., Oskoui, P. R., Banko, M. R., Maniar, J. M., Gygi, M. P., Gygi, S. P., and Brunet, A. (2007) *J. Biol. Chem.* 282, 30107–30119
38. Hedegaard, J., Horn, P., Lametsch, R., Søndergaard Møller, H., Roepstorff, P., Bendixen, C., and Bendixen, E. (2004) *Proteomics* 4, 2448–2454
39. Weigel, P. H., and DeAngelis, P. L. (2007) *J. Biol. Chem.* 282, 36777–36781
40. Athéa, Y., Viollet, B., Mateo, P., Rousseau, D., Novotova, M., Garnier, A., Vaulont, S., Wilding, J. R., Grynberg, A., Veksler, V., Hoerter, J., and Ventura-Clapier, R. (2007) *Diabetes* 56, 786–794
41. Foretz, M., Hebrard, S., Guihard, S., Leclerc, J., Do Cruzeiro, M., Harnard, G., Niedergang, F., Gaudry, M., and Viollet, B. (2011) *FASEB J.* 25, 337–347
42. Warden, S. M., Richardson, C., O'Donnell, J., Jr., Stapleton, D., Kemp, B. E., and Witters, L. A. (2001) *Biochem. J.* 354, 275–283
43. Goentzel, B. J., Weigel, P. H., and Steinberg, R. A. (2006) *Biochem. J.* 396, 347–354
44. Bourguignon, L. Y., Gilad, E., and Peyrollier, K. (2007) *J. Biol. Chem.* 282, 19426–19441
45. Karousou, E., Kamiryo, M., Skandalis, S. S., Ruusala, A., Asteriou, T., Passi, A., Yamashita, H., Hellman, U., Heldin, C. H., and Heldin, P. (2010) *J. Biol. Chem.* 285, 23647–23654
46. Wang, A., and Hascall, V. C. (2009) *Autophagy* 5, 864–865
47. Ren, J., Hascall, V. C., and Wang, A. (2009) *J. Biol. Chem.* 284, 16621–16632

THE JOURNAL OF BIOLOGICAL CHEMISTRY VOL. 285, NO. 32, pp. 24639–24645, August 6, 2010

Proinflammatory Cytokines Induce Hyaluronan Synthesis and Monocyte Adhesion in Human Endothelial Cells through Hyaluronan Synthase 2 (HAS2) and the Nuclear Factor-κB (NF-κB) Pathway*

Received for publication, April 15, 2010, and in revised form, June 1, 2010 Published, JBC Papers in Press, June 3, 2010, DOI 10.1074/jbc.M110.134536

Davide Vigetti*[1], Anna Genasetti*[1], Evgenia Karousou*, Manuela Viola*, Paola Moretto*, Moira Clerici*, Sara Deleonibus*, Giancarlo De Luca*, Vincent C. Hascall[§], and Alberto Passi*[2]

From the *Dipartimento di Scienze Biomediche Sperimentali e Cliniche, Università degli Studi dell'Insubria, via J. H. Dunant 5, 21100 Varese, Italy and the* [§]*Department of Biomedical Engineering, The Cleveland Clinic, Cleveland, Ohio 44195*

Chronic inflammation is now accepted to have a critical role in the onset of several diseases as well as in vascular pathology, where macrophage transformation into foam cells contributes in atherosclerotic plaque formation. Endothelial cells (EC) have a critical function in recruitment of immune cells, and proinflammatory cytokines drive the specific expression of several adhesion proteins. During inflammatory responses several cells produce hyaluronan matrices that promote monocyte/macrophage adhesion through interactions with the hyaluronan receptor CD44 present on inflammatory cell surfaces. In this study, we used human umbilical chord vein endothelial cells (HUVECs) as a model to study the mechanism that regulates hyaluronan synthesis after treatment with proinflammatory cytokines. We found that interleukin 1β and tumor necrosis factors α and β, but not transforming growth factors α and β, strongly induced HA synthesis by NF-κB pathway. This signaling pathway mediated hyaluronan synthase 2 (HAS2) mRNA expression without altering other glycosaminoglycan metabolism. Moreover, we verified that U937 monocyte adhesion on stimulated HUVECs depends strongly on hyaluronan, and transfection with short interference RNA of HAS2 abrogates hyaluronan synthesis revealing the critical role of HAS2 in this process.

Hyaluronan (HA)[3] is a linear glycosaminoglycan consisting of a disaccharide (glcUA-β1,3-glcNAc-β1,4) repeated several thousand times without any other chemical modifications (*i.e.* sulfation and epimerization) that are typical of the other glycosaminoglycans (1). HA is a multifunctional molecule in the extracellular matrix. In addition to its viscoelastic properties that modulate tissue hydration, HA can interact with cell surface receptors, including CD44, receptor for HA-mediated motility (RHAMM), Lyve-1 (lymphatic vessel endothelial receptor 1), HARE (HA receptor for endocytosis), intercellular adhesion molecule-1 (ICAM-1), and Toll-like receptor 4 (TLR4), and HA can initiate several signal transduction pathways (1). Chain lengths can depend on the activity of different isoforms of HA synthases (HAS1, -2, and -3) (2), or from the activity of degrading enzymes (*i.e.* hyaluronidases) (1). Short HA fragments produced after injuries or inflammation can interact with TLR4 and stimulate synthesis of macrophage chemokines and cytokines (3).

In vascular pathologies, HA accumulation can regulate the behavior of smooth muscle cells and contribute to vessel wall thickening by inducing cell migration and proliferation (4). Moreover, in the media and neointima, HA exerts a proatherosclerotic effect by promoting adhesion of immune cells and by recruiting monocytes/macrophages (5) that, through cholesterol rich lipoproteins endocytosis, contribute to progression of atherosclerotic plaque. The molecular mechanism involved in the interaction of immune cells with HA depends on CD44. Interestingly, the organization of HA in the extracellular matrix has a critical role in this process, and cells subjected to various stresses (endoplasmic reticulum stress, viral stimulus, and hyperglycemia) synthesize HA cable-like structures that interact with CD44 on monocyte surfaces and mediate adhesion (6). The organization of the HA cable structure largely is unknown and can contain additional molecules, including versican and the covalently linked heavy chains transferred from the chondroitin sulfate chain in inter-α-trypsin inhibitor to HA catalyzed by tumor necrosis factor α (TNF-α)-induced protein 6 (7). The recruited monocytes/macrophages are required to remove this abnormal matrix, and CD44 also is required. Mice null in CD44 do not survive a bleomycin-induced inflammation in the lung due to the continued accumulation of HA extracellular matrix and despite continued influx of monocytes/macrophages (8). Interestingly, dividing cells in hyperglycemia initiate HA synthesis in intracellular compartments (endoplasmic reticulum/Golgi/transport vesicles), which induces autophagy and cyclin D3 responses that initiate formation of HA cable structures after completion of cell division (9). This suggests that HA synthases located in these intracellular compartments

* This work was supported by Fondazione Comunitaria del Varesotto-ONLUS, PRIN 2007 (to G. D. L.) and a young researcher award from the Centro Insubre di Biotecnologie per la Salute Umana (to D. V.).

[1] Both authors contributed equally to this work.

[2] To whom correspondence should be addressed: Dipartimento di Scienze Biomediche Sperimentali e Cliniche, Università degli Studi dell'Insubria, via J. H. Dunant 5, 21100 Varese, Italy. Tel.: 39-0332397142; Fax: 39-0332 397119; E-mail: alberto.passi@uninsubria.it.

[3] The abbreviations used are: HA, hyaluronan; HAS, HA synthase(s); RT-PCR, reverse transcriptase-polymerase chain reaction; HPLC, high pressure liquid chromatography; TNF, tumor necrosis factor; TGF, tumor growth factor; HUVEC, human umbilical vein endothelial cells; ICAM-1, intercellular adhesion molecule-1; PAGE-FS, polyacrylamide gel electrophoresis of fluorophore-labeled saccharides; VCAM-1, vascular cell adhesion molecule-1; EC, endothelial cells; MHC, major histocompatibility complex.

can be activated and utilize the UDP-sugar substrates in the cytosol during HAS transport to and/or from the plasma membrane where it is normally active (6, 10, 11). Such HA cables have been described both *in vitro* and *in vivo* and appear to be associated to smooth muscle cells in gut mucosa of Crohn disease patients, in the lung of asthmatic patients, and in glomeruli of kidneys in the streptozotocin diabetic rat model (6). However, immune cells that circulate in the bloodstream have to cross the endothelium to reach the inflamed sites. Therefore, the role of endothelial cells is critical to "capture" circulating inflammatory cells only at specific sites where the immune response is required through interactions with cell membrane structures.

Proinflammatory mediators, including TNF-α and interleukin 1β (IL-1β), significantly alter expression of adhesion molecules on EC surfaces that determine the tethering, rolling, activation, arrest, and extravasation (diapedesis) of leukocytes from the bloodstream into the inflamed tissue. This complex set of successive events depends on many proteins (*i.e.* selectins and integrins) expressed on both ECs and the immune cells (12, 13). In addition, HA is known to have a critical role in this process (14). Interaction of leukocyte CD44 with HA on the EC surface determines their adhesion and activation (15). Interestingly, ECs normally synthesize very little HA, whereas its production dramatically increases after stimulation by proinflammatory cytokines (16). However, evidence for HA cable formation in ECs is lacking, and our data support a model in which EC synthesis of HA forms a structure bound to CD44 on the EC surface that can be recognized by CD44 on immune cells (17). In this study, we investigated the mechanism by which ECs increase HA synthesis at the molecular level and identify the pathway involved in this process.

EXPERIMENTAL PROCEDURES

Cell Culture—Human umbilical vein endothelial cells (HUVECs) were purchased from Lonza and were grown for 2–6 passages in EGM2 culture medium (Lonza) supplemented with 10% fetal bovine serum. The cultures were maintained in an atmosphere of humidified 95% air, 5% CO_2 at 37 °C. Six h before treatments, subconfluent HUVECs were cultured in EGM2 with 1% fetal bovine serum. The medium was then changed to EGM2 plus 10% fetal bovine serum with 5 μg/ml of IL-1β (Peprotech), or 0.1 μg/ml of TNF-α (Euroclone), or 0.3 μg/ml of TNF-β (Euroclone), or 1 μg/ml of tumor growth factor α (TGF-α Euroclone), or 0.01 μg/ml of tumor growth factor β (TGF-β, Euroclone) and incubated for 24 h. In some experiments, 2 μM (final concentration) of pyrolidine dithiocarbamate (PDTC, Sigma) was added to the cells. By using these cytokine concentrations, we did not measure any mortality effects detected by trypan blue staining (results not shown).

Glycosaminoglycan Quantification—HA and chondroitin sulfate released into the culture medium were quantified by polyacrylamide gel electrophoresis of fluorophore-labeled saccharides (PAGE-FS) and by HPLC analyses as described previously (18, 19). Briefly, proteins in the culture medium were digested with proteinase K, and the glycosaminoglycans were purified by ethanol precipitation. The specific unsaturated disaccharides of HA and chondroitin sulfate (ΔHA and ΔCS, respectively) were obtained by specific glycosidase digestions and derivatization with 2-aminoacridone. 2-Aminoacridone-labeled ΔHA and ΔCS disaccharides were separated and quantified by PAGE-FS or HPLC and normalized to the cell number. Agarose gel electrophoresis, as described by Vigetti *et al.* (5), was used to assess the molecular weight distributions of synthesized HA after IL-1β treatments.

HA Visualization—To visualize HA, HUVECs were grown on glass coverslips and either untreated or treated with IL-1β. They were processed using a biotinylated HA-binding protein and a green fluorescent reporter as described previously (20).

Quantitative RT-PCR—Total RNA samples were extracted from untreated or cytokine-treated HUVECs with TRIzol (Invitrogen), and contaminating DNA was removed by DNase (Ambion). cDNAs were generated by using the High Capacity cDNA synthesis kit (Applied Biosystems) and were amplified on an Abi Prism 7000 instrument (Applied Biosystems) using the Taqman Universal PCR Master Mix (Applied Biosystems) following the manufacturer's instructions. The following human TaqMan gene expression assays were used: HAS1 (Hs00155410_m1), HAS2 (Hs00193435_m1), HAS3 (Hs00193436_m1), CD44 (HS00174139_m1), and β-actin (Hs99999903_m1). The relative quantification of gene expression levels was determined by comparing ΔCt (5).

HAS Activity—To quantify the activity of HAS on cell membranes, we used the nonradioactive assay of HA synthesis as described previously (11).

Human HAS2 Silencing—Short interfering RNA (siRNA) was used to reduce the expression of human HAS2 in HUVECs by using HAS2 siRNA (ID117326, 5′-GCUGCUUAUAUUGUUGGCUtt-3′) and negative control siRNA kit (scramble, catalog no. 4611), both from Ambion. The transfections were done using a Nucleofector apparatus (Lonza) and the human HUVEC Nucleofector kit as described previously (21). After 48 h of incubation, the silencing efficiency was quantified by quantitative RT-PCR measuring the HAS2 mRNA transcript.

Monocytes Adhesion Assay—Adhesion of U937 monocytes to HUVEC cultures was assayed as described previously (22). 1×10^6 U937 monocytes were labeled with fluorescent green CytoTracker (Invitrogen) vital staining and plated on cytokine-treated or untreated HUVEC cultures followed by incubation at 4 °C for 30 min. After phosphate-buffered saline washing at 4 °C, the numbers of adherent cells were assessed under a fluorescent microscope (Olympus). As controls for binding to HA and CD44, HUVECs were pretreated with 2 units/μl of *Streptomyces* hyaluronidase (Seikagaku), or were incubated with monocytes in the presence of an antibody against CD44 (BRIC235, 5 μg/ml) that inhibits CD44/HA interaction, or were incubated with unrelated antibodies. Furthermore, monocytes were placed on HUVECs in the presence of 25 μg/ml high molecular mass HA (Healon, 4×10^6 Da) to compete with HA produced by treated cells.

Statistical Analyses—Statistical analysis of the data were done using analysis of variance, followed by post hoc tests (Bonferroni) using Origin 7.5 software (OriginLab). Probability values of $p < 0.01$ were considered statistically significant. Experiments were repeated three times each time in duplicate, and data are expressed as means ± S.E.

RESULTS AND DISCUSSION

Proinflammatory Cytokines Induce HA Synthesis—One of the main roles of ECs in inflammation is to regulate recruitment of immune cells from the bloodstream into the inflamed site. This mechanism involves not only expression of adhesive molecules on EC surfaces but also a coordinated expression of the corresponding ligands on the circulating cells. Diffusible alerting molecules (*i.e.* cytokines) bind to EC receptors and drive the expression of specific adhesion proteins, selectins, and integrins. Cytokines such as IL-1β and TNF-α are among the common proinflammatory-alerting molecules that are synthesized by immune cells such as macrophages in response to infection in an early phase of the process. The pioneering works of Siegelmen's research group clearly showed that HA is also involved in lymphocyte recruitment *in vivo* as well as *in vitro* (16, 23–26). Circulating leukocytes are activated by HA through CD44 interaction, whereas proinflammatory cytokines stimulate ECs to produce HA together with other well known adhesion molecules such as ICAM-1 and VCAM-1.

In our study, we focused on the mechanism of HA induction after IL-1β and TNF-α treatment. We used HUVECs because they are a convenient and broadly accepted artery EC model. After preliminary dose-response experiments, we found that a 24-h treatment of HUVEC cultures with 5 μg/ml of IL-1β induced a clear accumulation of HA secreted into the culture medium, which was quantitatively measured by PAGE-FS (Fig. 1*A*), and HA in the cell layer was qualitatively visualized by immunofluorescence (Fig. 1*B*). The band corresponding to HA disaccharides dramatically increased after IL-1β addition, whereas the bands corresponding to chondroitin sulfate disaccharides remained unchanged, indicating that IL-1β induces a specific alteration in the HA content without modifying chondroitin sulfate synthesis. The organization of HA in treated cells revealed a diffuse staining around HUVEC plasma membranes without showing the cable-like structures that are known to be adhesive toward monocytes in other cell models (6, 14). Moreover, analysis of the size of HA induced by IL-1β by agarose gel electrophoresis revealed the synthesis of a high molecular weight polymer of $>2 \times 10^6$ Da (results not shown).

Furthermore, we tested the responses of HUVECs to other proinflammatory cytokines (*i.e.* TNF-α and TNF-β) or to anti-inflammatory cytokines (*i.e.* TGF-α and TGF-β) (27). After preliminary dose-response experiments (data not shown), the proinflammatory TNF-α and TNF-β at plateau concentrations induced the highest HA secretion, ~3.5-fold over control, whereas IL-1β increased HA ~2-fold over control. In contrast, anti-inflammatory TGF-α and TGF-β treatments did not increase HA secretion over control (Fig. 2). These results suggest that macrovascular artery ECs, such as HUVECs, together with previously reported microvascular ECs (16), can respond to microenvironmental changes by activating HA synthesis after treatment with proinflammatory cytokines. Previous studies and our unpublished data have shown that HUVECs induce ICAM-1 and VCAM-1 expression after treatment with proinflammatory cytokines, whereas Mohamadzadeh *et al.* (16) reported that HUVECs did not increase HA synthesis after stimulation with 10 ng/ml of TNF-α or IL-1β for 4 h. These

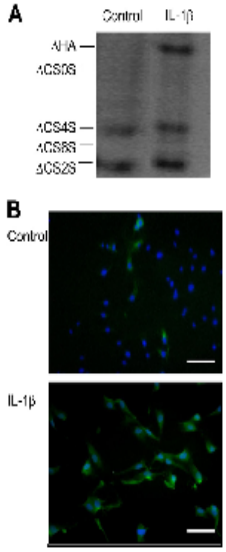

FIGURE 1. IL-1β induces HA biosynthesis in HUVECs. *A*, PAGE-FS analysis of the HUVEC culture medium in untreated (*CNT*) and 24-h treated cells with 5 μg/ml of IL-1β. *ΔHA* and *ΔCS0S* indicate HA and chondroitin disaccharides, respectively, while *ΔCS4S*, *ΔCS6S*, and *ΔCS2S* indicate chondroitin 4, 6, and 2 sulfate disaccharides, respectively. *B*, visualization of HA (*green*) and nuclei (*blue*) on untreated (*Control*) or 24-h treated cells with 5 μg/ml of IL-1β. The microphotographs show representative results of different experiments. *Scale bars*, 70 μm.

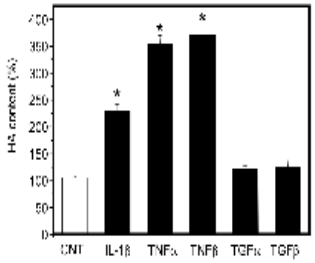

FIGURE 2. Effects of several cytokines on HA biosynthesis in HUVECs. Relative quantification by HPLC of ΔHA secreted into the culture medium in untreated (*CNT*, *white bar*) and 24-h treated (*black bars*) cells with 5 μg/ml of IL-1β, 0.1 μg/ml of TNF-α, 0.3 μg/ml of TNF-β, 1 μg/ml of TGF-α, and 0.01 μg/ml of TGF-β. Results are expressed as mean ± S.E. *, $p < 0.01$ control *versus* treated samples.

apparent differences in results can be explained considering the different cytokine concentrations and incubation times, as well as the different sensitivity of the HA quantification methods that we used in our experiments. Although the cytokine concentrations used in this study appear to be higher than physiological level, it was discussed elsewhere that as cytokines act locally, their concentration *in vivo* may be difficult to define and higher than expected (28).

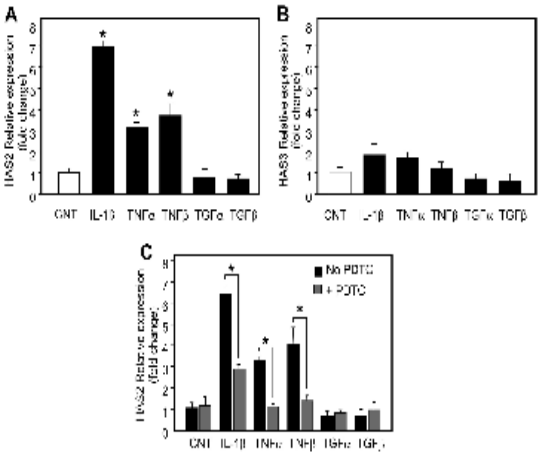

FIGURE 3. **Gene expression alteration after treating HUVECs with cytokines.** Relative quantification of transcripts coding for HAS2 (*A*) or HAS3 (*B*) in untreated (*CNT*, *white bar*) and after 24 h treated (*black bars*) cells with 5 μg/ml of IL-1β, 0.1 μg/ml of TNF-α, 0.3 μg/ml of TNF-β, 1 μg/ml of TGF-α, and 0.01 μg/ml of TGF-β. The lowest HAS2 or HAS3 mRNA level in three different untreated samples was set at 1, and the S.E. is shown on each *bar*. *, $p < 0.01$ control *versus* treated samples. *C*, relative quantification of HAS2 mRNA was done after cytokines exposure in the presence (*gray bars*) or absence (*black bars*) of PDTC (final concentration, 2 μM). The lowest HAS2 mRNA level in three different untreated samples was set at 1, and the S.E. is shown on each *bar*. *, $p < 0.01$ PDTC-untreated *versus* PDTC-treated samples.

Proinflammatory Cytokine-induced HA Depends on HAS2 and NF-κB—As the synthesis of HA depends on the activity of one or more of the three HA synthases, HAS1, -2, and -3, we measured their mRNA expression after cytokine treatments by using quantitative RT-PCR (Fig. 3, *A* and *B*). As HAS protein only is present at low levels at the plasma membrane (29), quantitative assessment at the protein level remains a technical challenge and could not be performed in a reliable manner. HAS1 mRNA was not detected in HUVECs, whereas HAS2 and HAS3 mRNAs were present at similar levels. Interestingly, only HAS2 mRNA significantly increased, ~7-fold after IL-1β treatment and ~3-fold after TNF-α and TNF-β treatments. In contrast, HAS2 mRNA did not change after treatment with the anti-inflammatory cytokines. It should be noted that the induction of HAS2 mRNA and HA levels after the cytokine treatments did not match exactly. This could be due to an earlier expression of HAS2 that we did not detect after 24 h of incubation, whereas HA accumulates during the whole incubation time. HAS2 enzymes synthesize HA of high molecular weight in agreement with the size that we observed after IL-1β stimulation. These results indicate that increased HA in response to the proinflammatory cytokines is regulated by expression of HAS2. In addition, we measured the HA synthetic activity in purified plasma membrane vesicles (11) isolated from control, IL-1β-, TNF-α-, and TNF-β-treated HUVEC cultures and found values of 22.4 ± 3, 91.1 ± 7, 78.9 ± 8, and 83.7 ± 5 pmol ΔHA/μg of protein/min, respectively. The cytokine treated cultures showed statistically significant increases ~4-fold over control of HAS activity in purified plasma membranes, consistent with the increases in HA in the culture medium. Interestingly, the proinflammatory cytokine treatments induced similar HAS activities, whereas IL-1β induced a much greater HAS2 mRNA response than did TNF-α and TNF-β. Therefore, this activity increase was not related completely to HAS2 gene expression as shown in Fig. 3*A*, because cytokine treatments caused a different degree of HAS2 messenger accumulation. These data could suggest the existence of complex post-translational processing of HAS mRNA as has been shown for the stability of other TNF-α-induced transcripts (30). Moreover, other additional factors, such as hyaluronidase activity and HA turnover could contribute to this issue. Previous data from TNF-α-treated lymph node ECs reported that increased HA synthesis did not involve a significant change in HAS gene expression (16). However, only HAS1 mRNA was investigated at that time as the other isoenzymes were just discovered, and their sequences were not available in public databases.

A large body of evidence (31) has demonstrated that many cellular responses to proinflammatory signals are mediated by NF-κB. This transcription factor normally is present in the cytoplasm in a complex with the protein IκBα that maintains NF-κB in an inactive state. IκBα phosphorylation, mediated by IκB kinase, induces a rapid degradation of IκBα via the ubiquitin-proteosome pathway, which leads to translocation of NF-κB into the nucleus and its transcriptional functions (31). IκB kinase activation can be induced by several stimuli including TNF receptors. Therefore, we investigated whether NF-κB is involved in the increased HAS2 transcript expression after proinflammatory cytokines treatment by using PDTC, a widely used chemical inhibitor of NF-κB (32). As shown in Fig. 3*C*, the simultaneous addition of IL-1β, or TNF-α, or TNF-β with PDTC caused a reduction of HAS2 transcription. Interestingly, in TNF-α- and TNF-β-treated cells, NF-κB inhibition inhibited HAS2 transcription to the level of control untreated cells. However, in IL-1β-treated cells, NF-κB inhibition did not lower HAS2 transcription to the level of control, which suggests a more complex mechanism of HAS2 transcription activation that could involve other factors in addition to NF-κB. In fact, in addition to NF-κB sites, the HAS2 promoter region contains putative binding sequences for other transcription factors (33). A previous study on human synoviocytes found that PDTC inhibited HAS1 transcription after IL-1β stimulation, confirming the critical role of NF-κB in HA metabolism (34). Interestingly, HA itself is able to modulate cytokine production via NF-κB, confirming its critical role in inflammation (35).

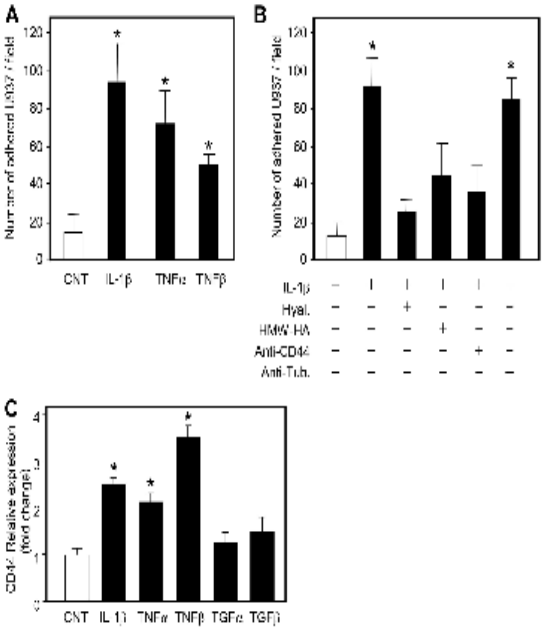

FIGURE 4. **Proinflammatory cytokine effects on HUVEC adhesiveness.** *A*, the adhesion assay was done on untreated (*CNT*, *white bars*) and after 24 h-treated (*black bars*) cells with 5 μg/ml of IL-1β, 0.1 μg/ml of TNF-α, and 0.3 μg/ml of TNF-β. Cytotracker-labeled monocytes (U937) were plated on treated and untreated HUVEC cultures, washed with phosphate-buffered saline, and counted under a fluorescent microscope. Results are expressed as the number of adherent U937 per field and represented as mean ± S.E. of six independent fields. *, $p < 0.01$; untreated *versus* the treated sample. *B*, the adhesion assay was done on untreated (*CNT*, *white bar*) and after 24 h-treated (*black bars*) cells with 5 μg/ml of IL-1β. Before adding monocytes, IL-1β-treated cells were incubated with 2 units/ml of hyaluronidase (*Hyal.*) for 20 min at 37 °C, or the monocytes were added with high molecular mass HA (Healon, 4 × 10^6 Da), or with 5 μg/ml CD44-blocking antibody (*anti-CD44*), or with 5 μg/ml anti-tubulin antibody (*anti-Tub.*). Results are expressed as the number of adherent U937 per field and represented as mean ± S.E. *, $p < 0.01$; untreated *versus* the treated sample. *C*, relative quantification of CD44 mRNA in untreated (*CNT*, *white bar*) and after 24 h-treated (*black bars*) cells with 5 μg/ml of IL-1β, 0.1 μg/ml of TNF-α, 0.3 μg/ml of TNF-β, 1 μg/ml of TGF-α, and 0.01 μg/ml of TGF-β. The lowest CD44 mRNA level in three different untreated samples was set at 1, and the S.E. is shown on each *bar*. *, $p < 0.01$ control *versus* treated samples.

HAS2 and CD44 Mediate HUVEC Monocyte Adhesive Property—Because some of the effect of HA is to modulate adhesion of immune cells on microvascular ECs (16), we investigated whether monocyte adhesion to HUVECs after treatment with proinflammatory cytokines could be modulated by HA. Fig. 4*A* shows that IL-1β, TNF-α, and TNF-β increased the number of adherent monocytes ~5-, ~4-, and ~3-fold, respectively. Furthermore, hyaluronidase treatment of HUVECs after IL-1β treatment decreased U937 monocyte binding to near control level (Fig. 4*B*). Moreover, the simultaneous addition of the monocytes with a pure HA preparation of high molecular weight (Healon) also inhibited binding. These data indicate the critical role of HA in monocytes adhesion in that removal of HA by hyaluronidase treatment as well as the competition with exogenous HA both reduced monocyte adhesion. This point is critical because lowering immune cell adhesion to vascular endothelium would reduce the number of inflammatory cells that reach an inflamed site, therefore reducing the inflammation. Several studies have highlighted the anti-inflammatory and protective effect of HA administered in an experimental model of restenosis (36) as well as in osteoarthritic joints injected with HA (37).

The molecular mechanism through which immune cells interact with HA is mainly mediated by CD44 (38). To confirm CD44 involvement, we simultaneously added monocytes together with a monoclonal antibody against CD44 known to block HA/CD44 binding and found a clear reduction of monocytes adherent to IL-1β-treated HUVECs, whereas an unrelated control antibody did not modify adhesion (Fig. 4*B*). We also measured CD44 mRNA expression by quantitative RT-PCR. Interestingly, proinflammatory cytokine treatments induced a significant increase of CD44 mRNA in HUVEC cultures, whereas anti-inflammatory cytokines maintained control CD44 levels (Fig. 4*C*). This finding could support the hypothesis that CD44 on the plasma membrane of HUVECs binds HA and presents HA to CD44 on circulating immune cells that can attach and form a "sandwich" structure (17). Notably, in this model, HA could remain in a soluble form without forming cable structures, as we found from the immunofluorescent experiments (Fig. 1*B*). It is of note that a previous work using an immortalized HUVEC cell line (*i.e.* Ea.hy.926) found an inhibition of neutrophil-EC adhesion by HA independent of CD44 and probably involving ICAM-1 (39), suggesting that *in vivo* multiple HA-interacting proteins may modulate interactions of immune cells with endothelium.

The main HAS isoform responsible for increased HA after treatment of HUVECs with proinflammatory cytokines was HAS2. Therefore, we assessed its involvement in monocyte binding by using an siRNA approach. HUVECs were transfected with commercial siRNA against HAS2 as well as with a scrambled control siRNA by using the Nucleofector apparatus to obtain a high transfection efficiency with a low mortality rate. After 24 h of incubation, nucleofected HUVECs were treated with or without IL-1β and incubated for 24 h. HUVEC cultures were then used for monocytes adhesion experiments or for RNA extraction and cDNA preparation. The effectiveness of HAS2 mRNA silencing was assessed with quantitative RT-PCR and, as shown in Fig. 5*A*,

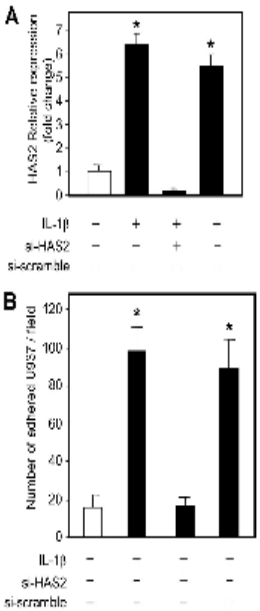

FIGURE 5. **HAS2 effects on IL-1β-induced monocyte adhesion.** *A*, relative quantification of the transcript coding for HAS2 in HUVECs silenced for HAS2 and treated with IL-1β (*black bars*). Cells were left untreated (*white bars*) or transfected with 50 μM of scramble siRNA (*si-scramble*) or with 50 μM of HAS2 siRNA (*si-HAS2*). After 24 h of incubation, 5 μg/ml of IL-1β was added, and, after 24 h, RNA was extracted for quantitative RT-PCR experiments. The lowest HAS2 mRNA level in three different untreated samples was set at 1, and the S.E. is shown on each *bar*. Results are expressed as mean ± S.E. *, $p < 0.01$ untreated *versus* treated samples. *B*, the adhesion assay was done on HUVECs silenced for HAS2 and treated with IL-1β. 24 h after siRNA transfections and subsequently after 24-h treatment with 5 μg/ml IL-1β, fluorescent monocytes were added, washed, and counted. Results are expressed as the number of adherent U937 per field and represented as mean ± S.E. of six independent fields. *, $p < 0.01$; untreated *versus* the treated samples.

after IL-1β treatment, HAS2 siRNA-nucleofected cells greatly reduced HAS2 expression. Control siRNA with a random sequence did not perturb the HAS2 mRNA increase due to IL-1β treatment. In parallel cultures, siRNA of HAS2 completely inhibited U937 binding, whereas control siRNA did not alter the adhesive property of HUVECs after IL-1β treatment (Fig. 5*B*).

Our results clearly demonstrate that HA synthesis in HUVECs is regulated strictly at the transcriptional level by proinflammatory cytokines. *In vivo*, this issue is of great importance, as HA can participate together with other adhesion molecules to recruitment of immune cells at inflamed sites. Although the generally accepted model foresees the formation of HA cables (6), we demonstrate that monocytes can bind to HA via CD44 without such filamentous structures, consistent with the recent model of Ruffell and Johnson (17). They proposed that HA can be maintained above the endothelium by CD44 on ECs, and leukocytes can bind to HA though their own CD44. Our findings highlight the critical role of HAS2 that could be

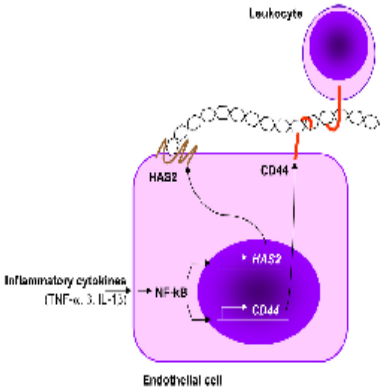

FIGURE 6. **Schematic representation of the line of events by which HA modulates the leukocyte-EC interaction.** Proinflammatory cytokines, through their receptors, activate NF-κB pathway that has a pivotal role in the inflammatory response by activating several genes including HAS2 (this work), CD44, and other adhesive molecules (ICAM-1, E-selectin, VCAM-1, and MHC class I genes) (41). High molecular weight HA synthesized by HAS2 interacts with CD44 present both on ECs and leukocytes in the "sandwich model" proposed by Ruffell and Johnson (17), which drives immune cells to adhere to ECs that eventually contribute to inflammation.

involved to maintain the nascent HA chain tethered on EC surfaces. *In vivo*, this model can be modulated by other players that include other cell types, other molecules, and other microenvironmental conditions such as free radical presence, enzyme activity, and shear stress. In fact, recently it has been shown that platelets can produce hyaluronidase 2 that can fragment HA and generate bioactive oligosaccharides that can trigger many cellular responses involving all the vasculature (40).

In conclusion, in this work, we provide evidence at molecular and functional levels that HA synthesis can modulate immune cell adhesion on HUVECs that, in turn, could regulate inflammatory responses (Fig. 6). In fact, proinflammatory cytokines induce HA synthesis through the NF-κB mediated expression of HAS2 that modulates monocyte adhesion by CD44, which represents the first step to start an inflammatory process. The central role of NF-κB in inflammation is highlighted by the induction also of other adhesion molecules (such as CD44, ICAM-1, E-selectin, VCAM-1, and MHC class I) (41), which, *in vivo*, may orchestrate all of the inflammatory responses that include cell adhesion, rolling, extravasation, migration, and specific cellular activity. In light of this model, the clinical relevance of HA administration to ameliorate inflammation (42) can be due to the competition with CD44 on ECs and leukocytes, thereby inhibiting the recruitment process.

Acknowledgments—We are grateful to Eleonora Solari (University of Insubria) and Giuseppe Campo (University of Messina) for technical support, Carol De La Motte (The Cleveland Clinic) for U937 cells, and Frances Spring (National Blood Service) for BRIC235 monoclonal antibodies. We acknowledge the "Centro Grandi Attrezzature per la Ricerca Biomedica" Università degli Studi dell'Insubria, for instruments availability.

REFERENCES

1. Jiang, D., Liang, J., and Noble, P. W. (2007) *Annu. Rev. Cell Dev. Biol.* **23**, 435–461
2. Itano, N., Sawai, T., Yoshida, M., Lenas, P., Yamada, Y., Imagawa, M., Shinomura, T., Hamaguchi, M., Yoshida, Y., Ohnuki, Y., Miyauchi, S., Spicer, A. P., McDonald, J. A., and Kimata, K. (1999) *J. Biol. Chem.* **274**, 25085–25092
3. Termeer, C. C., Hennies, J., Voith, U., Ahrens, T., Weiss, J. M., Prehm, P., and Simon, J. C. (2000) *J. Immunol.* **165**, 1863–1870
4. Vigetti, D., Viola, M., Karousou, E., Genasetti, A., Rizzi, M., Clerici, M., Bartolini, B., Moretto, P., De Luca, G., and Passi, A. (2008) *ScientificWorldJournal* **8**, 1116–1118
5. Vigetti, D., Rizzi, M., Viola, M., Karousou, E., Genasetti, A., Clerici, M., Bartolini, B., Hascall, V. C., De Luca, G., and Passi, A. (2009) *Glycobiology* **19**, 537–546
6. Hascall, V. C., Majors, A. K., De La Motte, C. A., Evanko, S. P., Wang, A., Drazba, J. A., Strong, S. A., and Wight, T. N. (2004) *Biochim. Biophys. Acta* **1673**, 3–12
7. Selbi, W., de la Motte, C. A., Hascall, V. C., Day, A. J., Bowen, T., and Phillips, A. O. (2006) *Kidney Int.* **70**, 1287–1295
8. Jiang, D., Liang, J., Fan, J., Yu, S., Chen, S., Luo, Y., Prestwich, G. D., Mascarenhas, M. M., Garg, H. G., Quinn, D. A., Homer, R. J., Goldstein, D. R., Bucala, R., Lee, P. J., Medzhitov, R., and Noble, P. W. (2005) *Nat. Med.* **11**, 1173–1179
9. Ren, J., Hascall, V. C., and Wang, A. (2009) *J. Biol. Chem.* **284**, 16621–16632
10. Majors, A. K., Austin, R. C., de la Motte, C. A., Pyeritz, R. E., Hascall, V. C., Kessler, S. P., Sen, G., and Strong, S. A. (2003) *J. Biol. Chem.* **278**, 47223–47231
11. Vigetti, D., Genasetti, A., Karousou, E., Viola, M., Clerici, M., Bartolini, B., Moretto, P., De Luca, G., Hascall, V. C., and Passi, A. (2009) *J. Biol. Chem.* **284**, 30684–30694
12. Mantovani, A., Bussolino, F., and Dejana, E. (1992) *FASEB J.* **6**, 2591–2599
13. Pober, J. S., and Cotran, R. S. (1990) *Physiol. Rev.* **70**, 427–451
14. Day, A. J., and de la Motte, C. A. (2005) *Trends Immunol.* **26**, 637–643
15. Johnson, P., and Ruffell, B. (2009) *Inflamm Allergy Drug Targets* **8**, 208–220
16. Mohamadzadeh, M., DeGrendele, H., Arizpe, H., Estess, P., and Siegelman, M. (1998) *J. Clin. Invest.* **101**, 97–108
17. Ruffell, B., and Johnson, P. (2009) in *Science of Hyaluronan Today* (Hascall, V. C., Yanagishita, M., and Toole, B. P., eds.)
18. Karousou, E. G., Viola, M., Genasetti, A., Vigetti, D., Luca, G. D., Karamanos, N. K., and Passi, A. (2005) *Biomed. Chromatogr.* **19**, 761–765
19. Viola, M., Karousou, E. G., Vigetti, D., Genasetti, A., Pallotti, F., Guidetti, G. F., Tira, E., De Luca, G., and Passi, A. (2006) *J. Pharm. Biomed Anal.* **41**, 36–42
20. Vigetti, D., Viola, M., Karousou, E., Rizzi, M., Moretto, P., Genasetti, A., Clerici, M., Hascall, V. C., De Luca, G., and Passi, A. (2008) *J. Biol. Chem.* **283**, 4448–4458
21. Vigetti, D., Moretto, P., Viola, M., Genasetti, A., Rizzi, M., Karousou, E., Pallotti, F., De Luca, G., and Passi, A. (2006) *Faseb J.* **20**, 1118–1130
22. de la Motte, C. A., Hascall, V. C., Drazba, J., Bandyopadhyay, S. K., and Strong, S. A. (2003) *Am. J. Pathol.* **163**, 121–133
23. DeGrendele, H. C., Estess, P., Picker, L. J., and Siegelman, M. H. (1996) *J. Exp. Med.* **183**, 1119–1130
24. DeGrendele, H. C., Estess, P., and Siegelman, M. H. (1997) *Science* **278**, 672–675
25. Estess, P., Nandi, A., Mohamadzadeh, M., and Siegelman, M. H. (1999) *J. Exp. Med.* **190**, 9–19
26. Nandi, A., Estess, P., and Siegelman, M. H. (2000) *J. Biol. Chem.* **275**, 14939–14948
27. Letterio, J. J., and Roberts, A. B. (1998) *Annu. Rev. Immunol.* **16**, 137–161
28. Kaplan, D. (1996) *Immunol. Today* **17**, 303–304
29. Rilla, K., Siiskonen, H., Spicer, A. P., Hyttinen, J. M., Tammi, M. I., and Tammi, R. H. (2005) *J. Biol. Chem.* **280**, 31890–31897
30. Anderson, P. (2009) *Nat. Immunol.* **10**, 233–234
31. Paparakis, M. (2009) *Nat. Rev. Immunol.* **9**, 778–788
32. Schreck, R., Meier, B., Männel, D. N., Dröge, W., and Baeuerle, P. A. (1992) *J. Exp. Med.* **175**, 1181–1194
33. Monslow, J., Williams, J. D., Fraser, D. J., Michael, D. R., Foka, P., Kift-Morgan, A. P., Luo, D. D., Fielding, C. A., Craig, K. J., Topley, N., Jones, S. A., Ramji, D. P., and Bowen, T. (2006) *J. Biol. Chem.* **281**, 18043–18050
34. Kao, J. J. (2006) *Exp. Gerontol.* **41**, 641–647
35. Campo, G. M., Avenoso, A., Campo, S., D'Ascola, A., Nastasi, G., and Calatroni, A. (2010) *Biochimie* **92**, 204–215
36. Savani, R. C., and Turley, E. A. (1995) *Int. J. Tissue React.* **17**, 141–151
37. Miltner, O., Schneider, U., Siebert, C. H., Niedhart, C., and Niethard, F. U. (2002) *Osteoarthritis Cartilage* **10**, 680–686
38. Khan, A. I., Kerfoot, S. M., Heit, B., Liu, L., Andonegui, G., Ruffell, B., Johnson, P., and Kubes, P. (2004) *J. Immunol.* **173**, 7594–7601
39. Alam, C. A., Seed, M. P., Freemantle, C., Brown, J., Perretti, M., Carrier, M., Divwedi, A., West, D. C., Gustafson, S., Colville-Nash, P. R., and Willoughby, D. A. (2005) *Inflammopharmacology* **12**, 535–550
40. de la Motte, C., Nigro, J., Vasanji, A., Rho, H., Kessler, S., Bandyopadhyay, S., Danese, S., Fiocchi, C., and Stern, R. (2009) *Am. J. Pathol.* **174**, 2254–2264
41. Mackay, F., Loetscher, H., Stueber, D., Gehr, G., and Lesslauer, W. (1993) *J. Exp. Med.* **177**, 1277–1286
42. Ialenti, A., and Di Rosa, M. (1994) *Agents Actions* **43**, 44–47